High-throughput OpenArray™: novel, swift TaqMan® Real-Time PCR chip for diagnostic biomarkers in *Oncorhynchus tshawytscha*

by

Xiaoqing Dang

A thesis

presented to the University of Waterloo

in fulfillment of the

thesis requirement for the degree of

Master of Science

in

Biology

Waterloo, Ontario, Canada, 2024

Author's Declaration

This thesis consists of material all of which I authored or co-authored: see Statement of Contributions included in the thesis. This is a true copy of the thesis, including any required final revisions, as accepted by my examiners. I understand that my thesis may be made electronically available to the public.

Statement of Contributions

Manuel Soto Dávila assisted with *Vibrio anguillarum* bacterial growth.

Kenneth Jeffries and Shahinur Islam assisted with OpenArray™ TaqMan® Real-Time PCR primer and probe design.

Jonathon LeBlanc assisted with OpenArray™ TaqMan® Real-Time PCR chip assays and provided raw data.

Abstract

In 2014, aquaculture replaced capture fisheries as the primary source of fish supply for human consumption for the first time in history, but to date, fish domestication has not developed enough to cope with the disease-related challenges. Members of the *Salmonidae* family are among the most popular commercialized fish species and salmon aquaculture has been the fastest growing food production system worldwide. An OpenArray™ device for Chinook Salmon (*Oncorhynchus tshawytscha*) health surveillance was validated in this thesis. On each microscope slide–sized OpenArray™ plate, 28 gene transcripts from 48 samples can be quantified using TaqMan® RT-qPCR. To evaluate the function of the chip, fish culture water, mucus, head kidney, spleen, and gill tissues were collected from Chinook salmon that were intraperitoneally injected with live *Vibrio anguillarum* within the course of 96 h. Based on the on-chip primer efficiency results, primers for 27 of the genes were considered acceptable for future validation. Based on the transcript expression patterns revealed by the OpenArray™ TaqMan® RT-qPCR chip, 6 immune genes (*calm*, *mhc-i*, *mhc-ii*, *il-1β*, *il-8*, *tapbp*) were selected and validated by SYBR RT-qPCR. Pearson's correlation analysis revealed that a moderate to strong correlation existed between the results generated by both RT-qPCR methods for the 6 genes analysed.

Both OpenArray™ TaqMan® and SYBR RT-qPCR detected significantly increased *il-1β* and *il-8* expression levels in spleen tissue at 72 h and 96 h, although the peaks of the expression were not recorded within the time point analysed. In head kidney tissue, *il-1β* expression level was also increased at 72 h, but there was no difference observed for *il-8* between the control and infected groups within any time points. A longer response initiation

time was observed in the Chinook salmon model in this trial. Comparing to previous studies in related salmon species, the pro-inflammatory cytokine *il-1β* was observed to increase as early as 6 h post infection *in vivo*. Nevertheless, mucus samples showed great potential as a minimally invasive sampling method if the transcripts were quantified by SYBR RT-qPCR. By comparison, in mucus the OpenArray™ TaqMan® RT-qPCR chip did not report as many quantification data as in spleen and head kidney tissue. In general, both RT-qPCR methods revealed an early systematic immune response induced by *Vibrio anguillarum* in spleen and head kidney, but the biological significance of the delayed immune response initiation will require further analysis to understand.

The OpenArray™ TaqMan® RT-qPCR chip validated in this thesis was designed to be specific to salmon species under the order *Salmoniformes*. By validating this health monitoring tool in other salmon species, it is possible that the interspecies physiological differences can be horizontally compared. This will enable the development of species-specific, more effective prophylactic and therapeutic approaches against the salmon diseases.

Acknowledgements

First, I would like to thank my supervisor Dr. Brian Dixon, who has been supporting me through a long journey in your lab. I joined your lab as a BIOL 499 student in 2018, and you changed my life by allowing me to continue as a MSc candidate. You are the best supervisor that any student could ever ask for, and I feel so lucky because of this. Thank you for all the advice and suggestions - you shaped me greatly through so many small talks in your office. It was such a fun and adventurous experience to work in your lab because you are always so supportive to the experiment ideas, and you are always so kind to me. During my MSc study, I attended my first academic conference in Banff, and I lived on a remote island in BC for a whole month to collect samples (that's crazy!). There are so many things that I never imagined to experience, and none of these would be possible if it is not you.

Secondly, I would like to thank my committee members, Dr. Daniel Heath, and Dr. Christine Dupont for their guidance on this journey. I am appreciative of your suggestions on my experimental design that completed the picture. Dr. Heath, thank you so much for the opportunity on the gene chip project. This thesis would not happen without you and your lab. I would like to give special thanks to John and Ann, for allowing inexperienced students like me to go to your fish farm and do experiment using live pathogen. Thank you for allowing us to stay in your cozy cottage by the sea.

I would like to thank Dr. Tania Rodriguez-Ramos, our lab manager, who has taught me all the lab techniques I know hand by hand. You are so knowledgeable about everything, from data analysis methods to the design of a tricky experiment. You just have the magic to make things happen, and you offered me with so many "daily hugs". I would like to thank

Dr. James Hugh Campbell, who was always so patient and helped me so much with all the "what if" I had for my project. I would like to thank Emily McKenzie, for being a dear sister that I never had. I would like to thank all members of the Dixon Lab, for all the laughs and happy memories. I truly enjoyed every moment that I spent with you all.

Table of Contents

List of Figures

List of Tables

List of Abbreviations

ACTH	Adrenocorticotropic hormone
AMP	antimicrobial peptides
ampkα	AMP-Activated Protein Kinase alpha
ANOVA	Analysis of variance
BC	British Columbia
BSC	brain-sympathetic-chromaffin cell
calm	Calmodulin
CaMK	Ca^{2+}/calmodulin-dependent kinase
casp	Caspase
CD	Cluster of differentiation
cDNA	Complementary deoxyribonucleic acid
CDS	Coding sequence
CFU	Colony forming unit
cirbp	Cold inducible RNA binding protein
CMC	Cell-mediated cytotoxicity
C_q	Cycle of quantification
C_{rt}	Cycle of relative threshold
CTL	CD8+ cytotoxic T lymphocyte
ctsd	Cathepsin D
DAMP	Damage-associated molecular pattern
DNA	Deoxyribonucleic acid
ef1α	Elongation factor 1 alpha
FAO	Food and Agriculture Organization of the United Nations
fasn	Fatty acid synthase
GALT	Gut-associated lymphoid tissue
GIALT	Gill-associated lymphoid tissue
gr	Glucocorticoid receptor
HK	Head kidney
HPI	Hypothalamus–pituitary–interrenal axis

HSP	Heat shock protein
IFN	Interferon
Ig	Immunoglobulin
IHNV	Infectious hematopoietic necrosis virus
Il	Interleukin
ilpea/b	Hormone-sensitive lipase a & b
ILT	Interbranchial lymphoid tissue
i.p.	intraperitoneal
IPNV	Infectious Pancreatic Necrosis Virus
ISAV	Infectious salmon anemia virus
JAK/STAT	Janus kinase/signal transducers and activators of transcription
lpl	Adipose triglyceride lipase/lipoprotein lipase
LPS	Lipopolysaccharide
MALT	Mucosal-associated lymphoid tissue
MDA	Melanoma differentiation-associated gene
MHC	Major histocompability complex class
mt	Metallothionein
mx	Mx protein
NALT	Nasal-associated lymphoid tissue
NK cells	Natural killer cells
PAMP	Pathogen-associated molecular pattern
PBS	Phosphate buffered saline
PCR	Polymerase chain reaction
PE	Primer efficiency
prdx	Peroxiredoxins
PRR	Pattern recognition receptors
PRV	Piscine orthoreovirus
PMCV	Piscine myocarditis virus
RIG	Retinoic acid-inducible gene
RNA	Ribonucleic acid
rpl13a	Ribosomal protein L13a

RT-qPCR	Quantitative reverse transcription polymerase chain reaction
SALT	Skin-associated lymphoid tissue
SAV	Salmonid alphavirus
serpinh1	Serpin Family H1
SRS	Salmonid Rickettsial Septicemia
stat1	Signal transducer and activator of transcription 1
TAP	Transporter of antigen processing
tapbp	Tapasin
Taq	*Thermus aquaticus*
TLR	Toll-like receptors
TNF	Tumor necrosis factor
TSA	Tryptic soy agar
TSB	Trypticase Soy Broth
UK	the United Kingdom
USD	United States Dollar
VHSV	Viral haemorrhagic septicaemia virus
WOAH	World organization of animal health
YIAL	Yellow Island Aquaculture Ltd.

Chapter 1: General Introduction

Salmon aquaculture was initially industrialized in Norway in the 1980s. After over 40 years of significant development, today it has risen to become one of the most profitable and fastest growing industries which is dominated by Norway, Chile, the United Kingdom (UK), and Canada (Asche & Bjørndal, 2011; Barton et al., 2023; Salazar & Dresdner, 2021). These four countries supplied 71.6% of global salmon production in 2021 (3.02 million tonnes) (FAO, 2023a). Salmon aquaculture has been well-integrated into the global food chain and salmonids are amongst the most successful commercialized species in the aquaculture industry. In 2013, salmon became the largest internationally traded fish product in value terms; in 2020, salmon accounted for 18.4% (USD 27.6 billion) of the total value of exported aquatic products globally, growing from 5.1% in 1976 (FAO, 2022).

Due to factors like overexploitation, loss of habitat and climate change, global capture fish production plateaued around 80 million tonnes annually in the late 1980s. Additionally, because of the various regulations designed to avoid overexploitation, capture fisheries can no longer meet the growing demand for fish meat as a source of high-quality protein and long-chain omega-3 polyunsaturated fatty acids, as well as various micronutrients (Costello & Ovando, 2019; Weichselbaum et al., 2013). In 1980, human fish consumption *per capita* was 11.5kg; in 2020, it increased to 20.2 kg, slightly declining from the record high of 20.5 kg in 2019. By 2030, the estimated *per capita* consumption will increase to 21.4 kg, while the global human population reached eight billion in November 2022 (Adam, 2022; FAO, 2020, 2022). In 2014, for the first time in history aquaculture replaced capture fisheries as the

primary source of fish supply for human consumption (FAO, 2016). The limited production of capture fisheries, alongside expanded global trade, competitive pricing, and rising incomes, have fueled the intensive and rapid growth of aquaculture (Bush et al., 2019; Little et al., 2016). From a trading point of view, in 2020 aquaculture provided 49.2% (87.5 million tonnes) of fish product by live weight (**Figure 1.1**), which generated 65.3% (USD 265 billion) of total first sale value (FAO, 2022).

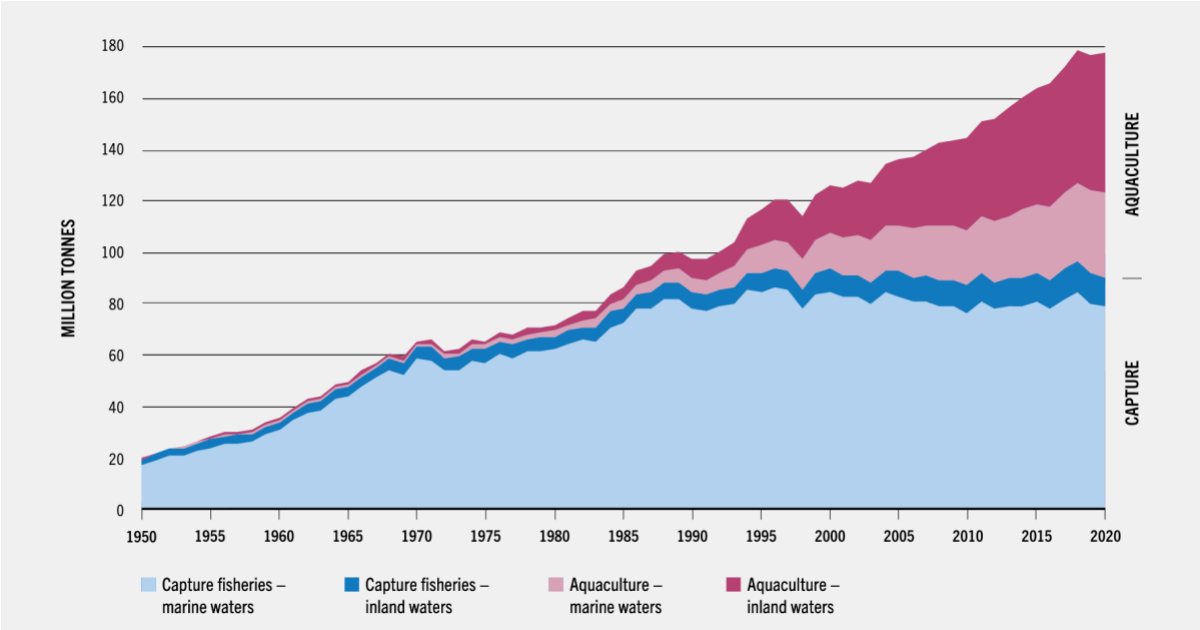

Figure 1.1 The comparison between world total production (live weight equivalent) by capture fisheries and aquaculture sectors, 1950 to 2020. The data excluded aquatic mammals, crocodiles, alligators, caimans and algae (FAO, 2022).

Salmon, or salmonid, is a blanket term referring to a variety of organisms in the family of Salmonidae, which include several versatile and high-value species that are suitable for intensive aquaculture (Gjedrem & Gunnes, 1978; Landry et al., 2023). Compared to other widely traded fish species, salmonid production is more dependent on aquaculture. From

2009 to 2021, aquaculture was responsible for increasing salmon production from 58.9% (1.45 million tonnes) to 80% (2.82 million tonnes) worldwide (Shahbandeh, 2023). It is estimated by the Food and Agriculture Organization (FAO) that in 2024, the global salmon aquaculture industry will grow by 4%, recovering from the disruptions of aquaculture operations during COVID-19 (FAO, 2023b).

From a global point of view, the major farmed salmon species are Atlantic salmon (*Salmo salar*), rainbow trout (*Oncorhynchus mykiss*), and coho salmon (*Oncorhynchus kisutch*). In 2021, they accounted for 68.9%, 22.6%, and 5.5% of the total world salmon production by weight respectively (FAO, 2023a). Norway is the world's largest producer of Atlantic salmon and rainbow trout. In 2022, Norwegian aquaculture provided 1.55 million tonnes of Atlantic salmon and 85,000 tonnes Rainbow trout (Directory of Fisheries, 2023). Representing only approximately 1% of the global total salmon production, Chinook Salmon (*Oncorhynchus tshawytscha*) is farmed because it frequently gains the highest price on the global market due to the excellent taste and texture (NIWA, 2020).

Farmed salmon are often exposed to various types of stressors, including infectious diseases, handling, sub-optimal water conditions, and crowding, that compromise fish welfare (Lai et al., 2021). For global salmon aquaculture, pathogens, parasites, and pests are considered the main barrier to industry expansion, as they cause consistent annual loss and pose chronic risks as well as new threats to salmon health management (Groner et al., 2016; Torrissen et al., 2013). Although numerus prophylactic and therapeutic approaches have been proposed to prevent and treat waterborne pathogens, the current disease management

strategies in salmon aquaculture do not effectively prevent outbreaks, leading to the increased risks of aquatic diseases with economic, social, and ecological ramifications (Bateman et al., 2021; Mordecai et al., 2021; Teffer et al., 2020). A deeper understanding of how cultured salmon species respond to diseases and the development of more efficient disease monitoring methods would lead to the development of immunomodulatory products, vaccines, and therapeutic treatments, which will be invaluable for the sustainable development of this industry.

1.1 Disease control in salmon aquaculture

With the intensive and extensive development of aquaculture, infectious diseases are becoming increasingly more difficult to control, especially with the emergence of novel and diverse pathogenic agents and wider geographical ranges (Mishra et al., 2023; Stentiford et al., 2012). Intensified aquaculture can facilitate disease outbreaks in both the farmed and wild populations, yet unfortunately the current disease control strategies, including vaccination, probiotics, and prebiotics, may not be effective in preventing outbreak events (Fregeneda-Grandes et al., 2023; Wang et al., 2023; Figueroa et al., 2022; Maisey et al., 2017). Although salmon vaccination programs for furunculosis and cold-water vibriosis have been successful and largely reduced the use of antibiotics, vaccines are designed for specific, known infectious agents and there are still many deadly pathogens that do not have a commercially available vaccine available yet, for example, piscine myocarditis virus (PMCV) (Sommerset et al., 2021). Nevertheless, as a prophylactic method, vaccination cannot help in monitoring a potential outbreak when there is a novel infectious agent, and it is also common that

vaccination does not generate adequate, long-lasting protection for the farmed salmon population for reasons that remain elusive (Figueroa et al., 2022). This is particularly problematic for large salmon producers because their sustainable development of salmon aquaculture is constrained by frequent disease outbreaks which causes large economic losses.

In Norway, a large-scale infectious salmon anaemia virus (ISAV) epidemic was recorded in the 1990s; despite of the availability of multiple commercialized ISAV vaccines, there were still 23 outbreaks in 2020 and 25 outbreaks in 2021 recorded (Dean et al., 2022; Sommerset et al., 2021). In Chile, Salmonid Rickettsial Septicemia (SRS) has been the most damaging and persistent disease to salmon aquaculture since its emergence in the 1980s even though various commercialized vaccines against its causative agent *Piscirickettsia salmonis* were available (Valenzuela-Aviles et al., 2022). To date, SRS is still the leading cause of death of the three major farmed salmon species in Chile, namely Atlantic salmon, Coho salmon, and rainbow trout, causing 9% of the total mortalities and an estimated annual loss of over USD 700 million (Dettleff et al., 2015; Jakob et al., 2014; Maisey et al., 2017; Miranda et al., 2018; Valenzuela-Aviles et al., 2022). Starting in 2019, Chile started to import smolts that are genetically resistant to Infectious Pancreatic Necrosis Virus (IPNV), but large-scale INPV outbreaks have still been reported and new INPV variants have been identified as the cause (Godoy et al., 2022). Moreover, the existence of crosstalk between several freshwater and marine pathogenic bacteria in British Columbia, Canada, was recently reported (Bateman et al., 2021). The piscine orthoreovirus-1 (PRV-1), originally a disease of the Atlantic Ocean, has become a critical infectious agent in endangered wild Pacific salmon

populations in Canada, and it has also been introduced to farms in Chile (Mordecai et al., 2021).

These disease outbreaks can pose significant threats not only to the farmed animals, but also to their sympatric wild compatriots. To date, there are 12 major fish diseases recognized by the world organization of animal health (WOAH). Several high-profile cases from this list, namely infectious salmon anemia virus (ISAV), viral haemorrhagic septicaemia virus (VHSV), salmonid alphavirus (SAV), and infectious hematopoietic necrosis virus (IHNV), have significantly impacted the salmon industry as well as other local species, causing an ecological burden (Dean et al., 2022; WOAH, 2023). It has also been reported that global climate change associated effects including increases in water body temperature, drastic temperature fluctuation, acidification and hypoxia, adversely influence fish physiology and increase their susceptibility to infectious diseases (Little et al., 2020; Melo et al., 2022; Perez -Casanova et al., 2008). As the result, the development of better health evaluation tools for an informed fish health management strategy will not only benefit the industry, but also wildlife alike by facilitating research into host-disease interactions.

1.2 Salmon immune system

It is estimated that 476-423 million years ago, Osteichthyes (bony fish) divided into two categories, namely Sarcopterygii (lobe-finned fish) and Actinopterygii (ray-finned fish) (Broughton et al., 2013). Sarcopterygii gave rise to the tetrapods that include the mammals and birds, while Actinopterygii evolved into the lineage of teleost fishes that includes the majority of the modern fish species including salmon (Sallan, 2014; Taylor & Leite, 2022).

Despite of the early separation, the teleost fishes and the tetrapods share a highly similar immune system, including some lymphoid organs and populations of immune cells, and immune responses in both groups can also be categorized into innate and adaptive branches. Some differences exist for teleost immune system, namely the lack of germinal centers, bone marrow, lymph nodes, and the development of a unique mucosal antibody IgT (Flajnik, 2018; Neely & Flajnik, 2016; Sepulcre et al., 2009; Zhang et al., 2011). The following information explains the salmon immune defenses that are related to the experiment in this thesis.

1.2.1 The salmon immune cells and organs

Interestingly, mammalian and teleostean immune cell types are very similar, including lymphocytes, monocytes, granulocytes, macrophages, mast cells, and dendritic cells (Espelid et al., 1996; Flajnik, 2018; Reite, 1997; Solem et al., 1995). B cells in fish do not mature and differentiate in germinal centres, and it has been suggested that they may proliferate in the melano-macrophage centres in head kidney and spleen instead (Muthupandian et al., 2021; Waly et al., 2022).

Following the order from cranial to caudal, fish lymphoid organs and tissues are nasal-associated lymphoid tissue (NALT), gill-associated lymphoid tissue (GIALT), interbranchial lymphoid tissue (ILT), thymus, head kidney, spleen, bursa, skin-associated lymphoid tissue (SALT), and gut-associated lymphoid tissue (GALT). Thymus and head kidney are regarded as the primary lymphoid organs as they are the sites of lymphocyte generation, and spleen and mucosal-associated lymphoid tissue (MALT) are regarded as the

secondary lymphoid organs as initiation of immune responses occurs there (Reviewed by Salinas, 2015). Like higher vertebrates, the kidney of fishes is also an important endocrine organ, which is innervated by sympathetic nervous systems and is involved in stress equilibrium (Madaro et al., 2023). Due to direct contact with pathogens and stimuli from the environment, MALT has been referred to the first line of immune defense in fish, and there have been many studies investigating MALT immune function, including its potential in vaccination delivery and as a diagnostic matrix (Echeverría-Bugueño et al., 2023; Fast et al., 2002; Franco-Martinez et al., 2022; Hoare et al., 2022; Madaro et al., 2023; Tartor et al., 2020).

1.2.2 Salmon immune response

There are many biochemical changes that happen during the early stage of infection and inflammation, caused by the activation by the fish innate immune- and stress response-systems. As the first response made to pathogen invasion, most of the features in fish innate immunity are highly conserved in comparison to higher vertebrates. Salmon innate immunity has been shown to have a greater role because of the limitations in their adaptive immune system, like the slow initiation in B cells and antibody production, and a lack of long-term immune memory (Kaattari, 2002; Ye et al., 2011).

Fish mucus matrix is rich in nutrients and harbors complex and dynamic microbiota. Under evolutionary selective forces, teleost have developed excellent innate and adaptive immune mechanisms to maintain microbiome homeostasis and to discriminate between pathogenic and commensal microorganisms in the MALTs (Pérez et al., 2010). Similar to

mammals, teleost mucus also contains innate humoral components like lysozyme, complements, antimicrobial peptides (AMP), lectins, and natural antibodies, and studies have demonstrated their ability to inhibit mucosal bacteria (Chen et al., 2023; Fast et al., 2002; Narvaez et al., 2010; Palaksha et al., 2008).

In teleost, opportunistic and pathogenic microorganisms are recognized by phagocytotic monocytes/macrophages, and neutrophiles. These antigen presenting cells express a variety of germline-coded pattern recognition receptors (PRR) that can recognize and bind to different damage-associated molecular patterns (DAMPs) and pathogen-associated molecular patterns (PAMP) like polysaccharides and lipopolysaccharide (LPS) (reviewed by Boltaña et al., 2011; Ingerslev et al., 2010). In humans, the activated macrophages secrete pro-inflammatory cytokines including interleukins and tumor necrosis factor (TNF, IL-1, IL-6, IL-8, and IL-12) and initiate phagocytosis for pathogen digestion and antigen presentation (reviewed by Duque and Descoteaux, 2014). For salmonids, rainbow trout and Atlantic salmon macrophages have been studied extensively in its cytokine production properties (TNF, IL-1B, IL-6, IL-8) (Castro et al., 2011b; Gjøen et al., 2004). Typically, the pro-inflammatory cytokines IL-1β, Il-8, and TNFα are the first effectors to be secreted in salmon (Fast et al., 2007; Seierstad et al., 2009).

In teleost, neutrophiles and monocytes/macrophages are phagocytes while B cells have been described as phagocytic as well (reviewed by Rieger & Barreda, 2011). The monocytes/macrophages destruct the internalized microorganisms by the various hydrolytic enzymes and low pH environment in phagolysosomes and respiratory burst. On

phagolysosomes membranes, nicotinamide adenine dinucleotide phosphate (NADPH) oxidase produces reactive oxygen species (ROS) like superoxide anion ($O2^{-}$) and hydrogen peroxide (H_2O_2). These ROS can produce bactericidal hypochlorous acid (HClO) after reacting with free chlorine ions (reviewed by Zhu & Su, 2022). The digested exogenous antigens are then presented to the $CD4^+$ Th cells using the surface major histocompability complex class II (MHC-II) (Castro et al., 2011a). At the same time, the activated macrophages and $CD4^+$ Th cells start to release cytokines and chemokines to recruit and activate more immune cells of both innate and adaptive response (granulocytes, monocytes, macrophages, natural killer cells, T cells and B cells). These immune cells are summoned to the site of infection and will perform a spectrum of antimicrobial activities until the elimination of infiltrating pathogens. Apart from phagocytosis, two types of natural killer (NK) cell homologues have been described in salmon: non-specific cytotoxic cells and NK-like cells (Øvergård et al., 2023; Ribera et al., 2020). As for the endogenous antigen derived from intracellular pathogens, they are presented by fish MHC-I, and they can be recognized by $CD8^+$ cytotoxic T lymphocyte (CTL). The activated CTLs then initiate pathogen-specific cell-mediated cytotoxicity (CMC) to control infection, including inducing apoptosis and cell rupture in the infected cell (Castro et al., 2011a). Previous studies strongly suggest that teleost CTLs share similar killing pathways with mammalians, including the $Ca2^+$-dependent perforin/granzyme pathway and FasL/Fas pathway (reviewed by Nakanishi et al., 2011).

Both MHC-I and MHC-II antigen presentation pathways can be induced by immunostimulants or pathogens in salmon (Hansen & La Patra, 2002; Jørgensen, Hetland, et

al., 2007; Kania et al., 2010). Their antigen presentation accessory molecules have also been identified in salmonids. Tapasin, also known as the "TAP binding protein", is a chaperone glycoprotein that is essential in MHC-I antigen loading because it stabilizes the multimeric peptide-loading complex in the endoplasmic reticulum and bridges it with the transporter of antigen processing (TAP) (Bangia et al., 1999; Rizvi & Raghavan, 2010). In salmon species, tapasin was observed to be up-regulated with MHC-I receptor genes post pathogen challenge, revealing its possible role in regulating endogenous antigen presentation (Jørgensen et al., 2007; Sever et al., 2014).

Calcium (Ca^{2+}) ions are a universally conserved intracellular messenger, and the Ca^{2+} binding protein, calmodulin, is one of the most conserved proteins in eukaryotes for Ca^{2+} signaling (Chin & Means, 2000; Luan & Wang, 2021). The Ca^{2+}/calmodulin complex regulates lymphocytes through a variety of kinases, mainly in the Ca^{2+}/calmodulin-dependent kinase (CaMK) family. The induced calmodulin kinase cascade controls signaling of Toll-like receptors (TLR), T cell activation and differentiation, and cytokine production (Illario et al., 2008; Ivanov et al., 2006; Kim & Leonard, 2007; Yang et al., 2008). Thus, calmodulin has a critical rule in immune responses and inflammation. Specifically in salmon, calmodulin was inducible by infectious hematopoietic necrosis virus (IHNV), LPS, and salmon louse (*Lepeophtheirus salmonis*) (MacKenzie et al., 2008; Skugor et al., 2008).

Peroxiredoxins (Prdx) are a family of antioxidant enzymes that may act as modulators of inflammation, iron metabolism, cell death, and tissue repair after damage, and their transcription is ubiquitously distributed in all fish tissues (reviewed by Valero et al., 2015).

Orthologues of *prdx* gene have been found in a wide range of teleost fish including rainbow trout and Atlantic salmon (Loo et al., 2012; Mourich et al., 1995). In salmonids, the function of Prdx has been linked to immune and stress responses, as it can be induced by a range of stimuli like LPS, bacterial/viral/parasitic pathogens, although the direct effect of Prdx on salmon immune system needs further study (Beemelmanns et al., 2021; Valero et al., 2015).

At the early stage of infection, a cascade of pro-inflammatory cytokines is first released to initiate inducible innate immune responses, by recruiting cells to the site of pathogen entry and activating more lymphocytes. The elevated expression of pro-inflammatory cytokines is often associated with acute pathogenesis (Kurpe et al., 2022). Three classical pro-inflammatory cytokines commonly studied in salmon immunology research, IL-1β, IL-8, and TNFα, are the focus of this thesis.

IL-1β is a potent inflammation inducer and in salmon it can be released by both immune cells (macrophages) and non-immune cells (epithelial cells) (Hong et al., 2001; Schmitt et al., 2015). IL-1β receptors are expressed on a range of immune cells and binding with IL-1β activates the NF-κB pathway, which will lead to the elevated transcription of a range of pro-inflammatory cytokines and chemokines (IL-1β, IL-6, IL-8, TNFα) and anti-apoptotic factors (caspase) (Liu et al., 2017; Weber et al., 2010). IL-8, also known as CXCL8, can also be released by salmon macrophages and epithelial cells upon infection (Komatsu et al., 2009; Laing et al., 2002). In mammals it is known to recruit neutrophils, basophils and eosinophils to the site of infection, while in trout it was shown to attract

macrophages and neutrophils (Grimholt et al., 2015; Montero et al., 2008; Omaima Harun et al., 2008).

Salmon TNFα is known as a regulator of leukocytes and systematic inflammatory responses (Hong et al., 2013). In mammals, TNFα has been regarded as a key mediator of both acute and chronic inflammation, by triggering the release of other pro-inflammatory cytokines and the activation of adaptive immune cells (reviewd by Bemelmans et al., 2017). TNFα expression in trout macrophage and epithelial cells was confirmed using the stimulation of recombinant IL-1β and a bacterial pathogen *Aeromonas salmonicida* (Komatsu et al., 2009; Laing et al., 2001). It was reported that in rainbow trout, TNFα can induce the expression of a range of pro-inflammatory cytokines including IL-1β, IL-6, IL-8, IL-17 and itself, as well as antimicrobial peptides (Hong et al., 2013).

Interferons (IFNs) are important antiviral cytokines in vertebrates. To date, three IFN families have been reported in mammals and two of them (type I and II IFN family) have been identified in teleost fish. In the past 20 years, the IFN receptors and signaling pathways have been extensively researched, and both fish IFN families have been reported to be induced in antiviral defense (reviewed by Zou & Secombes, 2011). In Atlantic salmon, six members of the type I IFN family have been identified and all six have been confirmed to be inducible by viral pathogens. Upon virus recognition by PRRs, for example retinoic acid-inducible gene I (RIG-I), anti-melanoma differentiation-associated gene 5 (MDA5), or toll-like receptor 3 (TLR3), the cytosolic IRFs and NF-κB pathways activated, which leads to the induction of type I IFN gene transcription (reviewed by Robertsen, 2018). Compared to the

type I IFNs where there are several forms, there are only two salmon type II IFN types, IFN-γ and IFN-γrel (Summathed et al., 2013). Salmon IFN-γ has a wide range of functions in regulating innate and adaptive immune responses, including antiviral responses, induction of MHC-II expression, and enhancement of respiratory burst activity in macrophages (Morales-Lange et al., 2021; Sun et al., 2011; Wiegertjes et al., 2016; Zou et al., 2005). It had also been suggested that both type I IFNs and IFN-γ use the same JAK/STAT signal transduction pathway as mammals (Skjesol et al., 2010).

1.3 Stress responses and metabolic reallocation during infection

During pathogen invasion and the development of infection, stress responses can also be initiated as a result of inflammation and tissue damage. Stress responses are key to maintaining homeostasis and they are some of the most conserved mechanisms in vertebrates (Balasch & Tort, 2019). Stress responses in salmon show many similarities to those of the higher vertebrates, from the principal axis to messenger molecules. For example, fish stress responses are controlled by two hormonal systems: 1) hypothalamus–pituitary–interrenal (HPI) axis, where adrenocorticotropic hormone (ACTH) is produced by the pituitary gland and induce cortisol from interrenal cells in the head kidney and 2) brain-sympathetic-chromaffin cell (BSC) axis that triggers the release of catecholamines (Sumpter, 1997; Wendelaar Bonga, 1997). It has been suggested that in salmonids cortisol is the main stress endocrine in the HPI axis (Gorissen & Flik, 2016; Krasnov et al., 2021).

The HPI axis restores homeostasis and adapts fishes to the stressors by reallocating resources to the mobilization of energy substrates. This process may include the activation of

the catabolic pathways to process fatty acids for energy, and the suppression of other high-cost energy and longer-term processes like immune responses, growth, and reproduction (Balasch & Tort, 2019; Mommsen et al., 1999). A recent transcriptomic study using an Atlantic salmon stress model examined the metabolic shift and stress responses under hypoxia and high temperature conditions. A range of highly interconnected metabolic processes was suppressed, including the carbohydrate metabolic process, fatty acid catabolic process, and lipid metabolic process (Beemelmanns et al., 2021). Meanwhile, to facilitate pathogen survival and replication, there is fierce competition between host and infectious agents. Alterations in host metabolome are a consequence of host-pathogen interactions, which include, but not limited to, the metabolism of glucose, fatty acids, and amino acids (Olive & Sassetti, 2016; van der Meer-Janssen et al., 2010).

1.4 Thesis objectives

The goal of this thesis was to validate an open array chip that was designed for a range of salmon species using Chinook salmon as a model. More specifically, the outcome of this research will help to understand responses generated to *Vibrio anguillarum* during an infection trial in a production facility. The two specific objectives of this MSc thesis were to:

1. Determine whether the novel nanofluidic OpenArray™ chip is a reliable tool to evaluate fish health status using *Vibrio anguillarum* as a disease model.
2. Determine whether mucus and culture water are a good source for mRNA transcripts that can indicate the physiological status of Chinook salmon, as a non-invasive sampling strategy.

To accomplish these objectives, two independent hypotheses were generated:

1. The OpenArray™ chip, as a novel tool to quantify transcript levels, would generate RT-qPCR results that strongly correlate with SYBR RT-qPCR results.
2. Water and mucus can be used for mRNA extraction and reveal the physiological changes during the infection as reliably as other lymphoid organs like spleen and head kidney.

Chapter 2. Validation of the OpenArray™ TaqMan® Real-Time PCR chip for diagnostic biomarkers in *Oncorhynchus tshawytscha*

2.1 Introduction

Vibrio anguillarum is a gram negative, extracellular bacterial pathogen that causes "vibriosis", a deadly haemorrhagic septicaemic disease of more than 50 fish species, including several economically important salmonids, such as Atlantic salmon (*Salmo salar*), rainbow trout (*Oncorhynchus mykiss*), and Chinook salmon (*Oncorhynchus tshawytscha*) (Chukwu-Osazuwa et al., 2022; Kurpe et al., 2022; Semple et al., 2022). This pathogen was reported as early as 1893 and it continues to cause high morbidity and mortality in aquaculture today, although various vaccines have been developed to counter this pathogen (Canestrini, 1893; reviewed by Ji et al., 2020). Thus, vibriosis is a highly relevant disease model for the improvement of salmon aquaculture. Because the *Vibrio anguillarum* is an opportunistic pathogen, outbreaks of vibriosis can be facilitated by suboptimal and immunosuppressive production conditions (Yu et al., 2021). Thus, a deeper understanding of the relationship between salmon immune, stress responses and the features of susceptibility to vibriosis would greatly assist in the control of this disease.

Sustainable aquaculture management and responsible decision-making require standardized, reliable fish disease diagnostics and surveillance systems (Semeniuk et al., 2022). Importantly, factors like salmon genetic background, age, diet, season, polyploidy, amongst many other factors, may result in deviations between different studies (Krasnov et al., 2021). To achieve the standardized transcriptional profiling of immune, metabolic, and

stress responses for different fish targets, researchers from the Genomic Network for Fish Identification, Stress and Health (GEN-FISH; https://gen-fish.ca) developed a suit of novel nanofluidic quantitative real-time quantitative PCR (qPCR) assays for use with the OpenArray™ chip platform. This OpenArray™ chip targets a range of fish species and it can be utilized as a standardized tool for large-scale health evaluation. The present study describes immune and stress responses from Chinook salmon that were infected with live *Vibrio anguillarum* and tested for gene transcription profile response using this nanofluidic TaqMan® assay on the OpenArray™ chip.

Current diagnostic methods for fish diseases, with a focus on clinical symptoms and molecular-level biomarker quantification, still involve invasive organ sampling and fish euthanasia; as a result, repeated sampling and longitudinal studies are difficult to perform. This approach also provides little information on the temporal development of immune responses at the individual level (Bateman et al., 2021; MacAulay et al., 2022; Mordecai et al., 2021). Meanwhile, infectious agents and inflammatory responses may be present long before the manifestation of visible symptoms such as lesions, and thus disease outbreaks may not be controlled in a timely manner. These methods are often costly, time-consuming, and not conducive to repeated measurements over the lifespan of a single fish, require killing several individuals per test. To address these issues, utilization of mucus and filtered water samples is gaining attention as an alternative source of biomarkers. Fish mucus is associated with mucosal-associated lymphoid tissue (MALT) that contains abundant immune cells and biomarkers, and water testing is theoretically based on quantifying biomarkers from the

constant fish mucus turnover filtered from culture water. Mucus has been widely explored as a diagnostic matrix, but the quantification targets are usually at the protein level (Birlanga et al., 2022; Djordjevic, Byron Morales-Lange, et al., 2021; Djordjevic, Morales-Lange, et al., 2021; Fast et al., 2002; Fernández-Alacid et al., 2018; Franco-Martinez et al., 2022; Santoso et al., 2020). On the other hand, fish culture water has been used for studies using environmental DNA (Bastos Gomes et al., 2017; Mächler et al., 2016), environmental RNA (Miyata et al., 2021), and microRNAs (Ikert et al., 2021).

This study describes a range of transcriptomic responses (immune, stress, apoptosis, growth and metabolism) measured using the novel OpenArray™ platform, after Chinook salmon juveniles were challenged with live *V. anguillarum*. Fish mucus and culture water, as well as spleen, head kidney and gill, were collected to assess if they can be used to quantify fish-sourced transcripts. The expression of six selected immune genes (*il-1β*, *il-8*, *calm*, *mhc-i*, *mhc-ii*, and *tapbp*) were validated with SYBR RT-qPCR. The significant positive correlations observed here indicate the reliability of the novel OpenArray™ platform for nanofluidic TaqMan® assays in Chinook salmon. Possible applications of this novel OpenArray™ chip might be in the fishery and aquaculture sectors that are directly involved with fish health assessment, management, and conservation. The transcriptional profiling of the farmed salmon immune responses may also assist in the development of species-specific vaccination plans and disease control strategies that may promote animal welfare and economic benefits.

2.2 Materials and Methods

2.2.1. Experimental Animals

Fish used in this experiment were provided by Yellow Island Aquaculture Ltd. (YIAL), on Quadra Island, British Columbia, Canada. All experimental procedures were approved and conducted per the University of Waterloo Animal Care Committee and the Canadian Council of Animal Care guidelines (Animal Care protocol #43212).

Four hundred diploid Chinook salmon (*Oncorhynchus tshawytscha*) juveniles were randomly selected and were housed with a 15:9 h (light: dark) photoperiod and fed twice a day with commercial dry pellets (EWOS Harmony 2 mm) to satiety. The Chinook salmon were organically reared in the YIAL fresh water tanks, and there was evidence of bacterial kidney disease symptoms prior to this experiment. Water was maintained at 11.6 ± 0.1°C, 87.7 ± 2.4 % dissolved oxygen, and water flow was maintained at 1000 mL/min. Fish were randomly distributed into four 250 L tanks at a density of 100 fish per tank (22.12 kg/m^3). One blank tank with no fish was designed as the control for water filter samples. To eliminate contamination, all of the five tanks were sprayed and scrubbed using 10% bleach prior to the trial. Experimental fish had a mean fork length of 20.3 ± 6.6 cm and a mass of 62.4 ± 37.2 g and were acclimated for 14 days before live pathogen exposure. To ensure the infectious agent used in this experiment were eliminated, the water outflow from the pathogen challenged tanks were treated with a UV sterilizer.

2.2.2 Culture conditions of *Vibrio anguillarum*

Vibrio anguillarum serotype O1 (J382) (Machimbirike et al., 2023) was isolated from a diseased winter Steelhead Trout in Little Campbell River (BC, Canada), and the bacteria stock was provided by Simon Jones of Pacific Biological Station, Fisheries and Oceans Canada. Tryptic soy agar (TSA) supplemented with 2% NaCl (TSA 2% NaCl; Multicell Wisent, Quebec, Canada) was used to subculture the frozen stocks of *V. anguillarum* for 48 h at room temperature, and a single colony from the agar plate was used for inoculating 2.5 mL Trypticase Soy Broth (TSB) supplemented with 2% NaCl (TSB 2% NaCl; Multicell Wisent, Quebec, Canada). The inoculated broth was incubated on a shaker at 20°C for 24h at 200rpm with aeration, then 150 μL of this overnight culture was used to inoculate 150 mL of TSB 2% NaCl media, which was incubated on a shaker at 20°C for 24h at 200rpm with aeration again. After incubation, the culture was centrifuged for 10 min, at 6,000 rpm, room temperature, to obtain the bacterial pellet. The pellet was then washed with phosphate buffered saline (PBS 1X, w/o Calcium & Magnesium; Multicell Wisent, Quebec, Canada) and centrifuged for 10 min, at 6,000 rpm, room temperature for three times. The pellet was resuspended in 25 mL of PBS to a concentration of 3.1×10^9 CFU mL^{-1}, which was confirmed by serial dilution and a 2-day TSA 2% NaCl plate culturing. The resuspended bacteria were diluted with sterile PBS to 6.2×10^4 CFU mL^{-1} for intraperitoneal injection. The final injection volume for each fish is 100 μL, and the application dose for each fish is 6.2×10^3 CFU.

2.2.3 Live *V. anguillarum* infection and sample collection

After the two-week acclimation Chinook salmon juveniles were randomly distributed into four experimental tanks, with two tank replicates being used for live *V. anguillarum* intraperitoneal pathogen injection (Tank V1 and V2), and the remaining two being used for sham injection with sterile PBS (Tank P1 and P2). On August 3rd, 2022, one day prior to the pathogen challenge (0 h), fish (n=6) from each tank were sampled as the unstimulated control. Water samples (n=3, 250 mL) were taken from Tank V1, V2, P1, P2, and the blank tank (Tank B). On August 4th, 2022, all fish from Tank V1 and V2 received intraperitoneal (i.p.) injections with 100 μL of live *V. anguillarum* (6.2×10^4 CFU mL^{-1}) and all fish from Tank P1 and P2 received intraperitoneal (i.p.) injections with 100 μL sterile PBS. At 12, 24, 72, and 96 hours (h) post treatment, fish (n=6) and water sample (n=3) from each tank were sampled as illustrated below. Fish survival rate was recorded for 14 days.

Water samples were taken before the fish were sampled from tanks. The fresh water used on YIAL locations was directly sourced from a nearby well on the Quadra island, and the water was not contaminated with external fish mRNA. The bottles used for fish culture water sampling were treated with 10% bleach overnight prior to each sampling time point. From each tank (V1, V2, P1, P2, B), water was sampled using a bleached 1 L glass bottle and was immediately stored in at 4°C. One hundred and fifty mL of each water sample was applied to a 0.45 μm filter from the Water RNA/DNA Purification Kit (Norgen Biotek Corp., Canada). The Filters were connected to a vacuuming apparatus to draw the water sample through filter. Subsequently, the filter was recovered using sterile forceps and stored in the

"Bead Tube" with 500 µL "Lysis Buffer E", as per manufacturer's instructions for the Water RNA/DNA Purification Kit (Cat. 26450; Norgen Biotek Corp., Canada). These filter samples were moved to liquid N_2 tank immediately.

Fish tissue samples were collected after the water sampling. Following sedation with clove oil, fish weights and lengths were measured, and spleen, head kidney, and gill were sampled from each individual then stored in RNAlater in 1.5 mL Eppendorf Tubes®, which were placed in liquid nitrogen tank immediately. Following sedation, fish were placed on individual plastic sheets to avoid cross contamination, and the mucus was gently scraped with a sterile glass slide, avoiding areas of possible blood and fecal contamination. The mucus samples were stored in 5 mL snap cap tubes (GeneBio Systems, Inc., Canada) directly in liquid nitrogen tank without RNAlater to avoid dilution (Fernández-Alacid et al., 2018). After shipping all samples were stored at -80°C at the University of Waterloo.

2.2.4 Sample processing

2.2.4.1 RNA extraction and DNase treatment

For water filter samples, total RNA extraction and DNAse treatment were conducted as described in the manufacturer's protocol. All the reagents were provided in the Water RNA/DNA Purification Kit (Norgen Biotek Corp., Canada), except for a compatible RNase-free DNase I Kit (Norgen Biotek Corp., Canada) used for on-column genomic DNA digestion. The DNase-treated water filter samples were quantified with Synergy H1 plate reader (Biotek Instruments, Inc., USA) and were stored at -80°C until further use.

For spleen, head kidney, and gill samples, RNA was extracted from 20-40 mg of tissue using 1 mL of TRIzol™ (Invitrogen™, USA) as described in the manufacturer's protocol. The total RNA extracted was quantified with a Synergy H1 hybrid reader (Biotek Instruments, Inc., USA). To remove the genomic DNA from the total RNA extracted, samples were treated with DNase I. Five µg RNA was added per DNase I (Invitrogen™, USA) treatment reaction as described in the manufacturer's protocol.

Considering the RNA concentration was lower in mucus compared to other tissue types, the RNeasy® Mini Kit (Qiagen, Germany) was used for mucus RNA extraction to ensure better recovery. For each sample, all 150 µL was thawed, well-mixed mucus was first pushed through a syringe with a 23G needle 20 times to break the cells. A RNase-Free DNase Set (Qiagen, Germany) was used for on-column DNA digestion as described in the manufacturer's protocol. The DNase-treated tissue samples were quantified with a Synergy H1 plate reader (Biotek Instruments, Inc., USA) and were stored at -80°C until further use.

2.2.4.2 cDNA synthesis

Complementary DNA (cDNA) was synthesized from 250 ng of DNase-treated RNA using the qScript cDNA Supermix (Quanta Biosciences, USA) as described in the manufacturer's protocol. A pool of DNase-treated RNA samples was prepared for each tissue type to make the controls for the downstream SYBR green RT-qPCR reactions. For the positive control, 250 ng of the pooled RNA sample was included in the cDNA synthesis reaction. For the non-template control, 250 ng of the pooled RNA sample was included in the cDNA synthesis reaction without qScript to create a reverse transcriptase-free reaction system. The cDNA

reaction system was incubated at 25°C for 5 min, at 42°C for 30 min, and at 85°C for 5 min. The cDNA samples were diluted 1:10 and stored at -20°C until further use.

2.2.5 Nanofluidic TaqMan® assays in the OpenArray™ platform

2.2.5.1 Validation of TaqMan® RT-qPCR primers and probes for Chinook salmon

The OpenArray™ TaqMan® RT-qPCR system (gene expression platform, Thermo Fisher Scientific, USA) allows 28 target genes from 48 samples to be tested on one chip, in technical duplicates. Thus, there are a range of target genes that were included in this assay, from immune response-related genes like pro-inflammatory cytokines, to stress-related genes like heat shock proteins (full list of genes in **Table 2.1**). The method for primer design was developed by Dr. Kenneth Jefferies's lab from the University of Manitoba. For this thesis, the primers and probes used on the chips were designed by Dr. Shahinur Islam from the University of Windsor.

Specifically, for each target gene, multiple alignment was performed using the coding sequences from a range of phylogenetically related salmon species in the Salmoniformes order. Subsequently, the conserved regions in the coding sequences (CDS) across salmon species were selected for primer and probe design for TaqMan® RT-qPCR. The specificity of each primer set may fluctuate between species, majorly affected by the availability of the CDS sequence of a certain target gene in a specific species. For the genes investigated in this study, Atlantic salmon (*Salmo salar*) from genus *Salmo* and rainbow trout (*Oncorhynchus mykiss*) from genus *Oncorhynchus* are the two species that had the highest CDS sequence

availability. Phylogenetically, Chinook salmon and rainbow trout are more closely related because they are both from the genus *Oncorhynchus* (Crawford & Muir, 2008), although all three of these species are within the family of Salmoninae (Stearley & Smith, 1993). Thus, a high specificity against Chinook salmon samples was expected with the primers and probes on this chip.

For species-specific primers, the efficiency is considered acceptable to use when the primer efficiency is within the range of 90-110%, which means that per each cycle of amplification, the primer and probe set can amplify 90-110% of the total number of the targeted DNA sequence (Taylor et al., 2010). The large majority (25) of the primers tested on chip had a primer efficiency within this range, indicating the robustness of cross-species detection using this OpenArray™ Taqman® RT-qPCR chip. Two genes, *ifn-1* and *cirbp*, had a slightly higher efficiency value at 111.15 and 111.45 (**Table 2.1**). These primers are considered acceptable for next-step validations, although the acceptable primer efficiency range on chip should be determined based on more chip analysis data involving more salmon species, or it should be case-specific.

The primer efficiency targeting Chinook salmon *tnfα* was not calculated due to poor data quality. Because there are no available Chinook salmon *tnfα* CDS sequence identified, six related species were included in the CDS alignment for conserved region analysis and primer design (coho salmon (*Oncorhynchus kisutch*), rainbow trout (*Oncorhynchus mykiss*), Atlantic salmon (*Salmo salar*), Arctic charr (*Salvelinus alpinus*), brook trout (*Salvelinus fontinalis*), and Dolly Varden trout (*Salvelinus malma*). As a result, there is a lack of primer and probe

specificity targeting *tnfα* in Chinook salmon and it is advisable to modify the primers and probes using the conserved regions within the genus *Oncorhynchus* for future OpenArray™ TaqMan® RT-qPCR analysis, although this may affect the primer specificity to other salmon species.

2.2.5.2 TaqMan® RT-qPCR reactions using Nanofluid OpenArray™ gene chip

The design of the novel OpenArray™ TaqMan® RT-qPCR system was kindly assisted by Jonathon LeBlanc and Shahinur Islam from the Great Lakes Institute for Environmental Research, University of Windsor. Ten chips that could test 480 samples were customized and manufactured by Thermo Fisher Scientific Inc. Because in total there were 555 samples collected during the live pathogen trial, it was not feasible to test all samples. To reduce the sample number, 10 out of the 12 samples were selected for chip analysis in each treatment group.

The cDNA samples were shipped to the University of Windsor for Nanofluidic TaqMan® assays in the OpenArray™ platform. The OpenArray™ TaqMan® RT-qPCR reaction cycles were proprietary to Thermo Fisher Scientific Inc., and the assays were run on the Applied Biosystems™ QuantStudio™ 12K Flex instrument (Thermofisher Scientific Inc., USA) as described by the manufacture's protocol. The raw data and data analysis method were provided by Jonathon LeBlanc and Shahinur Islam from the University of Windsor.

2.2.5.3 Statistical analyses of OpenArray™ TaqMan® RT-qPCR

2.2.5.3.1 Primer efficiency calculation

Two software packages, LinRegPCR (version 2021.2) and JMP (version 17.1) were used to calculate the primer efficiency for the 28 primers across the 10 chips. Firstly, the original data was reorganized in JMP (version 17.1) so that the readings for specific genes could be filtered and fetched. Then a new Excel file was created for each target gene to combine their reading results across chip. For each specific gene, its Excel file was then opened by LinRegPCR (version 2021.2) to calculate its primer efficiency. Lastly, the average primer efficiency for each of the 28 genes across the 10 chips (Table 2.1) were calculated and were used for downstream analysis.

Table 2.1 Primer and probe sequences of 28 genes for OpenArray™ TaqMan® RT-qPCR and their average primer efficiency (PE). All the 28 gene were reported with a primer efficiency value by LinRegPCR (version 2021.2) analysis, except for tumor necrosis factor α (*tnfα*). Interferon I (*ifn-1*) and cold inducible RNA binding protein (*cirbp*) were observed with a primer efficiency that exceeded 90-110%.

Function	Gene name	Primers and probe (5'-3')	PE (%)
Endogenous Control	Ribosomal protein L13a (*rpl13a*)	F: CACTGGAGAGGCTGAAGGTGT R: GTGGGCTTCAGACGGACAAT P: CATGGTCGTACCTGCT	102
	Elongation factor 1 alpha (*ef1α*)	F: GAAGCTTGAGGACAACCCCA R: GAAGCTCTCCACACACATGGG P: CCGCCATCATCGTCAT	109
Immune Function	Calmodulin (*calm*)	F: GAGGAGCAGATTGCCGAGTT R: CATGACAGTGCCCAGCTCTTT P: CGCTCTTTGACAAGGA	106

	Major histocompatibility complex class 1 (*mhc-i*)	F: AGTCCCTCCCTCAGTGTCTCTG R: AGGACACCATGACTCCACTGG P: AGTGACCTGCCACGCG	99
	Major histocompatibility complex class 2 (*mhc-ii*)	F: GACAGTTGAGCCCCATGTCAG R: AGAAGTCATAGGCGCTGCACAT P: CCCCAGTGGCAGACA	103
	Natural killer enhancing factor (*prdx*)	F: GGATCAACACCCCCAGGAA R: GTCCTCCTTCAGCACTCCGTA P: CCCTTGTGGCTGACCT	99
	Interleukin 1β (*il-1β*)	F: ACCTGTCCTGCTCCAAATCG R: TGCTGGCTGATGGACTTCAG P: CCCACCCTGCACCT	95
	Interferon γ (*ifn-γ*)	F: GGAAGGCTCTGTCCGAGTTC R: CTCTTCCTGCGGTTGTCCTT P: CCTCCAAACTGGCC	95
	Tumor necrosis factor α (*tnfα*)	F: AGTACCAGACGCTGCTCAACTC R: TTTTCCTTCACTCGCAGCCT P: TCTGTACGCACCGTGTGT	nr
	Mx protein (*mx*)	F: GGAGGAGATTGAGGACCCCT R: ATCACTGATACCCACCCCCA P: TGAAGCCCAGGATGAA	103
	Signal transducer and activator of transcription 1 (*stat1*)	F: CAGAAAGGCTTCCTGGAGGG R: CTCTGTGGATGTGTGGGCAT P: CGGGCCCTGTCACT	98
	Interferon I (*ifn-1*)	F: TGTGACTGGATCCGACACCA R: TGGGGCATTCTGCTTTGTG P: CCTGCTGGACCAGAT	111
	Interleukin 8 (*il-8*)	F: TGGCCCTCCTGACCATTACT R: GTCTCAATGCAGCGACATCG P: CATGGGGGCTGACC	101

	Tapasin (*tapbp*)	F: ACGGCAAGACTGACCGATTT R: CACTTCAGCTTCCTGCAGGAT P: AGCGGGGCTAGACTT	97
Growth and Metabolism	AMP-Activated Protein Kinase alpha (*ampkα*)	F: AAGTTTGAGTGCACCGAGGAG R: GACATAATGCGGCGGTTGTC P: CGCAACCACCACGAC	97
	Fatty acid synthase (*fasn*)	F: TGTGGGAGGTGTAGTCAAGCC R: TCCCTGGGCCATGTATCTGA P: AGGTGGAGGAGGCC	100
	Cathepsin D (*ctsd*)	F: TTCACAGACATCGCCTGCTT R: GGTACCCAGACAGACTGCCAG P: CCACAAGTATAACGGTGCC	108
	Hormone-sensitive lipase a & b (*ilpea/b*)	F: ACACTGGTCAAGGTGTTGCAGT R: TGCAGTTAGCGGCAATGTAGC P: CTTCTGCACATCATCCA	101
	Adipose triglyceride lipase/lipoprotein lipase (*lpl*)	F: TGACAGCGCTGTACAAGAGGG R: GGAGGTGAGGTAGTGCTGCTG P: TGGACTGGCTGACACGG	101
Stress Response	Glucocorticoid receptor 1 (*gr1*)	F: GACTCTGCTGCAGTGTTCCTG R: CACTGGTCTGCCATGTAGGG P: CCTTCGGCCTGGGC	96
	Glucocorticoid receptor 2 (*gr2*)	F: ATGGCAGACCAGTGTGAACAGAT R: GAGCAGCAGCAGAACCTTCAT P: AGACTGCAGGTGTCTCA	108
	Serpin Family H1 (*serpinh1*)	F: AGCGCTGTGAAGTCCATCAA R: TGATGATCATGGCCCCATC P: CGGCCAAGTCCACCGA	93
	Heat shock protein 70 (*hsp70*)	F: GAGAACACTGTCCTCCAGCTCC R: CCCTGAAGAGGTCGGAACAC P: ACACCTCCATCACCAGG	104
	Heat shock protein 90 (*hsp90*)	F: GAGGTGGAGGAGGACGAGTACA	100

		R: GCTGTGAAGTGGATGTGGGA P: TCTCCAGGGACACAGAC	
	Cold inducible RNA binding protein (*cirbp*)	F: CGGGAAGGTCTCGTGGATT R: TGGTTCTGCCATCGACAGACT P: CATTGGAGGGAATGAA	111
	Metallothionein 1 (*mt1*)	F: TGGATCCTTGTGAATGCTCCA R: CTTACAACTGGTGCATGCGC P: CGGTGGATCCTGCAAG	103
	Metallothionein 2 (*mt2*)	F: GAAAAGTTGCTGCCCCTGC R: AACAGCTGGTATCGCAGGTCTT P: TTCAGGCTGTGTGTGCA	107
Apoptosis	Caspase 9 (*casp9*)	F: GCCAGACAGTTGGTTCGAGAC R: GGCTATGCTGCCCTTTCTCA P: TCCCAGCTTTAATAGAG	94

2.2.5.3.2 Bias correction of C_{rt} value in hydrolysis probe based quantitative PCR

Different types of fluorescent reporters can be used to monitor real-time DNA amplification in quantitative PCR assays (qPCR). Generally, the fluorescent reporters can be categorized into DNA binding molecules and hybridization reporters and hydrolysis reporters. SYBR green can bind with the double-stranded DNA, and it is one of the most commonly used fluorescent reporters in qPCR. The DNA-SYBR green-complex emits a fluorescent signal that is non-cumulative, and the increase of the signal is positively associated with the increased amount of the double-stranded DNA during amplification (Dragan et al., 2012).

The OpenArray™ TaqMan® RT-qPCR system utilizes hydrolysis reporters. Theoretically, one fluorophore should be cleaved off the probe during every DNA amplification event, and the released fluorophores generate a cumulative fluorescence signal during further cycles. According to Tuomi et al., the cumulative nature of the fluorophore does not statistically affect the calculation of primer efficiency, but their mathematical modeling indicated that the ignoring this factor would cause an underestimation of the C_{rt} (cycle of relative threshold) value by at least one cycle, which means an overestimation of the target quantity by 2-fold (Tuomi et al., 2010). They developed a mathematical method to correct the biased C_{rt} value, by calculating C_{shift}, the cycle number difference between the cumulative and non-cumulative amplification curves. Briefly, for each of the target genes except for *tnfα*, the averaged primer efficiency calculated in the section 2.2.5.3.1 were used to calculate the C_{shift} value. Then the C_{shift} value was used to adjust the C_{rt} value for each sample. All the equations used for bias correction were described by Tuomi et al. without change (Tuomi et al., 2010).

2.2.5.3.3 Gene expression analysis

Two endogenous control genes were included for the chip analysis, *rpl13a* and *ef1a*. For *ef1a*, there was not an adequate number of signals generated on chip to support meaningful statistical analysis (data not shown). As a result, the transcript levels of the 26 genes of interest were analysed in each of the individual samples, with normalization to *rpl13a*. In all cases, the C_{shift}-corrected C_{rt} value were used for the calculation of $\Delta\Delta$ C_{rt}. This step included normalizing the target gene C_{rt} value to the *rpl13a* C_{rt} value for each sample and calculating

the target gene expression difference between the average of 0 h control samples and the samples from 12 h, 24 h, 72 h, and 96 h post pathogen challenge. Due to suboptimal transportation conditions where the nitrogen tank was not properly charged, mucus and gill samples collected at 0 h, 12 h, and 24 h post infection did not generate meaningful signals on chip to support statistical analysis. Therefore, mucus and gill samples from the control tanks collected at time points 72 h and 96 h were combined as the new control group to calculate $\Delta\Delta C_{rt}$. With water filter samples, there were not enough signals generated for housekeeping genes to support further analysis (data not shown).

Specifically, the $\Delta\Delta C_{rt}$ value were converted to $\log_{PE}$ (fold change) for normality test and two-way ANOVA. The primer efficiency (PE) for each gene were listed in Table 2.1. This was then followed by a Tukey's posthoc test to determine significant differences between the control and treatment groups at each timepoint. A p-value of less than 0.05 was considered statistically significant (α=0.05). All statistical analyses and graphing were completed using the software GraphPad Prism 9.5.1. The full list of figures is shown in Appendix, except for the 6 genes selected for validation (section 2.3.2).

2.2.6 Validation of OpenArray™ RT-qPCR results by SYBR RT-qPCR

SYBR RT-qPCR was performed to validate the results of gene expression analyses by the nanofluid OpenArray™ gene chip. Water filter samples were not used in this assay because of suboptimal sample quality. Spleen, head kidney, gill (72 h, 96 h), and mucus (72 h, 96 h) samples were included in the validation SYBR RT-qPCR. Three endogenous control genes

and six immune response-related genes were selected based on significant differences detected with OpenArray™ gene chips and the immune responses they were involved with.

2.2.6.1 SYBR RT-qPCR reactions using QuantStudio™ 5 Real-Time PCR Systems

The 10 μL SYBR RT-qPCR reaction system is described as below: 5μL of 2x WISENT ADVANCED™ qPCR master mix (Wisent, Quebec, Canada), 2.5 μL of forward and reverse primer mix (Sigma Aldrich, USA) with each primer diluted to 0.25 μM by application, and 2.5 μL of sample cDNA. All reactions were performed with QuantStudio™ 5 Real-Time PCR Systems (Thermo Fisher Scientific, USA). Each sample were tested by technical triplicates. The reaction mixtures were pre-incubated for 5 min at 95°C, followed by 40 cycles of denaturation for 10 s at 95°C, annealing for 5 s at 60°C, and finally extension for 8 s at 72°C. The melt curve was calculated at the end of the 40 amplification cycles. Product specificity was confirmed through single peak on the melt curve.

2.2.6.2 Primer efficiency and DNA electrophoresis using SYBR RT-qPCR products

The primers used in the SYBR RT-qPCR validation were consistent with the ones used on the chip with the following exceptions. Because with SYBR RT-qPCR method the primer efficiency for *il-1β* was too high in spleen samples, the primers for *il-1β* were substituted with a primer set that was designed to be specific to rainbow trout *il-1β* (F: ACCGAGTTCAAGGACAAGGA; R: CATTCATCAGGACCCAGCAC) (Awad et al., 2020). In addition to the two endogenous control genes tested on chip, a third endogenous control gene, 18S ribosomal RNA (*18S*) were also included to the SYBR RT-qPCR analysis (F: CGTCGTAGTTCCGACCATAAA; R: CCACCCACAGAATCGAGAAA) (Giroux et

al., 2019). Both primer sets were previously used and validated in Chinook salmon in the Dixon lab. QuantStudio™ Design and Analysis (2.7.0) software was used to calculate the SYBR RT-qPCR primer efficiencies (Table 2.2) and melting curves for the primer sets mentioned above. Product specificity was confirmed with a single peak in melting curves as well as DNA electrophoresis using the PCR products. Notably, based on the multiple peaks in the melting curves, unspecific amplifications were observed in all the four tissue types using the *ef1α* primer set.

Table 2.2 Primer efficiencies (PE) of the endogenous control and target gene primers used in SYBR RT-qPCR. The primer efficiencies (%) were tested for every tissue type, including spleen, gill, head kidney (HK), and mucus.

Function	Gene name	Spleen PE (%)	Gill PE (%)	HK PE (%)	Mucus PE (%)
Endogenous Control	*rpl13a*	110	110	110	109
	ef1α	107	105	109	113
	18S	101	97	109	98
Immune Function	*il-1β*	105	110	104	108
	il-8	106	109	107	97
	mhc-i	107	102	113	110
	mhc-ii	110	110	113	129
	calm	101	101	110	97
	tapbp	109	110	109	107

To further confirm the specificity of the primer sets, a DNA agarose gel electrophoresis was performed using SYBR RT-qPCR products (**Figure 2.1**). A cDNA pool was made using spleen, head kidney, gill, and mucus samples, and SYBR RT-qPCR reactions were performed with the cDNA pool and primers of *rpl13a*, *il-1β*, *il-8*, *mhc-i*, *mhc-ii*, *calm*, and *tapbp*. A 2 % agarose gel was made with 2 g agarose (Fisher Bioreagents, Canada), 100 mL 1x TAE (Tris-acetate-EDTA) buffer, and 3 μL GelGreen® Nucleic Acid Gel Stain (Biotium, Inc., Canada). In each well on the agarose gel, 10 μL PCR product of the above-mentioned genes were loaded with 2 μL 6x DNA loading dye (Fermentas China Co., Ltd., China). Lastly, 5 μL 100 bp DNA Ladder (Promega Corporation, USA) and 1 μL 6x DNA loading dye was loaded to mark DNA band sizes. The loaded gel was run in 1x TAE buffer under 90 V electric pressure for 2 h, at room temperature. Upon the completion of DNA electrophoresis, the gel was immediately placed in the ChemiDoc™ XRS+ Imaging Systems (Bio-Rad Laboratories, Inc., USA) for DNA band detection. As shown in Figure 2.1, there was only one DNA product band observed for all 7 primer sets tests. No unspecific amplification was observed.

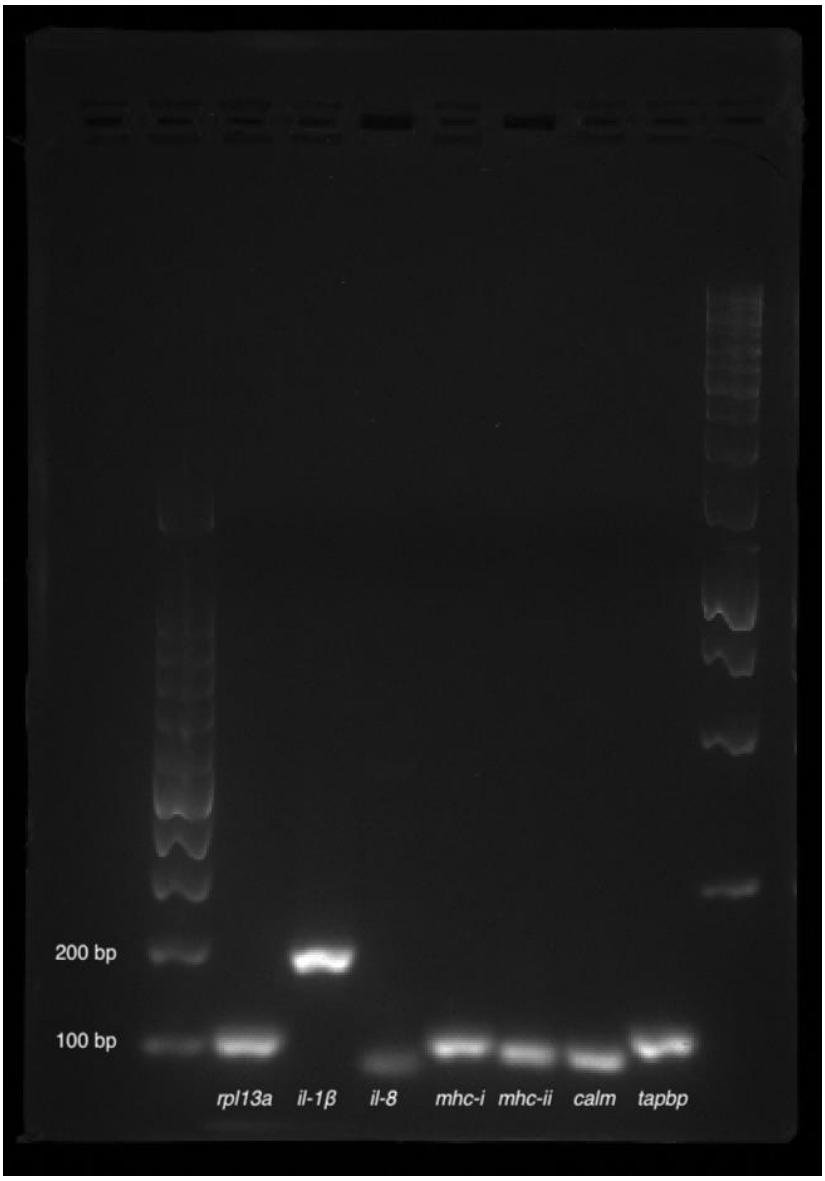

Figure 2.1 DNA electrophoresis using SYBR RT-qPCR products of *rpl13a, il-1β, il-8, mhc-i, mhc-ii, calm,* and *tapbp* primer sets. The SYBR RT-qPCR products was made using pooled cDNA samples (spleen, head kidney, gill, and mucus) and the primers of the target gene. Only one band was observed in each SYBR RT-qPCR product.

2.2.6.3 Statistical analyses of SYBR RT-qPCR results

Three endogenous control genes (*rpl13a*, *ef1a*, *18S*) were included in the SYBR RT-qPCR assays. Categorized by tissue type, cycle of quantification (C_q) values of these endogenous genes were used for reference gene evaluation using RefFinder (https://blooge.cn/RefFinder/), a web-based tool that mathematically integrates and ranks reference gene evaluation results from Genorm, NormFinder, BestKeeper, and the comparative Δ-Ct method (Andersen et al., 2004; Pfaffl et al., 2004; Silver et al., 2006; Vandesompele et al., 2002; Xie et al., 2012, 2023). According to the RefFinder analysis, *rpl13a* was the most stable endogenous control gene for spleen, head kidney, and gill samples, which is the same endogenous control gene selected to normalize OpenArray™ TaqMan® RT-qPCR results. For mucus samples, *ef1a* was the most stable endogenous control gene while *rpl13a* was ranked the second. Because the melting curves of *ef1a* SYBR RT-qPCR indicated unspecific amplifications, *rpl13a* was selected to normalize C_q values of mucus samples as well. **Figure 2.2** shows the RefFinder endogenous gene ranking for spleen samples as an example.

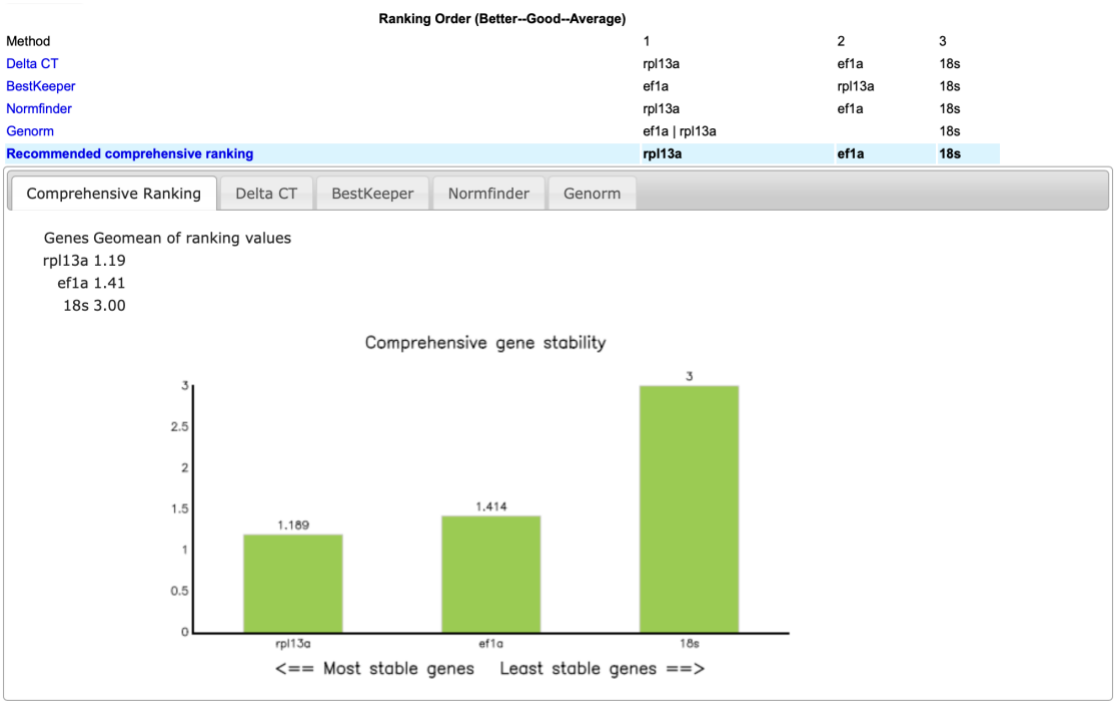

Figure 2.2 The SYBR RT-qPCR endogenous gene ranking result by RefFinder for Chinook salmon spleen tissue. The C_q values of three endogenous control genes (*rpl13a*, *ef1a*, *18S*) generated by SYBR RT-qPCR were analysed, and the endogenous control genes were ranked based on the mathematically integrated results by Genorm, NormFinder, BestKeeper, and the comparative delta-Ct method.

All SYBR qRT-PCR data was analysed using the $\Delta\Delta Cq$ method. This step was done using the web-based Relative Quantification (RQ) application module on Thermo Fisher Connect™ Cloud. As indicated in the chip result analysis, the gill and mucus samples collected at time point 0 h, 12 h, and 24 h post infection did not generate meaningful signals on chip to support statistical analysis. Thus, mucus and gill samples from the control tanks of 72 h and 96 h post infection were combined as the new control group to calculate $\Delta\Delta C_q$.

The $\Delta\Delta C_q$ values for spleen, head kidney, gill, and mucus samples were converted to $\log_2$(fold change) for normality test and two-way ANOVA. This was then followed by a

Tukey's posthoc test to determine significant differences between the control and treatment groups at each timepoint. A p-value of less than 0.05 was considered statistically significant. All statistical analyses and graphing were completed using the software GraphPad Prism 9.5.1.

2.2.7 Pearson's correlation analysis and simple linear regression analysis

In a previous transcriptomics study on the vaccine-induced responses in Arctic Charr (*Salvelinus alpinus*), Pearson's correlation analysis was used to validate the RNA-sequencing results with RT-qPCR (Braden et al., 2019). In another study investigating the salmon louse-induced immune response in Atlantic salmon, Pearson's correlation and linear regression analyses were applied to validate the microarray results using RT-qPCR results (Tadiso et al., 2011). In this thesis, to understand the relationship between the results generated by OpenArray™ TaqMan® RT-qPCR and SYBR RT-qPCR, both Pearson's correlation analysis and simple linear regression analysis were performed using $\log_{PE}$ (fold change) and $\log_2$(fold change) data, with the matched tissue type and target gene. For spleen and head kidney samples collected 0-96 h post infection, the six genes assessed with SYBR RT-qPCR were included in the above analysis. Considering there was no significant difference detected in mucus and gill samples, and the total sample numbers were smaller (only samples from time points 72 h and 96 h), data of mucus and gill samples were not included in the correlation and linear regression analyses.

Firstly, $\log_{PE}$ (fold change) data from OpenArray™ TaqMan® RT-qPCR and $\log_2$(fold change) data SYBR RT-qPCR were aligned and trimmed. Only the $\log_{PE}$ (fold

change) and $\log_2$(fold change) data with matched sample name were selected for the simple linear regression analyses and Pearson's correlation analyses. Both of the linear relationship and the correlation relationship were considered significant when p-value < 0.05. As for the Pearson's correlation analyses, normality test was performed and skewed data sets were transformed into Gaussian distribution. Notably, the matched $\log_{PE}$ (fold change) and $\log_2$(fold change) data were transformed using the same method. The mathematically transformed data set was then applied for Pearson's correlation analysis, and the correlation coefficient r were reported for each data pair. The correlation was considered "very strong" when r was greater than 0.80, "strong" when r was between 0.60-0.79, "moderate" when r was between 0.40-0.59, and "weak" when r was between "0.20-0.39" (Papageorgiou, 2022).

As for the simple linear regression analysis, a function describing the line of the best fit between the matched $\log_{PE}$ (fold change) and $\log_2$(fold change) data by OpenArray™ TaqMan® RT-qPCR and SYBR RT-qPCR method was reported. A slope greater than 0 was considered as a positive relationship. The R^2, coefficient of determination, measured the goodness of fit between the data set and the line of the best fit. Ideally when $R^2=1$, the dataset falls perfectly on the line of the best fit. All statistical analyses and graphing were completed using the software GraphPad Prism 9.5.1. The level of significance was noted with asterisks on r and R^2 in GraphPad style: p <0.0001****; p <0.0002***; p <0.0021**; p <0.0332*.

2.3 Results

2.3.1 Survival of Chinook salmon juveniles post live *V. anguillarum* challenge or sham injected.

Fish survival rates were monitored for 14 days after the live *V. anguillarum* i.p. injections. From days 0 to 4, a small reduction in survival was observed in both *V. anguillarum* injected and sham injected populations. This small reduction was likely caused by the handling stress and hypoxia during i.p. injections. At day 4, early symptoms of vibriosis-like skin lesions were first observed. A sharp drop in survival was observed between day 5 and day 10, which is typical of the time course of systemic vibriosis infection. After day 10, the survival rate remained stable in both groups until the end of recording. At day 14, the PBS sham injected group had a survival rate of 92% and the live *V. anguillarum* challenged group had a survival of 31% (**Figure 2.3**).

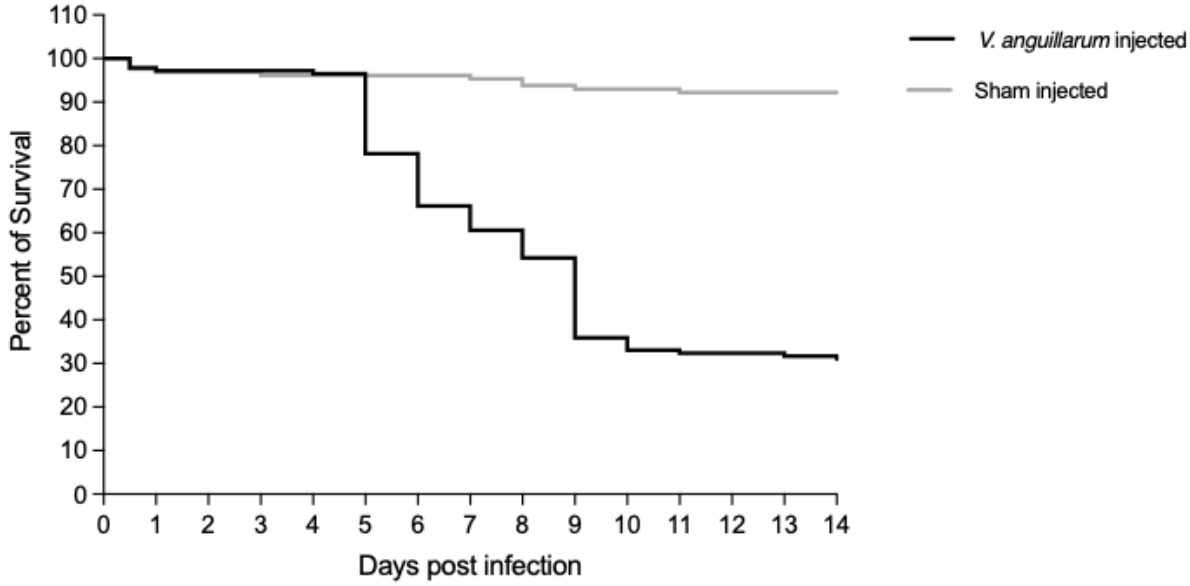

Figure 2.3. Survival rate curves for the Chinook salmon (*Oncorhynchus tshawytscha*) juveniles during the i.p. injected live *V. anguillarum* challenge. Individuals received either 100 µL of *Vibrio anguillarum* at a concentration of 6.2×10^4 CFU/mL or 100 µL of sterile PBS to act as a sham injected control. Both exposure conditions were completed in duplicate 250 L tanks (n=100 per tank).

2.3.2 Gene expression results by OpenArray™ TaqMan® RT-qPCR

The OpenArray™ TaqMan® RT-qPCR chip tested 26 target genes and 2 housekeeping genes were included as the endogenous control (*rpl13a* and *ef1a*). For *ef1a*, there was not an adequate number of signals generated on the chip to support meaningful statistical analysis, and across tissue types, the C_{shift}-corrected C_{rt} values of *ef1a* were very high (the average was 28.0). On the other hand, the average C_{shift}-corrected C_{rt} value of *rpl13a* was 22.8, and on the chip assay there was a good number of readings generated to support downstream analysis. The normality of *rpl13a* was tested by tissue and the target transcript levels were then

normalized to *rpl13a*. The immune transcripts expression level (*calm, mhc-i, mhc-ii, il-1β, il-8, tapbp*) are displayed by tissue type in the sections below. In general, the pro-inflammatory cytokine genes associated with early immune response increased injection in internal lymphoid organs starting at 72 h after live *V. anguillarum* i.p. injection, while no significant expression difference were observed in external MALT tissues, gill and skin mucus.

The rest of the target genes that were associated with stress, metabolism, and apoptosis showed no significant differences in transcript expression in spleen, head kidney, gill, or mucus samples. Although there was no difference in expression level observed, the primer efficiencies were calculated for all the primers and probes on chip, which can be used as a reference for future "on-chip" analysis (**Table 2.1**). Specifically, the primer efficiency of *tnfα* was not calculatable by LinRegPCR (version 2021.2) due to low C_{rt} data quality. The rest of the 27 genes had a cross-chip average primer efficiency within the range of 90% - 110%, except from *ifn-1* and *cirbp*, which had a slightly higher efficiency value at 111.15% and 111.45%. Because the primers were designed to target a range of salmon species, a primer efficiency slightly higher than 110% should be considered acceptable, although melting curves should be checked for product specificity.

2.3.2.1 Immune transcripts in spleen post V. anguillarum infection

Of the six immune transcript levels that were selected for data validation throughout the live *V. anguillarum* challenge in spleen, three genes (*il-1β, il-8, calm*) had an increased expression over time (**Figure 2.4A-C**). The pro-inflammatory cytokine *il-1β* stayed stable in the infected group (n=10) until 24 h post infection. At time point 72 h, the innate immune

response was initiated and *il-1β* transcript level started to elevate in the infected group. The *il-1β* level was significantly different in the infected group at the final time point of 96 h, compared to the infected groups sampled at 0 h - 24 h. The control group of time point 96 h was excluded from the analysis because it only had one data value. There was a significant difference observed between the *il-1β* transcript level between time points 24 h and 96 h ($p=0.0311$). In comparison, the control groups ($n=10$) that received i.p. injections of sterile PBS had no significant differences at the timepoints analysed (**Figure 2.4A**).

Similarly, the pro-inflammatory cytokine *il-8* also stayed stable in infected group until 24 h post infection. At 72 h and 96 h, a significant difference was observed in the infected group compared to the control group, and the infected groups did not show significant difference in between. There was a significant difference observed between the *il-8* transcript level between time points 24 h and 96 h ($p=0.0107$). The control group received i.p. injections of sterile PBS had no significant differences at the timepoints analysed (**Figure 2.4B**). At the timepoints analysed, the transcript expression level of Ca^{2+} regulatory gene *calm* had no significant difference observed within neither the control nor infected group. But at the final time point 96 h post infection, the *calm* transcript level was observed to be significantly different between the infected and control group. (**Figure 2.4C**).

As for the antigen-presenting molecules that are involved in the initiation of adaptive immune responses, *mhc-i* and *mhc-ii* were stable across the time points analysed (**Figure 2.4D, E**). The lack of adaptive immune responses was indirectly validated because *tapasin*,

the stabilizer for antigen peptide-loading complex for MHC class I, also had a stable transcript expression within the time frame analysed (**Figure 2.4D, F**).

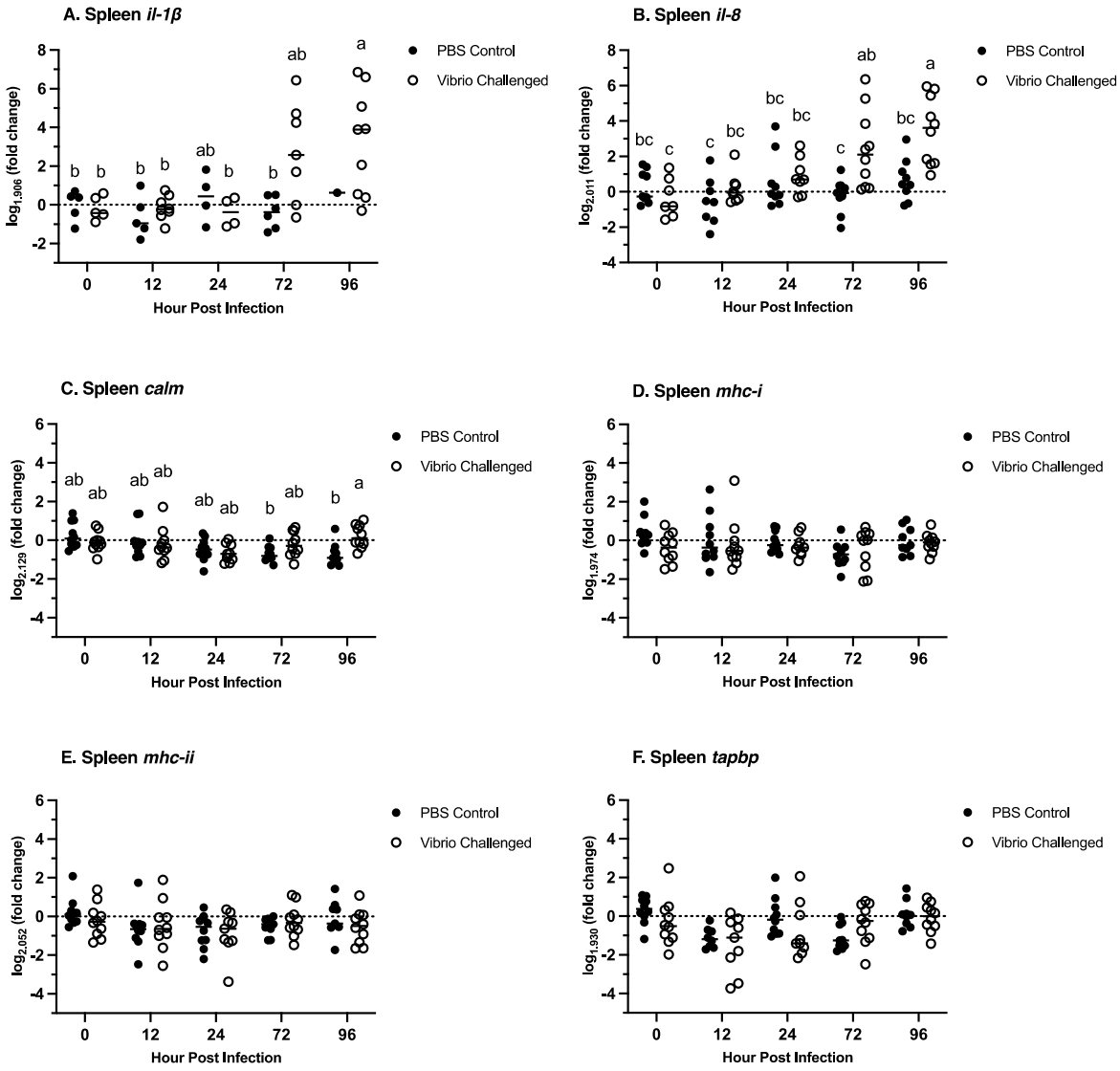

Figure 2.4. Spleen immune transcript expression throughout live *V. anguillarum* challenge, OpenArray™ TaqMan® RT-qPCR method. Transcript expression levels of pro-inflammatory cytokines *il-1β* (A), *il-8* (B), Ca^{2+} binding protein *calm* (C), antigen

presenting complex *mhc-i* (D) and *mhc-ii* (E), and MHC class I stabilizer *tapbp* (F) were assessed via OpenArray™ TaqMan® RT-qPCR on 12 h, 24 h, 72 h, and 96 h following i.p. injection with live *V. anguillarum*. Each treatment group had 10 individuals. All data was normalized to the reference gene *rpl13a* and expressed as a $\log_{PE}$ (fold change) over the 0 h control group. A p-value of less than 0.05 was considered to be statistically significant.

2.3.2.2 Immune transcripts in head kidney post V. anguillarum infection

When observing the six immune transcript levels throughout the live *V. anguillarum* challenge in head kidney, one gene (*il-1β*) had an increased expression over the time points analysed (**Figure 2.5A-C**). The pro-inflammatory cytokine *il-1β* was stable in the infected group (n=10) until time point 24 h post infection. The *il-1β* expression level was significantly different in the infected group at the final time point of 96 h, compared to the infected groups sampled at 0 h - 24 h. There was a significant difference observed between the *il-1β* transcript level between time points 24 h and 96 h (p=0.0069). In comparison, the control groups (n=10) that received i.p. injections of sterile PBS had no significant differences at the timepoints analysed (**Figure 2.5A**). The expression pattern of *il-1β* in head kidney was consistent to the expression pattern observed in spleen, although spleen *il-1β* transcripts was observed with a higher magnitude of increase by comparison.

On the other hand, no significant difference of the transcript expression of *il-8* was observed between treatment groups across the time points (**Figure 2.5B**). There was also no significant difference observed in the expression levels of *calm*, *mhc-i*, *mhc-ii*, and *tapasin* between treatment groups across the time points (**Figure 2.5C-F**).

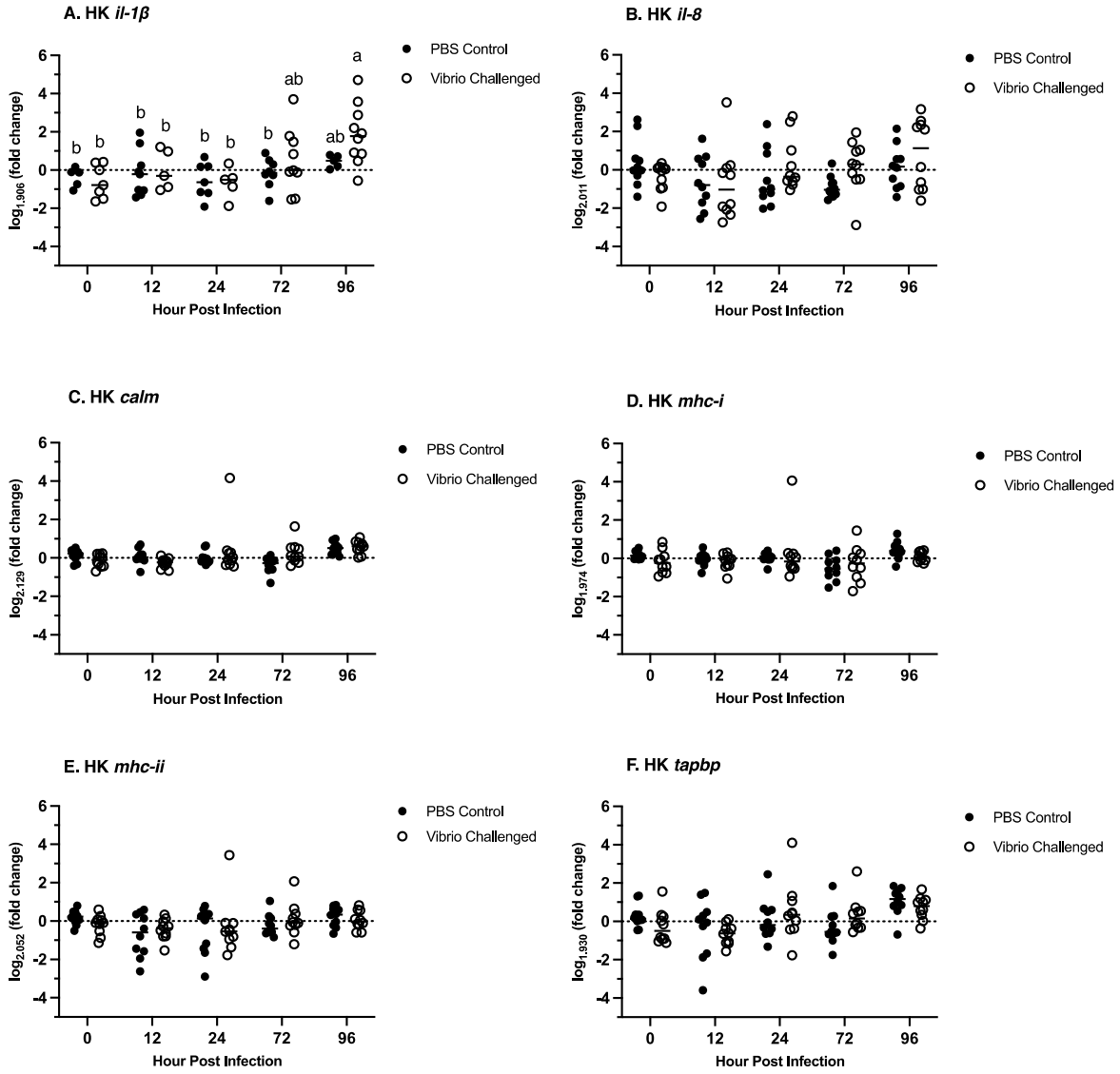

Figure 2.5. Head kidney immune transcript expression throughout live *V. anguillarum* challenge, OpenArray™ TaqMan® RT-qPCR method. Transcript expression levels of pro-inflammatory cytokines *il-1β* (A), *il-8* (B), Ca^{2+} binding protein *calm* (C), antigen presenting complex *mhc-i* (D) and *mhc-ii* (E), and MHC class I stabilizer *tapbp* (F) were assessed via OpenArray™ TaqMan® RT-qPCR on 12 h, 24 h, 72 h, and 96 h following i.p. injection with live *V. anguillarum*. Each treatment group had 10 individuals. All data was normalized to the reference gene *rpl13a* and expressed as a $\log_{PE}$ (fold change) over the 0 h control group. A p-value of less than 0.05 was considered to be statistically significant.

2.3.2.3 Immune transcripts in gill post V. anguillarum infection

Because of suboptimal transportation conditions for gill tissues, only samples taken at time point 72 h and 96 h were included in the figures. The immune transcripts (*calm*, *mhc-I*, *mhc-ii*, *il-1β*, *il-8*, *tapbp*) were expressed at a constant level post live *V. anguillarum* challenge in gill. There was no significant difference observed between the control group (n=10) and infected group (n=10) at the time points analysed (**Figure 2.6A-F**).

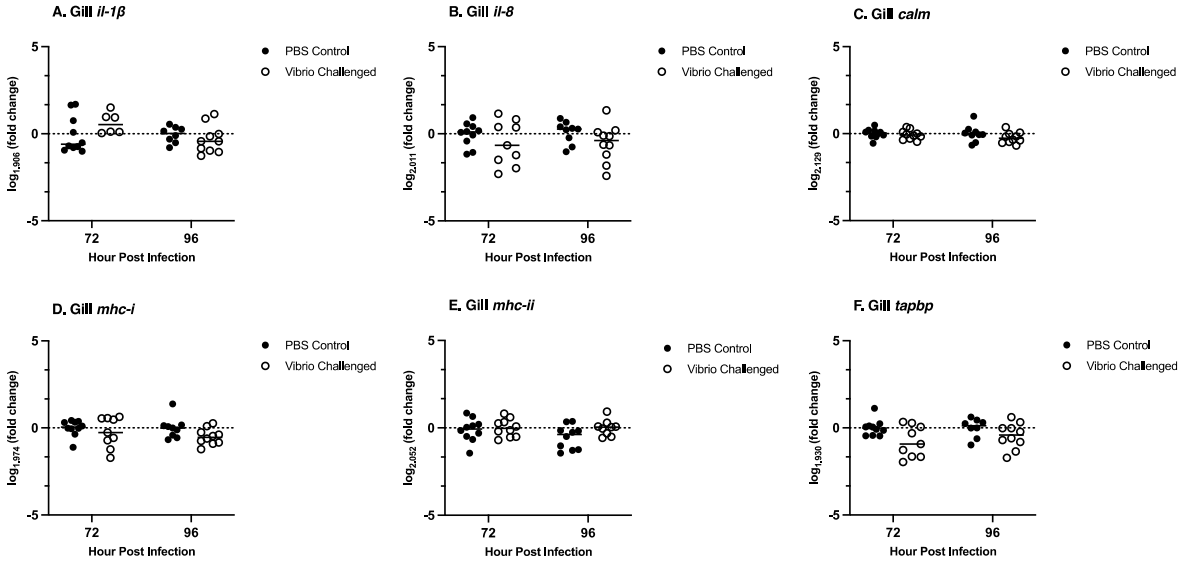

Figure 2.6. Gill immune transcript expression throughout live *V. anguillarum* challenge, OpenArray™ TaqMan® RT-qPCR method. Transcript expression levels of pro-inflammatory cytokines *il-1β* (A), *il-8* (B), Ca^{2+} binding protein *calm* (C), antigen presenting complex *mhc-i* (D) and *mhc-ii* (E), and MHC class I stabilizer *tapbp* (F) was assessed via OpenArray™ TaqMan® RT-qPCR on time points 72 h and 96 h following i.p. injection with live *V. anguillarum*. Each treatment group had 10 individuals. All data was normalized to the reference gene *rpl13a* and expressed as a $\log_{PE}$ (fold change) over the combined 72 h and 96 h control group. A p-value of less than 0.05 was considered to be statistically significant.

2.3.2.4 Immune transcripts in mucus post V. anguillarum infection

Also because of suboptimal transportation conditions only the mucus samples taken at time point 72 h and 96 h were included in the analysis. The immune transcripts were expressed at a constant level post live *V. anguillarum* challenge in mucus. There was no significant difference observed between the control group (n=10) and infected group (n=10) at the time points analysed (**Figure 2.7A-F**). The number of data points that were generated with the OpenArray™ TaqMan® RT-qPCR were fewer compared to spleen and gill tissues because of the interference of non-fish sourced environmental mRNA.

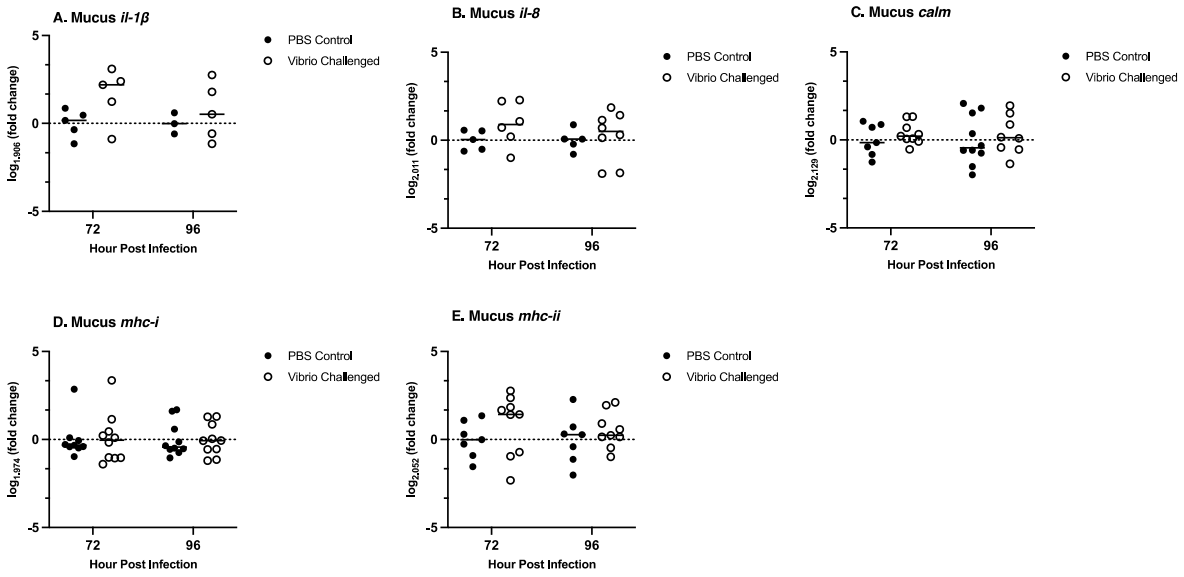

Figure 2.7. Mucus immune transcript expression throughout live *V. anguillarum* challenge, OpenArray™ TaqMan® RT-qPCR method. Transcript expression levels of pro-inflammatory cytokines *il-1β* (A), *il-8* (B), Ca^{2+} binding protein *calm* (C), antigen presenting complex *mhc-i* (D), and *mhc-ii* (E) was assessed via OpenArray™ TaqMan® RT-qPCR on time points 72 h and 96 h following i.p. injection with live *V. anguillarum*. Each treatment group had 10 individuals. All data was normalized to the reference gene *rpl13a* and

expressed as a $\log_{PE}$ (fold change) over the combined 72 h and 96 h control group. Data for *tapbp* was not shown due to poor quality. A p-value of less than 0.05 was considered to be statistically significant.

2.3.3 Gene expression results by SYBR RT-qPCR

To validate the immune transcripts expression patterns observed using OpenArray™ TaqMan® RT-qPCR, the six immune response-related genes that were discussed above in the gene-chip experiment (*calm*, *mhc-I*, *mhc-ii*, *il-1β*, *il-8*, *tapbp*) and three endogenous control genes (*rpl13a*, *ef1a*, *18s*) were tested with SYBR RT-qPCR. The RT-qPCR reactions used the same set of primers except for *il-1β* and 18S ribosomal RNA (*18s*). As mentioned in section 2.2.6.3, the *Cq* of all the samples were firstly normalized to *rpl13a*, the same endogenous control gene that was chosen for the OpenArray™ TaqMan® RT-qPCR result analysis. In brief, the immune transcript expression patterns found using OpenArray™ TaqMan® RT-qPCR method were repeated by SYBR RT-qPCR method.

2.3.3.1 Immune transcripts in spleen post V. anguillarum infection

When validating the six immune transcript levels throughout the live *V. anguillarum* challenge in spleen, two genes (*il-1β* and *il-8*) had an increased expression over time (**Figure 2.8A, B**). The transcript expression level of pro-inflammatory cytokine *il-1β* stayed stable until 24 h post injection. At both 72 h and 96 h, a significant difference was observed between the infected and control group (n=12). In the infected groups, there was a significant difference observed between the *il-1β* transcript levels at time points 12 h and 96 h (p

<0.0001). In comparison, the control groups (n=12) that received i.p. injections of sterile PBS had no significant differences at the timepoints analysed (**Figure 2.8A**).

As for the pro-inflammatory cytokine *il*-8, at both 72h and 96 h post injection, a significant difference was observed between infected group and control group. Between the infected groups, there was also a significant difference observed between the 12 h and 96 h post infection ($p < 0.0001$). The control had no significant differences at the timepoints analysed (**Figure 2.8B**). The expression level of Ca^{2+} regulatory gene *calm* had no significant difference observed in infected group at the timepoints analysed. The control groups that received i.p. injections of sterile PBS also had no significant differences across the time points (**Figure 2.8C**). For the expression levels of *mhc*-I, mhc-*ii*, and *tapasin*, there was also no significant difference observed across the time points in both infected and control groups (**Figure 2.8D-F**).

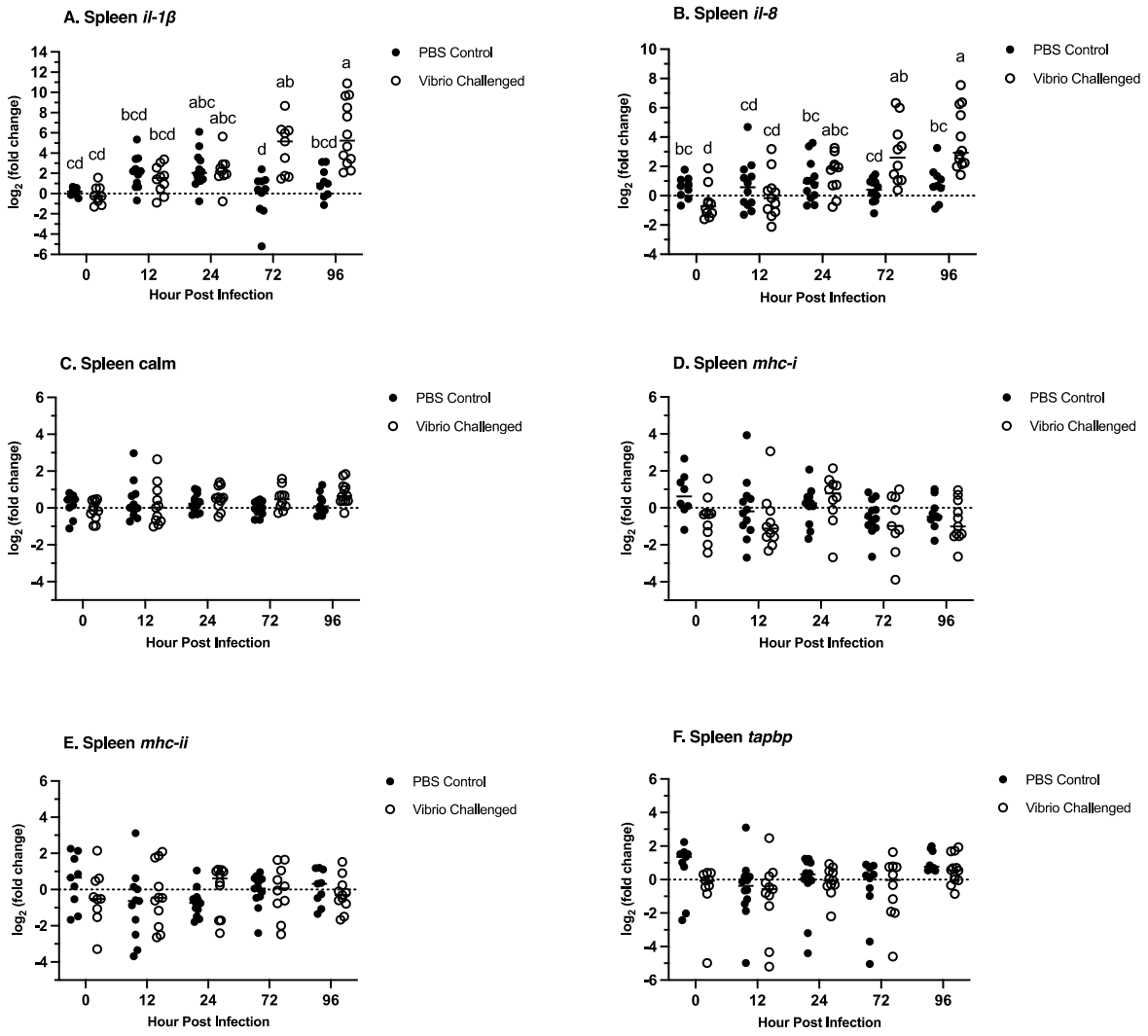

Figure 2.8. Spleen immune transcript expression throughout live *V. anguillarum* challenge, SYBR RT-qPCR method. Transcript expression levels of pro-inflammatory cytokines *il-1β* (A), *il-8* (B), Ca^{2+} binding protein *calm* (C), antigen presenting complex *mhc-i* (D) and *mhc-ii* (E), and MHC class I stabilizer *tapbp* (F) were assessed via SYBR RT-qPCR on 12 h, 24 h, 72 h, and 96 h following i.p. injection with live *V. anguillarum*. Each treatment group had 12 individuals. All data was normalized to the reference gene *rpl13a* and expressed as a $\log_2$(fold change) over the 0 h control group. A p-value of less than 0.05 was considered to be statistically significant.

2.3.3.2 Immune transcripts in head kidney post V. anguillarum infection

When validating the six immune transcript levels throughout the live *V. anguillarum* challenge in head kidney, three genes (*il-1β*, *il-8* and *tapbp*) had an increased expression over time points analysed (**Figure 2.9A, B, F**). The pro-inflammatory cytokine *il-1β* stayed stable in infected group (n=12) until time point 24 h post infection. At time point 72 h and 96 h, *il-1β* expression level was elevated in the infected group compared to the control group. In comparison, the control groups (n=12) had no significant differences at the timepoints analysed (**Figure 2.9A**). The transcript expression pattern of *il-1β* in head kidney was consistent to the expression pattern observed in spleen, where a significant difference within time point could be initially observed at 72 h post infection.

At 96 h post infection, the *il-8* transcript level increased in the infected group, with a significant difference observed between 12 h and 96 h (p=0.0024). The control groups had no significant differences from 0 h to 96 h post infection (**Figure 2.9B**). The expression of *il-8* in head kidney was weaker to the expression level observed in spleen, while no difference was observed between the infected and control groups within the same timepoint. Notably, the significant increase of *il-8* transcript detected by SYBR RT-qPCR method was not detected by OpenArray™ TaqMan® RT-qPCR method. Nevertheless, the expression level of *tapbp* was observed to increase between the infection groups at time point 12 h and 96 h (p=0.0117). The control groups had no significant differences from 0 h to 96 h post infection (**Figure 2.9F**). There was no significant difference observed of the expression level of *calm*, *mhc-i*, and *mhc-ii* between treatment groups across the time points (**Figure 2.9C-E**).

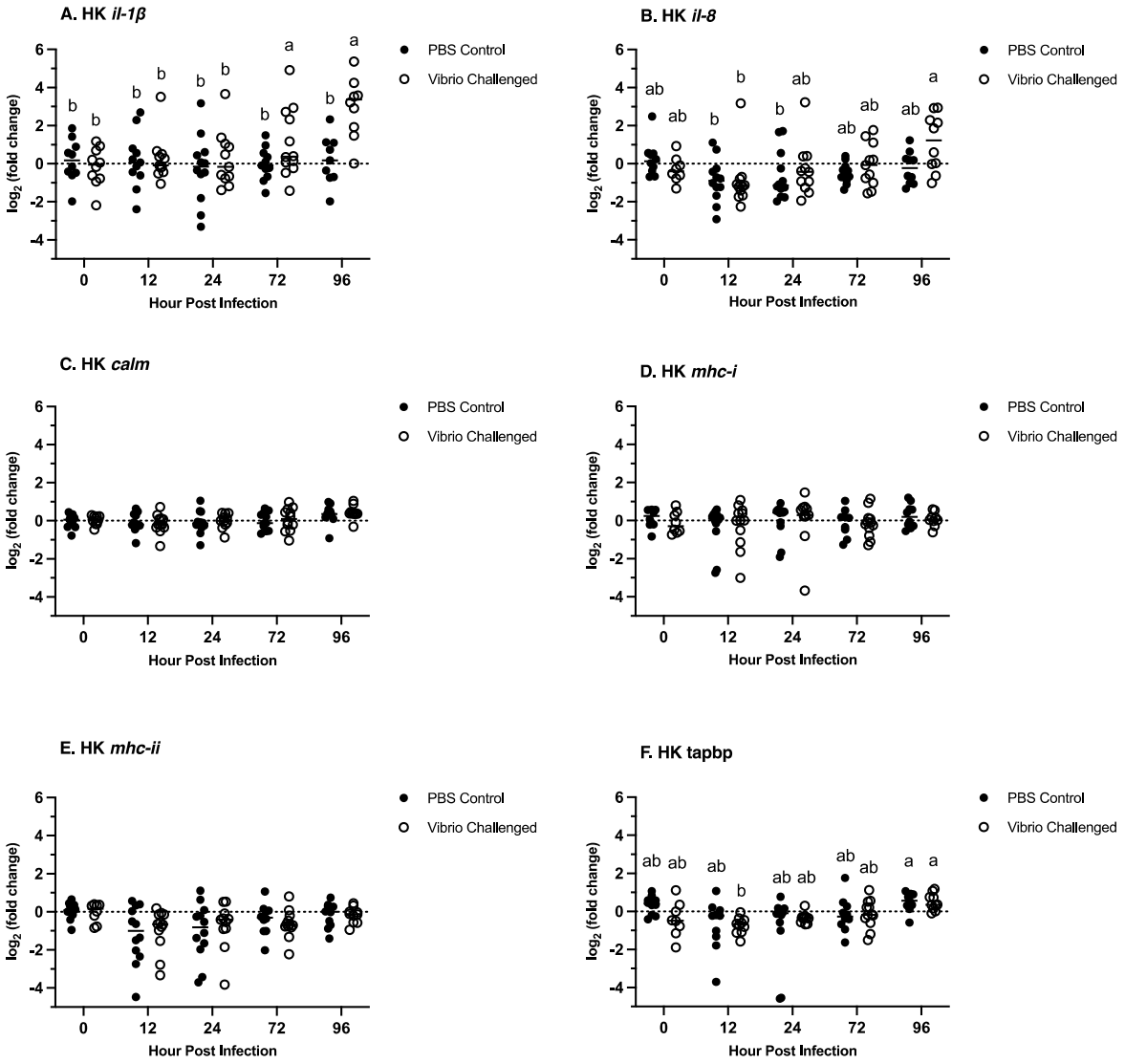

Figure 2.9. Head kidney immune transcript expression throughout live *V. anguillarum* challenge, SYBR RT-qPCR method. Transcript expression levels of pro-inflammatory cytokines *il-1β* (A), *il-8* (B), Ca^{2+} binding protein *calm* (C), antigen presenting complex *mhc-i* (D) and *mhc-ii* (E), and MHC class I stabilizer *tapbp* (F) were assessed via SYBR RT-qPCR on 12 h, 24 h, 72 h, and 96 h following i.p. injection with live *V. anguillarum*. Each treatment group had 12 individuals. All data was normalized to the reference gene *rpl13a* and expressed as a $\log_2$(fold change) over the 0 h control group. A p-value of less than 0.05 was considered to be statistically significant.

2.3.3.3 Immune transcripts in gill post V. anguillarum infection

Only the gill samples taken at time point 72 h and 96 h were included in the SYBR RT-qPCR analysis. The immune transcripts (*calm, mhc-I, mhc-ii, il-1β, il-8, tapbp*) were expressed at a constant level post live *V. anguillarum* challenge in gill tissue. There was no significant difference observed between the control group (n=12) and infected group (n=12) at the time points analysed (**Figure 2.10A-F**).

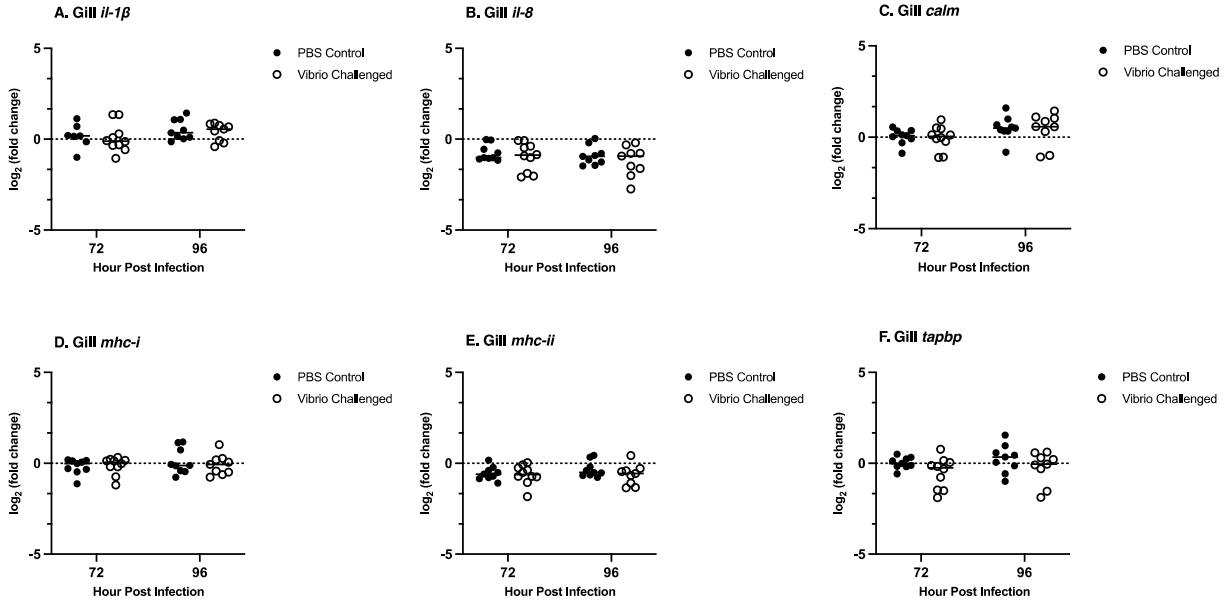

Figure 2.10. Gill immune transcript expression throughout live *V. anguillarum* challenge, SYBR RT-qPCR method. Transcript expression levels of pro-inflammatory cytokines *il-1β* (A), *il-8* (B), Ca^{2+} binding protein *calm* (C), antigen presenting complex *mhc-i* (D) and *mhc-ii* (E), and MHC class I stabilizer *tapbp* (F) were assessed via SYBR RT-qPCR on time points 72 h and 96 h following i.p. injection with live *V. anguillarum*. Each treatment group had 12 individuals. All data was normalized to the reference gene *rpl13a* and expressed as a $\log_2$(fold change) over the combined 72 h and 96 h control group. A p-value of less than 0.05 was considered to be statistically significant.

2.3.3.4 Immune transcripts in mucus post V. anguillarum infection

Only the mucus samples taken at time point 72 h and 96 h were included in the SYBR RT-qPCR analysis. The immune transcripts were expressed at a constant level post live *V. anguillarum* challenge in mucus. There was no significant difference observed between the control group (n=12) and infected group (n=12) at the time points analysed (**Figure 2.11A-F**).

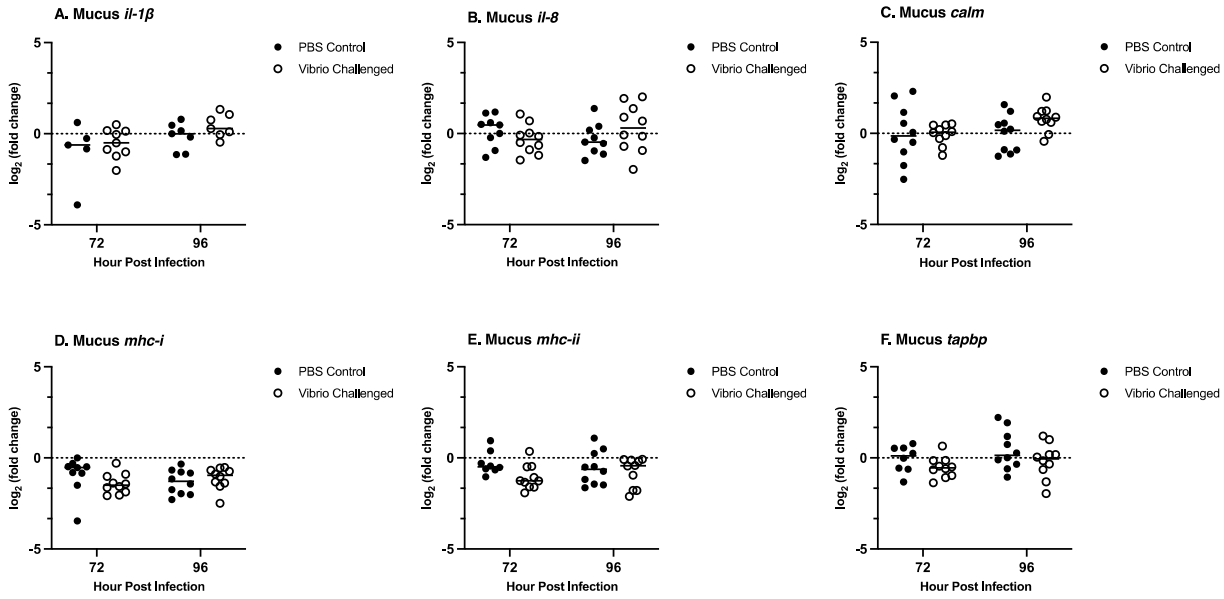

Figure 2.11. Mucus immune transcript expression throughout live *V. anguillarum* challenge, SYBR RT-qPCR method. Transcript expression levels of pro-inflammatory cytokines *il-1β* (A), *il-8* (B), Ca^{2+} binding protein *calm* (C), antigen presenting complex *mhc-i* (D) and *mhc-ii* (E), and MHC class I stabilizer *tapbp* (F) were assessed via SYBR RT-qPCR on time points 72 h and 96 h following i.p. injection with live *V. anguillarum*. Each treatment group had 12 individuals. All data was normalized to the reference gene *rpl13a* and expressed as a $\log_2$(fold change) over the combined 72 h and 96 h control group. A p-value of less than 0.05 was considered to be statistically significant.

2.3.4 Pearson's correlation and simple linear regression analyses

To compare the gene expression results (*calm*, *mhc-i*, *mhc-ii*, *il-1β*, *il-8*, *tapbp*) of the OpenArray™ TaqMan® RT-qPCR and SYBR RT-qPCR methods, the matched $\log_{PE}$ (fold change) and $\log_2$(fold change) values for spleen and head kidney samples were analysed using Pearson's correlation and linear regression analyses. In general, for the six target genes from both spleen and head kidney tissue, all the correlation and regression relationships were significant ($p<0.0001$). A moderate to strong positive correlation (correlation coefficient r between 0.4242 to 0.7307) and a slope ranged between 0 to 1 for the line of the best fit were observed, where x and y were assigned with $\log_{PE}$ (fold change) and $\log_2$(fold change) values by OpenArray™ TaqMan® RT-qPCR and SYBR RT-qPCR, respectively.

2.3.4.1 Correlation and regression analyses for spleen tissue

The Pearson's correlation and simple linear regression relationships of the six immune transcripts (*calm*, *mhc-i*, *mhc-ii*, *il-1β*, *il-8*, *tapbp*) from the spleen samples, using $\log_{PE}$ (fold change) and $\log_2$(fold change) values of OpenArray™ TaqMan® and SYBR RT-qPCR methods, are displayed in **Figure 2.12A-F**. As for the correlation analysis, all six genes showed a positive correlation significance ($p<0.0001$). The Pearson's correlation coefficient r indicated that *il-1β*, *il-8*, and *mhc-ii* had a strong correlation between the $\log_{PE}$ (fold change) and $\log_2$(fold change) data (**Figure 2.12A, B, E**), while *calm*, *mhc-i*, and *tapbp* had a moderate correlation (**Figure 2.12C, D, F**). The linear regression analysis of the six genes indicated a positive relationship between $\log_{PE}$ (fold change) and $\log_2$(fold change) values generated by OpenArray™ TaqMan® and SYBR RT-qPCR with a significance ($p<0.0001$)

and the slopes of the lines of the best fit were all below 1 (**Figure 2.12A-F**). As the result, a general trend was observed: the overall $\log_{PE}$ (fold change) values generated by OpenArray™ TaqMan® RT-qPCR method were lower than the $\log_2$(fold change) values generated by SYBR RT-qPCR method. As for the linear regression analysis, two genes (*il-1β* and *il-8*) were observed to have an elevation in transcript expression in spleen using both RT-qPCR methods, and a high R^2 value was reported for both cases (0.7939 and 0.7943 respectively) (**Figure 2.12A. B**). For genes that did not have an increased expression at the time points analysed, like *mhc-i* and *tapbp*, the R^2 value was observed to be lower (0.2381 and 0.2611) (**Figure 2.12D, F**).

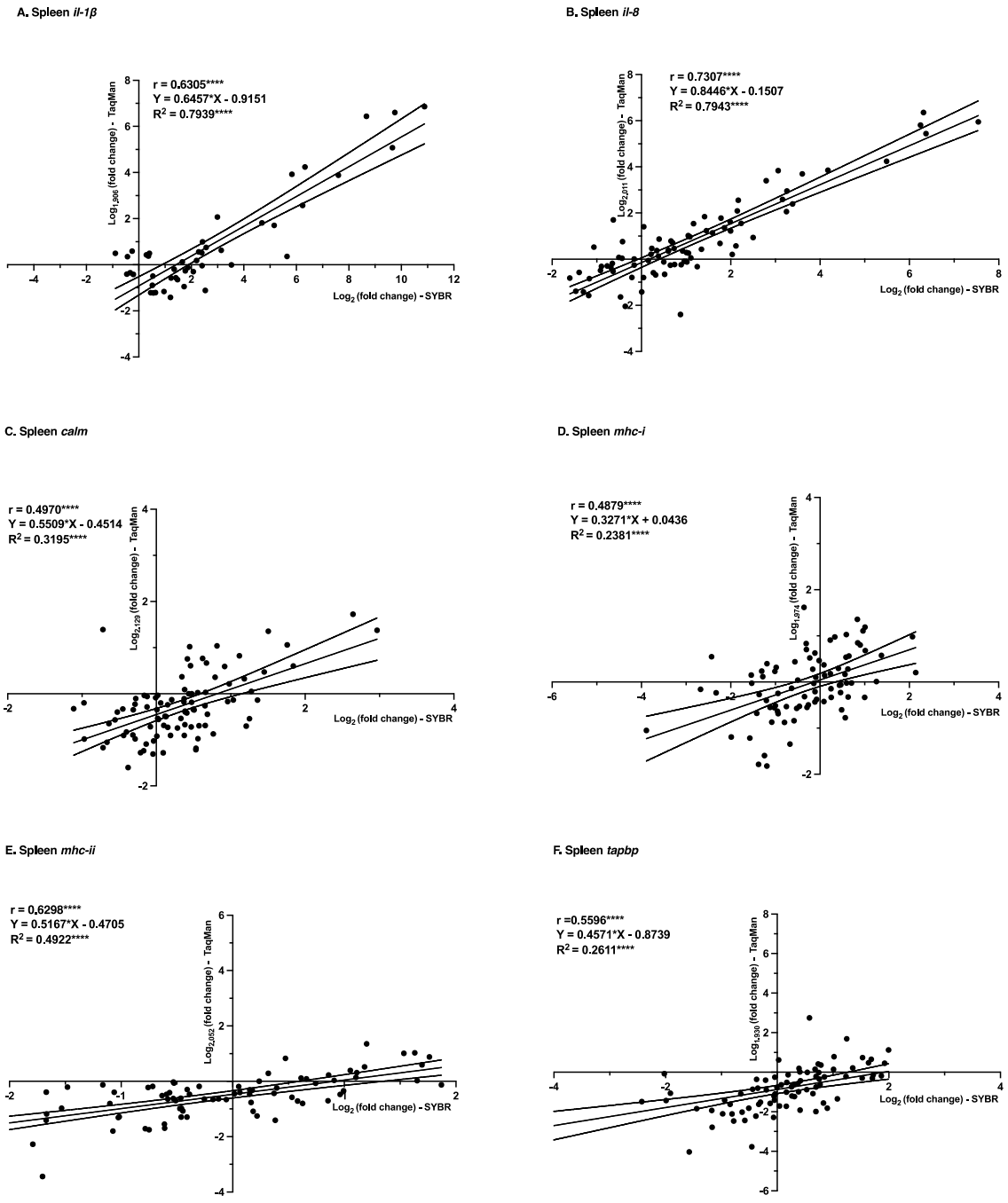

Figure 2.12. Pearson's correlation and simple linear regression between $\log_{PE}$ (fold change) and $\log_2$(fold change) values of OpenArray™ TaqMan® and SYBR RT-qPCR using spleen samples. The matched $\log_{PE}$ (fold change) and $\log_2$(fold change) values of six genes, *il-1β* (A), *il-8* (B), *calm* (C), *mhc-i* (D), *mhc-ii* (E), and *tapbp* (F) were assessed. The

relationship between data obtained by both methods was estimated using Pearson's correlation and simple linear regression. The line of the best fit was presented with the 95% confidence interval. The Pearson's correlation coefficient r, the function of the line of the best fit, the coefficient of determination R^2 for the simple linear regression are presented in the figure. The level of significance was displayed in GraphPad style ($p < 0.0001$****; $p < 0.0002$***; $p < 0.0021$**; $p < 0.0332$*).

2.3.4.2 Correlation and regression analyses for head kidney tissue

The Pearson's correlation and simple linear regression relationships of the six immune transcripts (*calm*, *mhc-i*, *mhc-ii*, *il-1β*, *il-8*, *tapbp*) from the head kidney samples, using $\log_{PE}$ (fold change) and $\log_2$(fold change) values of OpenArray™ TaqMan® and SYBR RT-qPCR methods, are displayed in **Figure 2.13A-F**. As for the correlation analysis, all six genes showed a positive correlation with significance ($p<0.0001$). The r, correlation coefficient, indicated *il-1β*, *il-8* and *tapbp* had a strong correlation (**Figure 2.13A, B, F**), and *calm*, *mhc-i* and *mhc-ii* had a moderate correlation (**Figure 2.13C, D, E**).

The linear regression analysis of the six genes indicated a positive relationship between $\log_{PE}$ (fold change) and $\log_2$(fold change) values generated by OpenArray™ TaqMan® and SYBR RT-qPCR with significance ($p<0.0001$) and the slopes of the lines of the best fit were all below 1 (**Figure 2.13A-F**). Thus, like what was observed in spleen samples, the overall $\log_{PE}$ (fold change) values were also lower than the $\log_2$(fold change) values in head kidney samples. Three genes (*il-1β*, *il-8*, and *tapbp*) were observed with significant expression elevations by either RT-qPCR methods, and the matched $\log_{PE}$ (fold change) and $\log_2$(fold change) data had a R^2 value of 0.6476, 0.5781, and 0.3431 respectively

(**Figure 2.13A, B, F**). For genes that did not elevate at the time points analysed (*calm* and *mhc-i*), the R^2 value was observed to be lower (0.1469 and 0.2058) (**Figure 2.13C, D).**

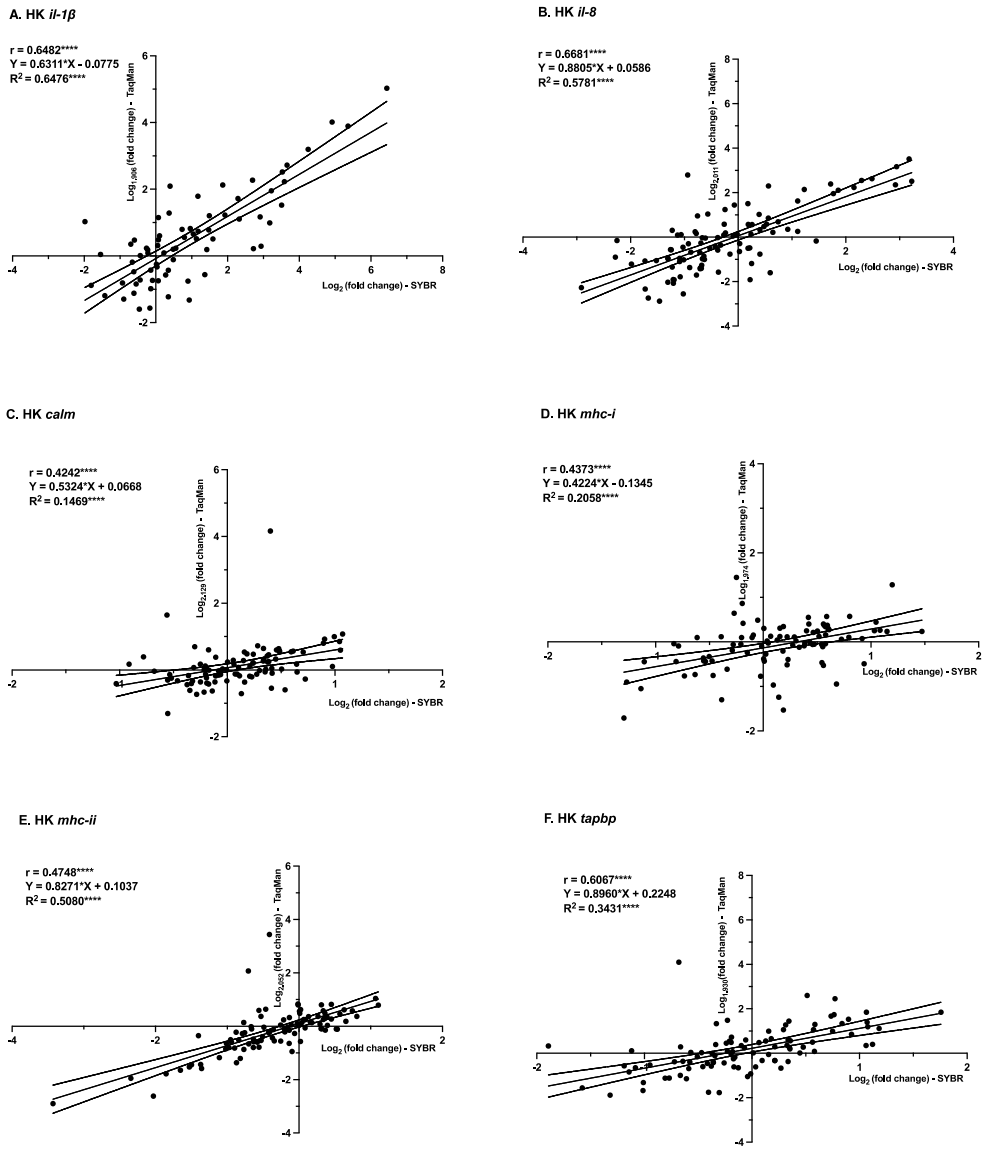

Figure 2.13. Pearson's correlation and simple linear regression between $\log_{PE}$ (fold change) and $\log_2$(fold change) values of OpenArray™ TaqMan® and SYBR RT-qPCR using head kidney samples. The matched $\log_{PE}$ (fold change) and $\log_2$(fold change) values of six genes, *il-1β* (A), *il-8* (B), *calm* (C), *mhc-i* (D), *mhc-ii* (E), and *tapbp* (F) were assessed.

The relationship between data obtained by both methods was estimated using Pearson's correlation and simple linear regression. The line of the best fit was presented with the 95% confidence interval. The Pearson's correlation coefficient r, the function of the line of the best fit, the coefficient of determination R^2 for the simple linear regression are presented in the figure. The level of significance was displayed in GraphPad style ($p < 0.0001$****; $p < 0.0002$***; $p < 0.0021$**; $p < 0.0332$*).

2.4 Discussion

The purpose of this study was to determine 1) if the novel nanofluidic OpenArray™ chip is a reliable tool to evaluate fish health status using a Chinook salmon disease model; 2) if mucus and culture water are a good source for mRNA transcripts and capable of indicating the physiological status of fish while allowing non-invasive sampling. To address these questions diploid Chinook salmon juveniles were divided into two groups (infected group and sham control group) and transcriptomic differences were measured using a novel nanofluidic OpenArray™ chip. Lymphoid organs (spleen and head kidney), mucus-associated lymphoid tissue (skin mucus and gill), and water samples were taken for assessment.

2.4.1 Performance assessment of the novel nanofluidic OpenArray™ chip

The novel nanofluidic OpenArray™ Taqman® RT-qPCR chip used in this experiment was developed to assess the transcriptomic responses for a range of salmon species under the order Salmoniformes, including Chinook salmon (*Oncorhynchus tshawytscha*), for purposes like fish health assessment, management, and conservation. In total, 28 genes were tested on the chip using samples taken from a Chinook salmon disease model. Six immune response-related genes (*calm*, *mhc-I*, *mhc-ii*, *il-1β*, *il-8*, and *tapbp*) were selected based on significant differences detected with OpenArray™ gene chips and the immune responses they were involved

with for the next-step validations using SYBR RT-qPCR. The amplicon products of these genes made using SYBR RT-qPCR method was run on an agarose gel (**Figure 2.1**). For SYBR RT-qPCR reactions, the primer set for *il-1β* was changed while the primers for the rest of the genes were consistent to the primers used on chip. Only a single product (band) was identified for each gene, which indicated that the primers were highly specific to the conserved regions of the CDSs, and the primers were not able to differentiate between isoforms. As a close relative to Chinook salmon, Rainbow trout has two isoforms of *il-1β* transcripts and five isoforms of *il-8* transcripts (Frenette et al., 2023; Zuo et al., 2020).

To further investigate the reliability of the OpenArray™ TaqMan® RT-qPCR chip, the gene expression results of *calm*, *mhc-i*, *mhc-ii*, *il-1β*, *il-8*, and *tapbp* were repeated using the SYBR RT-qPCR method. Similar transcript expression patterns were discovered in all the six genes analysed in both spleen and head kidney samples, especially in terms of the induction time point of pro-inflammatory cytokine transcripts. Notably, no significant difference was observed in the expression level of *il-8* in head kidney tissues using OpenArray™TaqMan® RT-qPCR method, but a decrease at was observed using SYBR RT-qPCR at 12 h in both control and infected groups. Similarly, at 72 h, OpenArray™TaqMan® RT-qPCR result indicated *calm* expression level in the infected group was significantly different to the control group but this elevation was not detected by SYBR RT-qPCR. As for *tapbp*, although no difference was observed between treatment groups in the same time point, an increased expression was discovered in the infected group from 12 h to 96 h using SYBR RT-qPCR. This elevation was not detected by OpenArray™TaqMan® RT-qPCR. The

discrepancies of the results may be caused by the sample number difference. In OpenArray™TaqMan® RT-qPCR assay, in each treatment group n=10, while in SYBR RT-qPCR n=12. The difference in signal specificity of these two methods may also influenced the 2-way ANOVA results.

The Pearson's correlation was performed on the matched $\log_{PE}$ (fold change) and $\log_2$(fold change) data generated by OpenArray™ TaqMan® RT-qPCR and SYBR RT-qPCR method, and a moderate to strong correlation was observed in all cases. These correlation results strongly proves the robustness of this OpenArray™ TaqMan® RT-qPCR chip as a tool for transcriptomics analysis for Chinook salmon. A simple linear relationship analysis was also performed. A positive linear relationship was discovered in all cases. If the OpenArray™ TaqMan® RT-qPCR chip could provide the same cycle readings as the SYBR RT-qPCR method, the line of the best fit between the two data set would be y = x, where the slope=1. Interestingly, the slope of the line of the best fit was lower than 1 in all regression models, where x was assigned with $\log_2$(fold change) data from SYBR RT-qPCR, and y was assigned with $\log_{PE}$ (fold change) data from OpenArray™ TaqMan® RT-qPCR. The overall lower readings generated by the OpenArray™ TaqMan® RT-qPCR can be explained by the different signalling mechanisms utilised by these two methods. Both RT-qPCR methods use a forward and reverse primer set that is specific to the target gene sequence. But for the on-chip TaqMan® RT-qPCR, a probe attached with a fluorophore and a quencher is also designed to be specific to the coding strand of the DNA. Because the Thermus aquaticus (Taq) DNA polymerase also has the 5'-3' exonuclease activity, the elongation of the DNA

strand will lead to the dissociation of the probe and the release of the fluorophore (Holland et al., 1991). As a result, only the specific amplification will be recorded by TaqMan® RT-qPCR. On the other hand, the fluorescent dye SYBR green can bind with any double stranded DNA in the reaction system, meaning the non-specific PCR products will also generate signals, although in this experiment the primer set specificity was confirmed with the single product band in DNA electrophoresis gel (**Figure 2.1**) (Dragan et al., 2012). To summarize, TaqMan® RT-qPCR result should be more specific compared to SYBR RT-qPCR result, which supports the discovery that the OpenArray™ TaqMan® RT-qPCR provided an overall lower reading value.

2.4.2 Fish culture water and mucus as sources of transcripts

To investigate whether mucus and culture water are a good source for transcripts that indicate the physiological status of fish, Chinook salmon skin mucus and filtered culture water were collected post live *V. anguillarum* i.p. injection. To ensure an abundant amount of shed mucus and fish-sourced transcripts in the water body, a high fish density was maintained at the start of the trial (100 fish per 250 L tank, 22.12 kg/m^3). By comparison, a previous study measuring the rainbow trout microRNA from the filtered water had a fish density of 0.644 kg/m^3 (4 fish per 200 L tank) and a water flow rate of 1.0 L/min (Ikert et al., 2021). The water flow rate was maintained at 1.0L/min, so that the water was renewed about 6 times a day and there should be a low microorganism accumulation.

The water filter samples were analysed using the OpenArray™ TaqMan® RT-qPCR chip. Unfortunately, there was no or very few signals generated for all the 28 genes even

though 250 ng of RNA per sample was used for filter cDNA synthesis. This means that most of the mRNA recovered from the filters were from the waterborne microorganisms. Additionally, the filters used in this experiment were from Norgen Water RNA/DNA Purification Kit (Cat. 26450). The filter provided was small in size with a diameter of approximately 2.5 cm, and it was saturated after application of 150 mL fish culture water, preventing the collection of more fish mRNA materials. However, there was no signal generated from the water samples taken from the blank tank (no fish), which means the OpenArray™ TaqMan® RT-qPCR chip was robust in not generating false positive results.

Mucus samples were analysed using both the OpenArray™ TaqMan® RT-qPCR chip and the SYBR RT-qPCR on plate. Although there was no induced expression observed by either method, it was interesting that the immune response related genes, especially *calm*, *mhc-I*, *mhc-ii*, were detected in the infected and control samples. On the other hand, the test failed to detect genes involved with the lipid and protein metabolism (*fasn*, *lpl*, and *ilpea/b*) and stress response (*hsp70*, *hsp90*, *gr1* and *gr2*). The functions of fish skin mucus include sensory perception, locomotion, respiration, excretion, ionic and osmotic regulation. More importantly, it is also the first line of defense against various pathogens for the rich immune factors in it (reviewed by Esteban, 2012). Considering the mucus being a gelatinous, protein and carbohydrate-rich matrix that also inhibit a complex network of commensal and pathogenic microbiota, evidence have shown that there is a variety of leukocytes in teleost skin-associated lymphoid tissue (SALT), including T cells, B cells, plasma cells, macrophages and granulocytes (Salinas et al., 2011).

Salmon skin mucus has been studied for stress related biomarkers, mainly cortisol, stress-related proteins and enzymes, and glucose (Franco-Martinez et al., 2022; Madaro et al., 2023). To date, the repertoire of immune factors present in the salmon skin mucus is not well understood, and these studies were more focused on non-specific humoural parameters like cortisol, peroxidase, esterase, lysozyme, protease, alkaline phosphatase, immunoglobulins, complement (Djordjevic, Byron Morales-Lange, et al., 2021; Echeverría-Bugueño et al., 2023; Fast et al., 2002; Madaro et al., 2023; Tartor et al., 2020). Salmon skin mucus transcripts like cytokines (*il-1β* and *il-10*) and heat shock proteins (*hsp70* and *hsp90*) were also successfully quantified after stressor exposure (Osório et al., 2022).

In the current study, antigen presentation-related genes (*mhc-i* and *mhc-ii*) and immune response signalling gene *calm* were expressed constitutively, and no induction was observed until 96 h post infection. This can be explained by the fact that the regional immune response in fish skin mucus is dependent on the recognition of pathogens by PRRs. In this experiment, the live *V. anguillarum* were intraperitoneally injected, and thus the amount of pathogen the mucosal-associated lymphoid tissue was exposed to directly was limited, leading to the result that the induced pro-inflammatory cytokines were observed in both spleen and head kidney tissues at time point 72 h and 96 h post infection, but not in mucus. Based on the survival curve, a sharp drop in survival was observed between day 5 and day 10. An immune response should be observed between this time window when the pathogen was starting to be shed into the water.

2.4.3 Short-term response using *Vibrio anguillarum* as a disease model

To date, the molecular mechanisms underlying *V. anguillarum* pathogenesis in salmon are not well understood. This is an important topic because host-pathogen interactions may directly shape the result of an infection. A disease model was used using Chinook salmon juveniles and live *V. anguillarum* to investigate the early-stage responses by Chinook salmon. When the Chinook salmon juveniles were i.p. injected with live *V. anguillarum*, different immune responses were observed between internal lymphoid organs (spleen, head kidney) and mucosal lymphoid tissues (skin mucus, gill), although stress and metabolic responses were not observed in all samples. At 72 h and 96 h post infection, no immune responses were observed from skin mucus (SALT) or gill (GIALT) tissue. By contrast, at 72 h, expression of pro-inflammatory cytokine genes *il-1β* and *il-8* were increased in spleen and head kidney. Increased expression was continued up to 96 h, although the full course of immune response against *V. anguillarum* was not described in this study.

Notably, during the course of sampling (0-96 h post infection), the control group and the infected group had a similar fish survival rate. Starting at day 5 (120 h) post infection, the survival rate in the infected group started to drop significantly while it was stable in the control group until the end of observation. The early mortalities were more likely to be caused by the stress from handling and injection wound. A previous study in Coho salmon (*Oncorhynchus kisutch*) discovered that hand injection could cause a two-time higher cortisol response compared to automated injection procedures (Sharpe, 2007). During an oil-based vaccination trial in Atlantic salmon, an increased number of mast cells and macrophages

were observed at the injection site, which have been previously associated with wound healing and the initiation of inflammation (Mutoloki et al., 2006; 2010).

Natural *V. anguillarum* infection in teleost fishes either occurs through penetration of the fish skin, or by oral intake of contaminated water. Subsequently, the pathogen enters the blood stream and replicates, resulting in septicaemia and infection of various organs like spleen and head kidney (reviewed by Frans et al., 2011). The teleost head kidney is the primary lymphoid organ where leukocytes are generated and pathogens are filtered from blood, but it is also an endocrine organ that is a part of both hypothalamus–pituitary–interrenal (HPI) and brain-sympathetic-chromaffin cell (BSC) axes. Thus, the teleost head kidney is the centre of immune–endocrine interactions. On the other hand, the spleen is a secondary lymphoid organ where blood is filtered and immune responses are initiated against extracellular pathogens like *V. anguillarum* (reviewed by Secombes & Wang, 2012). As a result, transcript expression in the head kidney and spleen reflect systemic immune responses and the stress status of infected fish. A previous study investigating the transcriptional profiles of *V. anguillarum* infected Rainbow trout using spleen and head kidney indicated that proinflammatory cytokine transcripts (*il-6, il-1β, tnfα*) were upregulated and transcripts of glucocorticoid and mineralocorticoid receptors (*grα, grβ, mrα, mrβ*) were downregulated 120 h post infection (Hou et al., 2021). The induced proinflammatory cytokines *il-6, il-1β, tnfα*, along with *il-8*, have been regarded as the markers for M1 macrophage polarization, which is crucial for the activation of proinflammatory cytokine cascade (Shapouri-Moghaddam et al., 2018).

Locally, there was no immune or stress responses observed at 72 h and 96 h post infection in mucus and gill samples. It has been reported that in salmon, gill and skin mucus are essential for local pathogen recognition, immune response initiation, and stress response (Lazado et al., 2021; Valdenegro-Vega et al., 2014). Because there was no vibriosis-like symptom (for instance, skin lesion) observed until 96 h post infection and the initial systemic immune response was not observed until 72 h post infection, there was a limited amount of *V. anguillarum* released into the water that could challenge SALT and GIALT and induce a response. A previous study investigating the *Vibrio anguillarum* bacterin vaccine-induced immune response in rainbow trout discovered that, after 1 min vaccine immersion challenge, transcript expressions of lysozyme, complement 3, heat shock protein 70 and cyclo-oxygenas-2 and transforming growth factor-beta was significantly elevated in skin mucus and gill tissue, while pro-inflammatory cytokines *il-1β*, *il-6*, and *il-10* were only observed to increase in gill (Khansari et al., 2018).

At the systemic level, expression of *il-1β* and *il-8* transcripts were significantly induced in spleen at time point 72h and 96 h. In head kidney, *il-1β* was also induced at 72 h and 96 h, but *il-8* was not detected with significant increase between the control and infected groups at time point 72 h and 96 h. Although *tnfα* was not tested in this study, these three cytokines are expected to increase early in the innate immune response in salmon bacterial disease models (Fast et al., 2007). As a gram-negative bacterium, *V. anguillarum* is coated with LPS and flagellin that can be recognized by a range of surface Toll-like receptors (TLRs), mostly on macrophages, which immediately activates the NF-κB signaling pathway

and downstream cytokine production (Gao et al., 2022; Tiainen et al., 1994; Tsujita et al., 2004; Tsukada et al., 2005). In an *in vitro* challenge model made of heat-killed *V. anguillarum* and rainbow trout macrophage cell line, increases of *il-1β* transcripts initiated at 4 h and peaked at 12 h post challenge (Frenette et al., 2023). Another study investigated using an *Aeromonas salmonicida* challenge in pink salmon (*Oncorhynchus gorbuscha*) and chum salmon (*Oncorhynchus keta*) *in vivo.* They reported that in head kidney, increases of *il-1β, il-8, and tnfα* transcripts was observed 6 h post infection in both species, but discrepancies appeared at 24 h (Fast et al., 2007). Specifically, they pointed out that the expression of *il-8* can be enhanced by *il-1β* and *tnfα*, but this potent chemotactic factor then recruits neutrophils that release more *il-8*, resulting in a longer time window of *il-8* expression. Thus, in this experiment expression levels of *il-1β* and *il-8* were not examined for the full course of infection, and it is anticipated that *il-1β* would peak earlier than *il-8.* The reaction time for increased pro-inflammatory cytokine expression is dependent on species, pathogen dose, and the age of the host. To summarize, the innate immune response observed in this study was presumably still in progress at the last timepoint, which would include longer expression of *il-1β* and *il-8* as well as the recruitment of more leukocytes.

In this study, the expression levels of stress and metabolism-related genes were found to be stable in Chinook salmon spleen, head kidney, gill, and mucus. This may suggest that *V. anguillarum* infection did not cause metabolic remodelling or impairment on stressors coping mechanisms in Chinook salmon within 96 h of infection. In previous studies, evidence was found that a 2-week parasitic infection (*Ceratonova shasta* and *Parvicapsula*

minibicornis) resulted high pathogen load and general stress responses in Chinook salmon gill, as well as depleted hepatic glycogen stores (Mauduit et al., 2022). Another study described the metabolic remodeling caused by *Pseudomonas plecoglossicida* infection in orange-spotted grouper (*Epinephelus coioides*) spleen tissue, where lipids and amino acid metabolism were found to be significantly down regulated at 96 h post infection (Zeng et al., 2022).

2.5 Conclusions

In this study, the novel nanofluidic OpenArray™ chip was shown to be a reliable tool to characterize early immune response over the course of *V. anguillarum* infection in Chinook salmon. The OpenArray™ chip data was validated with SYBR RT-qPCR data by Pearson's correlation and simple linear regression analyses. Based on on-chip primer efficiency tests, the following list of genes, *rpl13a*, *ef1α*, *calm*, *mhc-i*, *mhc-ii*, *prdx*, *il-1β*, *ifn-γ*, *mx*, *stat1*, *il-8*, *tapbp*, *ampkα*, *fasn*, *ctsd*, *ilpea/b*, *lpl*, *gr1*, *gr2*, *serpinh1*, *hsp70*, *hsp90*, *mt1*, *mt2*, *casp9*, *ifn-1* and *cirbp*, were good candidates for future validations. Based on the Pearson's correlation analysis, the OpenArray™ chip was proven to be a reliable device to quantify the following genes: *calm*, *mhc-i*, *mhc-ii*, *il-1β*, *il-8*, and *tapbp*. In Chinook salmon, *rpl13a* was a better endogenous control compared to *ef1α* and *18S*. Nevertheless, multiple endogenous controls should be used to counteract possible variations within the endogenous gene expressions. Compared to spleen and head kidney, salmon skin mucus can be a good immune transcript matrix, although its ability to reflect acute systemic immune responses was not observed. The fish culture water was proven to be not useful for biomarker recovery based on current

sample processing methods. Based on the data from spleen and head kidney tissues, an typical early pro-inflammatory response was observed.

2.6 Future directions

Accordingly, future research should emphasize testing OpenArray™ chip using more salmon species before the chip to be applied as a standard tool for disease and physiological status monitoring. As an important pro-inflammatory cytokine, *tnfα* transcript expression was missing in this study. The primers and probe for *tnfα* should be modified to increase the specificity for Chinook salmon *tnfα* sequence. The survival curves indicated that the full course of acute immune response in Chinook salmon juveniles may take longer than 96 h (a sharp drop in survival observed between day 5 and day 10), thus a longer pathogen exposure trial should be designed in future trials.

Salmon skin mucus may be a good option for diagnostics monitoring at the transcript level, but a different pathogen exposure method (for instance, pathogen emersion) should be used instead of i.p. injection to illicit a stronger local immune response. As for the sampling methods, scraping method was used in this thesis but it may cause substantial damage to skin epithelium. Instead, sampling mucus using absorptive materials is recommended because it has been proven to be less invasive, and between these two methods there was no difference in the quantity of antigen specific immunoglobulin M and complement component 5 retrieved (Tartor et al., 2020). Although in this trial the Chinook salmon were maintained in fresh water, most salmonids are anadromous, and the type of water environment should also be considered when evaluating salmon immune responses using skin mucus. It is believed

that the skin mucosal immunity is gradually developed during salmon smoltification, and it was observed that compared to fish in seawater, the mucosal alkaline phosphatase and protease activities were significantly lower in freshwater in three salmon species (Fast et al., 2002; Karlsen et al., 2018). These findings could be furtherly investigated using transcriptomics. As for the culture water samples, the major concern is the mRNA stability in environment (5 min by average) (Moran et al., 2013). In future trials, water samples should be filtered and frozen within this time window.

Globally, salmonid aquaculture is one of the fastest expanding food production industries. Along with the fast development of salmon aquaculture, pathogens, parasites, and pests are considered the main barrier to industry expansion, causing consistent annual loss and pose chronic risks to salmon health management. In this thesis, a novel, swift OpenArray™ Taqman® RT-qPCR chip was validated in testing six immune response-related genes using a Chinook salmon disease model. This research provides valuable reference to the methodologies of OpenArray™ Taqman® RT-qPCR chip design and validation. As a promising high-throughput tool that can be included in the standardized fish disease diagnostics and surveillance systems, the OpenArray™ Taqman® RT-qPCR chip can be applied in multiple scenarios like fish stock selection, wild animal preservation, and vaccination development, which may significantly expand the current understandings in combating salmon waterborne diseases.

References

Adam, D. (2022). World population hits eight billion—Here's how researchers predict it will grow. *Nature*, d41586-022-03720–03726. https://doi.org/10.1038/d41586-022-03720-6

Andersen, C. L., Jensen, J. L., & Ørntoft, T. F. (2004). Normalization of Real-Time Quantitative Reverse Transcription-PCR Data: A Model-Based Variance Estimation Approach to Identify Genes Suited for Normalization, Applied to Bladder and Colon Cancer Data Sets. *Cancer Research*, *64*(15), 5245–5250. https://doi.org/10.1158/0008-5472.CAN-04-0496

Arango Duque, G., & Descoteaux, A. (2014). Macrophage cytokines: involvement in immunity and infectious diseases. *Frontiers in immunology*, *5*, 491.

Asche, F., & Bjørndal, T. (2011). *The economics of salmon aquaculture* (2nd ed). Wiley-Blackwell.

Awad, E., El-Fiqi, A., Austin, D., & Lyndon, A. (2020). Possible effect of lesser galangal (*Alpinia officinarum*) extracts encapsulated into mesoporous silica nanoparticles on the immune status of rainbow trout (*Oncorhynchus n*). *Aquaculture Research*, *51*(9), 3674–3684. https://doi.org/10.1111/are.14717

Balasch, J. C., & Tort, L. (2019). Netting the Stress Responses in Fish. *Frontiers in Endocrinology*, *10*, 62. https://doi.org/10.3389/fendo.2019.00062

Bangia, N., Lehner, P. J., Hughes, E. A., Surman, M., & Cresswell, P. (1999). The N-terminal region of tapasin is required to stabilize the MHC class I loading complex.

European Journal of Immunology, *29*(6), 1858–1870. https://doi.org/10.1002/(SICI)1521-4141(199906)29:06<1858::AID-IMMU1858>3.0.CO;2-C

Barton, J. R., Baeza-González, S., & Román, Á. (2023). Unravelling sustainable salmon aquaculture: An historical political ecology of a business responsibility discourse, 1970–2020. *Maritime Studies*, *22*(2), 10. https://doi.org/10.1007/s40152-023-00297-2

Bastos Gomes, G., Hutson, K. S., Domingos, J. A., Chung, C., Hayward, S., Miller, T. L., & Jerry, D. R. (2017). Use of environmental DNA (eDNA) and water quality data to predict protozoan parasites outbreaks in fish farms. *Aquaculture*, *479*, 467–473. https://doi.org/10.1016/j.aquaculture.2017.06.021

Bateman, A. W., Schulze, A. D., Kaukinen, K. H., Tabata, A., Mordecai, G., Flynn, K., Bass, A., Di Cicco, E., & Miller, K. M. (2021). Descriptive multi-agent epidemiology via molecular screening on Atlantic salmon farms in the northeast Pacific Ocean. *Scientific Reports*, *11*(1), 3466. https://doi.org/10.1038/s41598-020-78978-9

Beemelmanns, A., Zanuzzo, F. S., Xue, X., Sandrelli, R. M., Rise, M. L., & Gamperl, A. K. (2021). The transcriptomic responses of Atlantic salmon (Salmo salar) to high temperature stress alone, and in combination with moderate hypoxia. *BMC Genomics*, *22*(1), 261. https://doi.org/10.1186/s12864-021-07464-x

Bemelmans, M. H. A., Van Tits, L. J. H., & Buurman, W. A. (2017). Tumor Necrosis Factor: Function, Release and Clearance. *Critical Reviews in Immunology*, *37*(2–6), 249–259. https://doi.org/10.1615/CritRevImmunol.v37.i2-6.50

Birlanga, V. B., McCormack, G., Ijaz, U. Z., MacCarthy, E., Smith, C., & Collins, G. (2022). Dynamic gill and mucus microbiomes during a gill disease episode in farmed Atlantic salmon. *Scientific Reports*, *12*(1), 16719. https://doi.org/10.1038/s41598-022-17008-2

Boltaña, S., Roher, N., Goetz, F. W., & MacKenzie, S. A. (2011). PAMPs, PRRs and the genomics of gram negative bacterial recognition in fish. *Developmental & Comparative Immunology*, *35*(12), 1195–1203. https://doi.org/10.1016/j.dci.2011.02.010

Braden, L. M., Whyte, S. K., Brown, A. B., Iderstine, C. V., Letendre, C., Groman, D., ... & Fast, M. D. (2019). Vaccine-induced protection against furunculosis involves pre-emptive priming of humoral immunity in Arctic charr. Frontiers in immunology, 10, 120.

Broughton, R. E., Betancur-R., R., Li, C., Arratia, G., & Ortí, G. (2013). Multi-locus phylogenetic analysis reveals the pattern and tempo of bony fish evolution. *PLoS Currents*. https://doi.org/10.1371/currents.tol.2ca8041495ffafd0c92756e75247483e

Bush, S. R., Belton, B., Little, D. C., & Islam, M. S. (2019). Emerging trends in aquaculture value chain research. *Aquaculture*, *498*, 428–434. https://doi.org/10.1016/j.aquaculture.2018.08.077

Canestrini, G. (1893). La malattia dominante delle anguille. *Atti Ist. Veneto Sci. Lett. Arti Cl. Sci. Mat. Nat.*, *7*, 809-814.

Castro, R., Bernard, D., Lefranc, M. P., Six, A., Benmansour, A., & Boudinot, P. (2011a). T cell diversity and TcR repertoires in teleost fish. *Fish & Shellfish Immunology*, *31*(5), 644–654. https://doi.org/10.1016/j.fsi.2010.08.016

Castro, R., Zou, J., Secombes, C. J., & Martin, S. A. (2011b). Cortisol modulates the induction of inflammatory gene expression in a rainbow trout macrophage cell line. Fish & Shellfish Immunology, 30(1), 215-223.

Chen, J., Liu, C., & Yang, T. (2023). Killing effect of fish serum and mucus on Gyrodactylus cichlidarum (Platyhelminthes, Monogenea) mediated by complement. Aquaculture, 567, 739248.

Chin, D., & Means, A. R. (2000). Calmodulin: A prototypical calcium sensor. *Trends in Cell Biology*, *10*(8), 322–328. https://doi.org/10.1016/S0962-8924(00)01800-6

Chukwu-Osazuwa, J., Cao, T., Vasquez, I., Gnanagobal, H., Hossain, A., Machimbirike, V. I., & Santander, J. (2022). Comparative Reverse Vaccinology of Piscirickettsia salmonis, Aeromonas salmonicida, Yersinia ruckeri, Vibrio anguillarum and Moritella viscosa, Frequent Pathogens of Atlantic Salmon and Lumpfish Aquaculture. *Vaccines*, *10*(3), 473. https://doi.org/10.3390/vaccines10030473

Costello, C., & Ovando, D. (2019). Status, Institutions, and Prospects for Global Capture Fisheries. *Annual Review of Environment and Resources*, *44*(1), 177–200. https://doi.org/10.1146/annurev-environ-101718-033310

Crawford, S. S., & Muir, A. M. (2008). Global introductions of salmon and trout in the genus Oncorhynchus: 1870–2007. *Reviews in Fish Biology and Fisheries*, *18*(3), 313–344. https://doi.org/10.1007/s11160-007-9079-1

Dean, K. R., Oliveira, V. H. S., Wolff, C., Moldal, T., & Jansen, M. D. (2022). Description of ISAV-HPRΔ-positive salmon farms in Norway in 2020. *Journal of Fish Diseases*, *45*(1), 225–229. https://doi.org/10.1111/jfd.13538

Dettleff, P., Bravo, C., Patel, A., & Martinez, V. (2015). Patterns of Piscirickettsia salmonis load in susceptible and resistant families of Salmo salar. *Fish & Shellfish Immunology*, *45*(1), 67–71. https://doi.org/10.1016/j.fsi.2015.03.039

Directory of Fisheries. (2023). Atlantic salmon and rainbow trout. Retrieved July 9, 2023, from https://www.fiskeridir.no/English/Aquaculture/Statistics/Atlantic-salmon-and-rainbow-trout

Djordjevic, B., Morales-Lange, B., McLean Press, C., Olson, J., Lagos, L., Mercado, L., & Øverland, M. (2021). Comparison of Circulating Markers and Mucosal Immune Parameters from Skin and Distal Intestine of Atlantic Salmon in Two Models of Acute Stress. *International Journal of Molecular Sciences*, *22*(3), Article 3. https://doi.org/10.3390/ijms22031028

Djordjevic, Byron Morales-Lange, Margareth Øverland, Luis Mercado, & Leidy Lagos. (2021). Immune and proteomic responses to the soybean meal diet in skin and intestine mucus of Atlantic salmon (Salmo salar L.). *Aquaculture Nutrition*. https://doi.org/10.1111/anu.13248

Dragan, A. I., Pavlovic, R., McGivney, J. B., Casas-Finet, J. R., Bishop, E. S., Strouse, R. J., Schenerman, M. A., & Geddes, C. D. (2012). SYBR Green I: Fluorescence Properties and Interaction with DNA. *Journal of Fluorescence*, *22*(4), 1189–1199. https://doi.org/10.1007/s10895-012-1059-8

Echeverría-Bugueño, M., Irgang, R., Mancilla-Schulz, J., & Avendaño-Herrera, R. (2023). Healthy and infected Atlantic salmon (Salmo salar) skin-mucus response to

Tenacibaculum dicentrarchi under in vitro conditions. *Fish & Shellfish Immunology*, *136*, 108747. https://doi.org/10.1016/j.fsi.2023.108747

Espelid, S., Løkken, G. B., Steiro, K., & Bøgwald, J. (1996). Effects of cortisol and stress on the immune system in Atlantic Salmon (Salmo salarL.). *Fish & Shellfish Immunology*, *6*(2), 95–110. https://doi.org/10.1006/fsim.1996.0011

Esteban, M. (2012). An Overview of the Immunological Defenses in Fish Skin. *ISRN Immunology*, *2012*, 1–29. https://doi.org/10.5402/2012/853470

FAO. (2016). *Contributing to food security and nutrition for all*. FAO (Food and Agriculture Organization of the United Nations). https://www.fao.org/3/i5555e/i5555e.pdf

FAO. (2020). *The State of World Fisheries and Aquaculture (SOFIA)*. FAO (Food and Agriculture Organization of the United Nations). https://doi.org/10.4060/ca9229en

FAO. (2022). *The State of World Fisheries and Aquaculture 2022*. FAO (Food and Agriculture Organization of the United Nations). https://doi.org/10.4060/cc0461en

FAO. (2023a). *Fishery and Aquaculture Statistics. Global aquaculture production 1950-2021 (FishStatJ)*. In: FAO Fisheries and Aquaculture Division [online]. Rome. Updated 2023. www.fao.org/fishery/statistics/software/fishstatj/en

FAO. (2023b). *Salmon—Main producers see record-breaking exports | GLOBEFISH |* Food and Agriculture Organization of the United Nations. Retrieved July 10, 2023, from https://www.fao.org/in-action/globefish/market-reports/resource-detail/en/c/1640993/

Fast, M. D., Johnson, S. C., & Jones, S. R. M. (2007). Differential expression of the pro-inflammatory cytokines IL-1β-1, TNFα-1 and IL-8 in vaccinated pink (Oncorhynchus

gorbuscha) and chum (Oncorhynchus keta) salmon juveniles. *Fish & Shellfish Immunology*, *22*(4), 403–407. https://doi.org/10.1016/j.fsi.2006.06.012

Fast, M. D., Sims, D. E., Burka, J. F., Mustafa, A., & Ross, N. W. (2002). Skin morphology and humoral non-specific defence parameters of mucus and plasma in rainbow trout, coho and Atlantic salmon. *Comparative Biochemistry and Physiology Part A: Molecular & Integrative Physiology*, *132*(3), 645–657. https://doi.org/10.1016/S1095-6433(02)00109-5

Fernández-Alacid, L., Sanahuja, I., Ordóñez-Grande, B., Sánchez-Nuño, S., Viscor, G., Gisbert, E., Herrera, M., & Ibarz, A. (2018). Skin mucus metabolites in response to physiological challenges: A valuable non-invasive method to study teleost marine species. *Science of The Total Environment*, *644*, 1323–1335. https://doi.org/10.1016/j.scitotenv.2018.07.083

Figueroa, C., Torrealba, D., Morales-Lange, B., Mercado, L., Dixon, B., Conejeros, P., Silva, G., Soto, C., & Gallardo, J. A. (2022). Commercial Vaccines Do Not Confer Protection against Two Genogroups of Piscirickettsia salmonis, LF-89 and EM-90, in Atlantic Salmon. *Biology*, *11*(7), 993. https://doi.org/10.3390/biology11070993

Flajnik, M. F. (2018). A cold-blooded view of adaptive immunity. *Nature Reviews Immunology*, *18*(7), 438–453. https://doi.org/10.1038/s41577-018-0003-9

Franco-Martinez, L., Brandts, I., Reyes-López, F., Tort, L., Tvarijonaviciute, A., & Teles, M. (2022). Skin Mucus as a Relevant Low-Invasive Biological Matrix for the Measurement of an Acute Stress Response in Rainbow Trout (Oncorhynchus mykiss). *Water*, *14*(11), 1754. https://doi.org/10.3390/w14111754

Frans, I., Michiels, C. W., Bossier, P., Willems, K. A., Lievens, B., & Rediers, H. (2011). *Vibrio anguillarum* as a fish pathogen: Virulence factors, diagnosis and prevention. *Journal of Fish Diseases*, *34*(9), 643–661. https://doi.org/10.1111/j.1365-2761.2011.01279.x

Fregeneda-Grandes, J. M., González-Palacios, C., Pérez-Sánchez, T., Padilla, D., Real, F., & Aller-Gancedo, J. M. (2023). Limited Probiotic Effect of Enterococcus gallinarum L1, Vagococcus fluvialis L21 and Lactobacillus plantarum CLFP3 to Protect Rainbow Trout against Saprolegniosis. *Animals*, *13*(5), 954.

Frenette, A. P., Rodríguez-Ramos, T., Zanuzzo, F., Ramsay, D., Semple, S. L., Soullière, C., Rodríguez-Cornejo, T., Heath, G., McKenzie, E., Iwanczyk, J., Bruder, M., Aucoin, M. G., Gamperl, A. K., & Dixon, B. (2023). Expression of Interleukin-1β protein in vitro, ex vivo and in vivo salmonid models. *Developmental & Comparative Immunology*, *147*, 104767. https://doi.org/10.1016/j.dci.2023.104767

Gao, S., Liu, X., Han, B., Wang, N., Lv, X., Guan, X., Xu, G., Huang, J., Shi, W., & Liu, M. (2022). Salmonid alphavirus non-structural protein 2 is a key protein that activates the NF-κB signaling pathway to mediate inflammatory responses. *Fish & Shellfish Immunology*, *129*, 182–190. https://doi.org/10.1016/j.fsi.2022.08.059

Garseth, Å. H., Ekrem, T., & Biering, E. (2013). Phylogenetic Evidence of Long Distance Dispersal and Transmission of Piscine Reovirus (PRV) between Farmed and Wild Atlantic Salmon. *PLOS ONE*, *8*(12), e82202. https://doi.org/10.1371/journal.pone.0082202

Giroux, M., Gan, J., & Schlenk, D. (2019). The effects of bifenthrin and temperature on the endocrinology of juvenile Chinook salmon. *Environmental Toxicology and Chemistry*, *38*(4), 852–861. https://doi.org/10.1002/etc.4372

Gjedrem, T., & Gunnes, K. (1978). Comparison of growth rate in Atlantic salmon, pink salmon, Arctic char, sea trout and rainbow trout under Norwegian farming conditions. *Aquaculture*, *13*(2), 135–141. https://doi.org/10.1016/0044-8486(78)90107-2

Gjøen, T., Obach, A., Røsjø, C., Helland, B. G., Rosenlund, G., Hvattum, E., & Ruyter, B. (2004). Effect of dietary lipids on macrophage function, stress susceptibility and disease esistance in Atlantic Salmon (Salmo salar). Fish Physiology and Biochemistry, 30, 149-161.

Godoy, M., Kibenge, M. J. T., Montes De Oca, M., Pontigo, J. P., Coca, Y., Caro, D., Kusch, K., Suarez, R., Burbulis, I., & Kibenge, F. S. B. (2022). Isolation of a New Infectious Pancreatic Necrosis Virus (IPNV) Variant from Genetically Resistant Farmed Atlantic Salmon (Salmo salar) during 2021–2022. *Pathogens*, *11*(11), 1368. https://doi.org/10.3390/pathogens11111368

Gorissen, M., & Flik, G. (2016). 3 - The Endocrinology of the Stress Response in Fish: An Adaptation-Physiological View. In C. B. Schreck, L. Tort, A. P. Farrell, & C. J. Brauner (Eds.), *Fish Physiology* (Vol. 35, pp. 75–111). Academic Press. https://doi.org/10.1016/B978-0-12-802728-8.00003-5

Grimholt, U., Hauge, H., Hauge, A. G., Leong, J., & Koop, B. F. (2015). Chemokine receptors in Atlantic salmon. *Developmental & Comparative Immunology*, *49*(1), 79–95. https://doi.org/10.1016/j.dci.2014.11.009

Groner, M. L., Rogers, L. A., Bateman, A. W., Connors, B. M., Frazer, L. N., Godwin, S. C., Krkošek, M., Lewis, M. A., Peacock, S. J., Rees, E. E., Revie, C. W., & Schlägel, U. E. (2016). Lessons from sea louse and salmon epidemiology. *Philosophical Transactions of the Royal Society B: Biological Sciences*, *371*(1689), 20150203. https://doi.org/10.1098/rstb.2015.0203

Hansen, J., & La Patra, S. (2002). Induction of the rainbow trout MHC class I pathway during acute IHNV infection. *Immunogenetics*, *54*(9), 654–661. https://doi.org/10.1007/s00251-002-0509-x

Hoare, R., Shahin, K., McLean, K., Adams, A., & K. D. Thompson. (2022). Skin mucus proteins of rainbow trout (*Oncorhynchus mykiss*) in response to mucosal vaccination and challenge with *Flavobacterium psychrophilum*. *Journal of Fish Diseases*, *45*(3), 491–495. https://doi.org/10.1111/jfd.13562

Holland, P. M., Abramson, R. D., Watson, R., & Gelfand, D. H. (1991). Detection of specific polymerase chain reaction product by utilizing the 5'—3' exonuclease activity of Thermus aquaticus DNA polymerase. *Proceedings of the National Academy of Sciences*, *88*(16), 7276–7280. https://doi.org/10.1073/pnas.88.16.7276

Hong, S., Li, R., Xu, Q., Secombes, C. J., & Wang, T. (2013). Two Types of TNF-α Exist in Teleost Fish: Phylogeny, Expression, and Bioactivity Analysis of Type-II TNF-α3 in Rainbow Trout *Oncorhynchus mykiss*. *The Journal of Immunology*, *191*(12), 5959–5972. https://doi.org/10.4049/jimmunol.1301584

Hong, S., Zou, J., Crampe, M., Peddie, S., Scapigliati, G., Bols, N., Cunningham, C., & Secombes, C. J. (2001). The production and bioactivity of rainbow trout

(Oncorhynchus mykiss) recombinant IL-1β. *Veterinary Immunology and Immunopathology*, *81*(1–2), 1–14. https://doi.org/10.1016/S0165-2427(01)00328-2

Hou, Z. S., Xin, Y. R., Yang, X. D., Zeng, C., Zhao, H. K., Liu, M. Q., ... & Wen, H. S. (2021). Transcriptional profiles of genes related to stress and immune response in rainbow trout (Oncorhynchus mykiss) symptomatically or asymptomatically infected with vibrio anguillarum. *Frontiers in Immunology*, *12*, 639489.

Ikert, H., Lynch, M. D. J., Doxey, A. C., Giesy, J. P., Servos, M. R., Katzenback, B. A., & Craig, P. M. (2021). High Throughput Sequencing of MicroRNA in Rainbow Trout Plasma, Mucus, and Surrounding Water Following Acute Stress. *Frontiers in Physiology*, *11*, 588313. https://doi.org/10.3389/fphys.2020.588313

Illario, M., Giardino-Torchia, M. L., Sankar, U., Ribar, T. J., Galgani, M., Vitiello, L., Masci, A. M., Bertani, F. R., Ciaglia, E., Astone, D., Maulucci, G., Cavallo, A., Vitale, M., Cimini, V., Pastore, L., Means, A. R., Rossi, G., & Racioppi, L. (2008). Calmodulin-dependent kinase IV links Toll-like receptor 4 signaling with survival pathway of activated dendritic cells. *Blood*, *111*(2), 723–731. https://doi.org/10.1182/blood-2007-05-091173

Ingerslev, H. C., Lunder, T., & Nielsen, M. E. (2010). Inflammatory and regenerative responses in salmonids following mechanical tissue damage and natural infection. *Fish & Shellfish Immunology*, *29*(3), 440–450. https://doi.org/10.1016/j.fsi.2010.05.002

Ivanov, I. I., McKenzie, B. S., Zhou, L., Tadokoro, C. E., Lepelley, A., Lafaille, J. J., Cua, D. J., & Littman, D. R. (2006). The Orphan Nuclear Receptor RORγt Directs the

Differentiation Program of Proinflammatory IL-17+ T Helper Cells. *Cell*, *126*(6), 1121–1133. https://doi.org/10.1016/j.cell.2006.07.035

Jakob, E., Stryhn, H., Yu, J., Medina, M. H., Rees, E. E., Sanchez, J., & St-Hilaire, S. (2014). Epidemiology of Piscirickettsiosis on selected Atlantic salmon (Salmo salar) and rainbow trout (Oncorhynchus mykiss) salt water aquaculture farms in Chile. *Aquaculture*, *433*, 288–294. https://doi.org/10.1016/j.aquaculture.2014.06.018

Ji, Q., Wang, S., Ma, J., & Liu, Q. (2020). A review: Progress in the development of fish Vibrio spp. vaccines. *Immunology Letters*, *226*, 46–54. https://doi.org/10.1016/j.imlet.2020.07.002

Jørgensen, S. M., Grimholt, U., & Gjøen, T. (2007). Cloning and expression analysis of an Atlantic salmon (Salmo salar L.) tapasin gene. *Developmental & Comparative Immunology*, *31*(7), 708–719. https://doi.org/10.1016/j.dci.2006.10.004

Jørgensen, S. M., Hetland, D. L., Press, C. McL., Grimholt, U., & Gjøen, T. (2007). Effect of early infectious salmon anaemia virus (ISAV) infection on expression of MHC pathway genes and type I and II interferon in Atlantic salmon (Salmo salar L.) tissues. *Fish & Shellfish Immunology*, *23*(3), 576–588. https://doi.org/10.1016/j.fsi.2007.01.005

Kaattari, S. (2002). Affinity maturation in trout: Clonal dominance of high affinity antibodies late in the immune response. *Developmental & Comparative Immunology*, *26*(2), 191–200. https://doi.org/10.1016/S0145-305X(01)00064-7

Kania, P. W., Evensen, O., Larsen, T. B., & Buchmann, K. (2010). Molecular and immunohistochemical studies on epidermal responses in Atlantic salmon *Salmo salar*

L. induced by *Gyrodactylus salaris* Malmberg, 1957. *Journal of Helminthology*, *84*(2), 166–172. https://doi.org/10.1017/S0022149X09990460

Karlsen, C., Ytteborg, E., Timmerhaus, G., Høst, V., Handeland, S., Jørgensen, S. M., & Krasnov, A. (2018). Atlantic salmon skin barrier functions gradually enhance after seawater transfer. *Scientific Reports*, *8*(1), 9510. https://doi.org/10.1038/s41598-018-27818-y

Khansari, A. R., Balasch, J. C., Vallejos-Vidal, E., Parra, D., Reyes-López, F. E., & Tort, L. (2018). Comparative immune-and stress-related transcript response induced by air exposure and Vibrio anguillarum bacterin in rainbow trout (Oncorhynchus mykiss) and gilthead seabream (Sparus aurata) mucosal surfaces. Frontiers in immunology, 9, 856.

Kim, H.-P., & Leonard, W. J. (2007). CREB/ATF-dependent T cell receptor–induced *FoxP3* gene expression: A role for DNA methylation. *The Journal of Experimental Medicine*, *204*(7), 1543–1551. https://doi.org/10.1084/jem.20070109

Komatsu, K., Tsutsui, S., Hino, K., Araki, K., Yoshiura, Y., Yamamoto, A., Nakamura, O., & Watanabe, T. (2009). Expression profiles of cytokines released in intestinal epithelial cells of the rainbow trout, Oncorhynchus mykiss, in response to bacterial infection. *Developmental & Comparative Immunology*, *33*(4), 499–506. https://doi.org/10.1016/j.dci.2008.09.012

Krasnov, A., Johansen, L.-H., Karlsen, C., Sveen, L., Ytteborg, E., Timmerhaus, G., Lazado, C. C., & Afanasyev, S. (2021). Transcriptome Responses of Atlantic Salmon (Salmo

salar L.) to Viral and Bacterial Pathogens, Inflammation, and Stress. *Frontiers in Immunology*, *12*. https://www.frontiersin.org/articles/10.3389/fimmu.2021.705601

Kurpe, S. R., Sukhovskaya, I. V., Borvinskaya, E. V., Morozov, A. A., Parshukov, A. N., Malysheva, I. E., Vasileva, A. V., Chechkova, N. A., & Kuchko, T. Y. (2022). Physiological and Biochemical Characteristics of Rainbow Trout with Severe, Moderate and Asymptomatic Course of Vibrio anguillarum Infection. *Animals*, *12*(19), 2642. https://doi.org/10.3390/ani12192642

Lai, F., Royan, M. R., Gomes, A. S., Espe, M., Aksnes, A., Norberg, B., Gelebart, V., & Rønnestad, I. (2021). The stress response in Atlantic salmon (Salmo salar L.): Identification and functional characterization of the corticotropin-releasing factor (crf) paralogs. *General and Comparative Endocrinology*, *313*, 113894. https://doi.org/10.1016/j.ygcen.2021.113894

Laing, K. J., Wang, T., Zou, J., Holland, J., Hong, S., Bols, N., Hirono, I., Aoki, T., & Secombes, C. J. (2001). Cloning and expression analysis of rainbow trout *Oncorhynchus mykiss* tumour necrosis factor-α. *European Journal of Biochemistry*, *268*(5), 1315–1322. https://doi.org/10.1046/j.1432-1327.2001.01996.x

Laing, K. J., Zou, J. J., Wang, T., Bols, N., Hirono, I., Aoki, T., & Secombes, C. J. (2002). Identification and analysis of an interleukin 8-like molecule in rainbow trout Oncorhynchus mykiss. *Developmental & Comparative Immunology*, *26*(5), 433–444. https://doi.org/10.1016/S0145-305X(01)00092-1

Landry, J. D., Blanch, E. W., & Torley, P. J. (2023). Chemical Indicators of Atlantic Salmon Quality. *Food Reviews International*, 1–31. https://doi.org/10.1080/87559129.2023.2221332

Lazado, C. C., Timmerhaus, G., Breiland, M. W., Pittman, K., & Hytterød, S. (2021). Multiomics Provide Insights into the Key Molecules and Pathways Involved in the Physiological Adaptation of Atlantic Salmon (Salmo salar) to Chemotherapeutic-Induced Oxidative Stress. *Antioxidants*, *10*(12), 1931. https://doi.org/10.3390/antiox10121931

Little, A. G., Loughland, I., & Seebacher, F. (2020). What do warming waters mean for fish physiology and fisheries? *Journal of Fish Biology*, *97*(2), 328–340. https://doi.org/10.1111/jfb.14402

Little, Newton, R. W., & Beveridge, M. C. M. (2016). Aquaculture: A rapidly growing and significant source of sustainable food? Status, transitions and potential. *Proceedings of the Nutrition Society*, *75*(3), 274–286. https://doi.org/10.1017/S0029665116000665

Liu, T., Zhang, L., Joo, D., & Sun, S.-C. (2017). NF-κB signaling in inflammation. *Signal Transduction and Targeted Therapy*, *2*(1), Article 1. https://doi.org/10.1038/sigtrans.2017.23

Loo, G. H., Sutton, D. L., & Schuller, K. A. (2012). Cloning and functional characterisation of a peroxiredoxin 1 (NKEF A) cDNA from Atlantic salmon (Salmo salar) and its expression in fish infected with Neoparamoeba perurans. *Fish & Shellfish Immunology*, *32*(6), 1074–1082. https://doi.org/10.1016/j.fsi.2012.03.002

Luan, S., & Wang, C. (2021). Calcium Signaling Mechanisms Across Kingdoms. *Annual Review of Cell and Developmental Biology*, *37*(1), 311–340. https://doi.org/10.1146/annurev-cellbio-120219-035210

MacAulay, S., Ellison, A. R., Kille, P., & Cable, J. (2022). Moving towards improved surveillance and earlier diagnosis of aquatic pathogens: From traditional methods to emerging technologies. *Reviews in Aquaculture*, *14*(4), 1813–1829. https://doi.org/10.1111/raq.12674

Machimbirike, V. I., Vasquez, I., Cao, T., Chukwu-Osazuwa, J., Onireti, O., Segovia, C., Khunrae, P., Rattanarojpong, T., Booman, M., Jones, S., Soto-Davila, M., Dixon, B., & Santander, J. (2023). Comparative Genomic Analysis of Virulent Vibrio (Listonella) anguillarum Serotypes Revealed Genetic Diversity and Genomic Signatures in the O-Antigen Biosynthesis Gene Cluster. *Microorganisms*, *11*(3), 792. https://doi.org/10.3390/microorganisms11030792

Mächler, E., Deiner, K., Spahn, F., & Altermatt, F. (2016). Fishing in the Water: Effect of Sampled Water Volume on Environmental DNA-Based Detection of Macroinvertebrates. *Environmental Science & Technology*, *50*(1), 305–312. https://doi.org/10.1021/acs.est.5b04188

MacKenzie, S., Balasch, J. C., Novoa, B., Ribas, L., Roher, N., Krasnov, A., & Figueras, A. (2008). Comparative analysis of the acute response of the trout, O. mykiss, head kidney to in vivo challenge with virulent and attenuated infectious hematopoietic necrosis virus and LPS-induced inflammation. *BMC Genomics*, *9*(1), 141. https://doi.org/10.1186/1471-2164-9-141

Madaro, A., Nilsson, J., Whatmore, P., Roh, H., Grove, S., Stien, L. H., & Olsen, R. E. (2023). Acute stress response on Atlantic salmon: A time-course study of the effects on plasma metabolites, mucus cortisol levels, and head kidney transcriptome profile. *Fish Physiology and Biochemistry*, *49*(1), 97–116. https://doi.org/10.1007/s10695-022-01163-4

Maisey, K., Montero, R., & Christodoulides, M. (2017). Vaccines for piscirickettsiosis (salmonid rickettsial septicaemia, SRS): The Chile perspective. *Expert Review of Vaccines*, *16*(3), 215–228. https://doi.org/10.1080/14760584.2017.1244483

Mauduit, F., Segarra, A., Mandic, M., Todgham, A. E., Baerwald, M. R., Schreier, A. D., Fangue, N. A., & Connon, R. E. (2022). Understanding risks and consequences of pathogen infections on the physiological performance of outmigrating Chinook salmon. *Conservation Physiology*, *10*(1), coab102. https://doi.org/10.1093/conphys/coab102

Melo, R. M. C., Cruz, C. K. F., Weber, A. A., Luz, R. K., Bazzoli, N., & Rizzo, E. (2022). Effects of temperature manipulation on gamete development and reproductive activity in the farmed catfish Lophiosilurus alexandri. *Animal Reproduction Science*, 107100. https://doi.org/10.1016/j.anireprosci.2022.107100

Miranda, C. D., Godoy, F. A., & Lee, M. R. (2018). Current Status of the Use of Antibiotics and the Antimicrobial Resistance in the Chilean Salmon Farms. *Frontiers in Microbiology*, *9*, 1284. https://doi.org/10.3389/fmicb.2018.01284

Mishra, S., Seshagiri, B., Rathod, R., Sahoo, S. N., Choudhary, P., Patel, S., Behera, D. K., Ojha, D. K., Jena, A., Namburu, P. K., & Swain, P. (2023). Recent advances in fish

disease diagnosis, therapeutics, and vaccine development. In *Frontiers in Aquaculture Biotechnology* (pp. 115–145). Elsevier. https://doi.org/10.1016/B978-0-323-91240-2.00011-7

Miyata, K., Inoue, Y., Amano, Y., Nishioka, T., Yamane, M., Kawaguchi, T., Morita, O., & Honda, H. (2021). Fish environmental RNA enables precise ecological surveys with high positive predictivity. *Ecological Indicators*, *128*, 107796. https://doi.org/10.1016/j.ecolind.2021.107796

Mommsen, T. P., Vijayan, M. M., & Moon, T. W. (1999). Cortisol in teleosts: Dynamics, mechanisms of action, and metabolic regulation. *Reviews in Fish Biology and Fisheries*, *9*(3), 211–268. https://doi.org/10.1023/A:1008924418720

Montero, J., Coll, J., Sevilla, N., Cuesta, A., Bols, N. C., & Tafalla, C. (2008). Interleukin 8 and CK-6 chemokines specifically attract rainbow trout (Oncorhynchus mykiss) RTS11 monocyte–macrophage cells and have variable effects on their immune functions. *Developmental & Comparative Immunology*, *32*(11), 1374–1384. https://doi.org/10.1016/j.dci.2008.05.004

Morales-Lange, B., Ramírez-Cepeda, F., Schmitt, P., Guzmán, F., Lagos, L., Øverland, M., Wong-Benito, V., Imarai, M., Fuentes, D., Boltaña, S., Alcaíno, J., Soto, C., & Mercado, L. (2021). Interferon Gamma Induces the Increase of Cell-Surface Markers (CD80/86, CD83 and MHC-II) in Splenocytes From Atlantic Salmon. *Frontiers in Immunology*, *12*. https://doi.org/10.3389/fimmu.2021.666356

Moran, M. A., Satinsky, B., Gifford, S. M., Luo, H., Rivers, A., Chan, L.-K., Meng, J., Durham, B. P., Shen, C., Varaljay, V. A., Smith, C. B., Yager, P. L., & Hopkinson, B.

M. (2013). Sizing up metatranscriptomics. *The ISME Journal*, *7*(2), Article 2. https://doi.org/10.1038/ismej.2012.94

Mordecai, G. J., Miller, K. M., Bass, A. L., Bateman, A. W., Teffer, A. K., Caleta, J. M., Di Cicco, E., Schulze, A. D., Kaukinen, K. H., Li, S., Tabata, A., Jones, B. R., Ming, T. J., & Joy, J. B. (2021). Aquaculture mediates global transmission of a viral pathogen to wild salmon. *Science Advances*, *7*(22), eabe2592. https://doi.org/10.1126/sciadv.abe2592

Mutoloki, S., Reite, O. B., Brudeseth, B., Tverdal, A., & Evensen, Ø. (2006). A comparative immunopathological study of injection site reactions in salmonids following intraperitoneal injection with oil-adjuvanted vaccines. *Vaccine, 24*(5), 578-588.

Mutoloki, S., Cooper, G. A., Marjara, I. S., Koop, B. F., & Evensen, Ø. (2010). High gene expression of inflammatory markers and IL-17A correlates with severity of injection site reactions of Atlantic salmon vaccinated with oil-adjuvanted vaccines. *BMC genomics*, *11*, 1-15.

Mourich, DanV., Hansen, J., & Leong, J. (1995). Natural killer cell enhancement factor-like gene in rainbow trout (Oncorhynchus mykiss). *Immunogenetics*, *42*(5). https://doi.org/10.1007/BF00179413

Muthupandian, A., Waly, D., & Magor, B. G. (2021). Do ectothermic vertebrates have a home in which to affinity mature their antibody responses? *Developmental & Comparative Immunology*, *119*, 104021. https://doi.org/10.1016/j.dci.2021.104021

Narvaez, E., Berendsen, J., Guzmán, F., Gallardo, J. A., & Mercado, L. (2010). An immunological method for quantifying antibacterial activity in Salmo salar (Linnaeus, 1758) skin mucus. Fish & Shellfish Immunology, 28(1), 235-239.

Neely, H. R., & Flajnik, M. F. (2016). Emergence and Evolution of Secondary Lymphoid Organs. *Annual Review of Cell and Developmental Biology*, *32*(1), 693–711. https://doi.org/10.1146/annurev-cellbio-111315-125306

NIWA. (2020). Retrieved on July 01, 2023. https://niwa.co.nz/aquaculture/species/chinook-salmon

Olive, A. J., & Sassetti, C. M. (2016). Metabolic crosstalk between host and pathogen: Sensing, adapting and competing. *Nature Reviews Microbiology*, *14*(4), Article 4. https://doi.org/10.1038/nrmicro.2016.12

Omaima Harun, N., Zou, J., Zhang, Y.-A., Nie, P., & Secombes, C. J. (2008). The biological effects of rainbow trout (Oncorhynchus mykiss) recombinant interleukin-8. *Developmental & Comparative Immunology*, *32*(6), 673–681. https://doi.org/10.1016/j.dci.2007.10.005

Øvergård, A. C., Eichner, C., Nuñez-Ortiz, N., Kongshaug, H., Borchel, A., & Dalvin, S. (2023). Transcriptomic and targeted immune transcript analyses confirm localized skin immune responses in Atlantic salmon towards the salmon louse. *Fish & Shellfish Immunology*, *138*, 108835.

Palaksha, K. J., Shin, G. W., Kim, Y. R., & Jung, T. S. (2008). Evaluation of non-specific immune components from the skin mucus of olive flounder (Paralichthys olivaceus). Fish & shellfish immunology, 24(4), 479-488.

Papageorgiou, S. N. (2022). On correlation coefficients and their interpretation. *Journal of Orthodontics*, *49*(3), 359–361. https://doi.org/10.1177/14653125221076142

Pérez, T., Balcázar, J. L., Ruiz-Zarzuela, I., Halaihel, N., Vendrell, D., de Blas, I., & Múzquiz, J. L. (2010). Host–microbiota interactions within the fish intestinal ecosystem. Mucosal immunology, 3(4), 355-360.

Perezcasanova, J., Rise, M., Dixon, B., Afonso, L., Hall, J., Johnson, S., & Gamperl, A. (2008). The immune and stress responses of Atlantic cod to long-term increases in water temperature. *Fish & Shellfish Immunology*, *24*(5), 600–609. https://doi.org/10.1016/j.fsi.2008.01.012

Pfaffl, M. W., Tichopad, A., Prgomet, C., & Neuvians, T. P. (2004). Determination of stable housekeeping genes, differentially regulated target genes and sample integrity: BestKeeper – Excel-based tool using pair-wise correlations. *Biotechnology Letters*, *26*(6), 509–515. https://doi.org/10.1023/B:BILE.0000019559.84305.47

Reite, O. B. (1997). Mast cells/eosinophilic granule cells of salmonids: Staining properties and responses to noxious agents. *Fish & Shellfish Immunology*, *7*(8), 567–584. https://doi.org/10.1006/fsim.1997.0108

Rieger, A. M., & Barreda, D. R. (2011). Antimicrobial mechanisms of fish leukocytes. Developmental & Comparative Immunology, 35(12), 1238-1245.

Rizvi, S. M., & Raghavan, M. (2010). Mechanisms of Function of Tapasin, a Critical Major Histocompatibility Complex Class I Assembly Factor. *Traffic*, *11*(3), 332–347. https://doi.org/10.1111/j.1600-0854.2009.01025.x

Robertsen, B. (2018). The role of type I interferons in innate and adaptive immunity against viruses in Atlantic salmon. *Developmental & Comparative Immunology*, *80*, 41–52. https://doi.org/10.1016/j.dci.2017.02.005

Salazar, L., & Dresdner, J. (2021). Market integration and price leadership: The U.S. Atlantic salmon market. *Aquaculture Economics & Management*, *25*(3), 245–259. https://doi.org/10.1080/13657305.2020.1843562

Salinas, I. (2015). The Mucosal Immune System of Teleost Fish. *Biology*, *4*(3), 525–539. https://doi.org/10.3390/biology4030525

Salinas, I., Zhang, Y.-A., & Sunyer, J. O. (2011). Mucosal immunoglobulins and B cells of teleost fish. *Developmental & Comparative Immunology*, *35*(12), 1346–1365. https://doi.org/10.1016/j.dci.2011.11.009

Sallan, L. C. (2014). Major issues in the origins of ray-finned fish (A ctinopterygii) biodiversity. *Biological Reviews*, *89*(4), 950–971. https://doi.org/10.1111/brv.12086

Santoso, H., Suhartono, E., Yunita, R., & Biyatmoko, D. (2020). Epidermal mucus as a potential biological matrix for fish health analysis. *Egyptian Journal of Aquatic Biology and Fisheries*, *24*(6), 361–382. https://doi.org/10.21608/ejabf.2020.114402

Schmitt, P., Wacyk, J., Morales-Lange, B., Rojas, V., Guzmán, F., Dixon, B., & Mercado, L. (2015). Immunomodulatory effect of cathelicidins in response to a β-glucan in

intestinal epithelial cells from rainbow trout. *Developmental & Comparative Immunology*, *51*(1), 160–169. https://doi.org/10.1016/j.dci.2015.03.007

Secombes, C. J., & Wang, T. (2012). The innate and adaptive immune system of fish. In *Infectious Disease in Aquaculture* (pp. 3–68). Elsevier. https://doi.org/10.1533/9780857095732.1.3

Seierstad, S. L., Haugland, Ø., Larsen, S., Waagbø, R., & Evensen, Ø. (2009). Pro-inflammatory cytokine expression and respiratory burst activity following replacement of fish oil with rapeseed oil in the feed for Atlantic salmon (Salmo salar L.). *Aquaculture*, *289*(3–4), 212–218. https://doi.org/10.1016/j.aquaculture.2008.12.004

Semeniuk, C. A. D., Jeffries, K. M., Li, T., Bettles, C. M., Cooke, S. J., Dufour, B. A., Halfyard, E. A., Heath, J. W., Keeshig, K., Mandrak, N. E., Muir, A. J., Postma, L., & Heath, D. D. (2022). Innovating transcriptomics for practitioners in freshwater fish management and conservation: Best practices across diverse resource-sector users. *Reviews in Fish Biology and Fisheries*, *32*(3), 921–939. https://doi.org/10.1007/s11160-022-09715-w

Semple, S. L., Heath, G., Filice, C. T., Heath, D. D., & Dixon, B. (2022). The impact of outbreeding on the immune function and disease status of eight hybrid Chinook salmon crosses after *Vibrio anguillarum* challenge. *Aquaculture Research*, *53*(3), 957–973. https://doi.org/10.1111/are.15636

Sepulcre, M. P., Alcaraz-Pérez, F., López-Muñoz, A., Roca, F. J., Meseguer, J., Cayuela, M. L., & Mulero, V. (2009). Evolution of Lipopolysaccharide (LPS) Recognition and

Signaling: Fish TLR4 Does Not Recognize LPS and Negatively Regulates NF-κB Activation. *The Journal of Immunology*, *182*(4), 1836–1845. https://doi.org/10.4049/jimmunol.0801755

Sever, L., Vo, N. T. K., Bols, N. C., & Dixon, B. (2014). Expression of tapasin in rainbow trout tissues and cell lines and up regulation in a monocyte/macrophage cell line (RTS11) by a viral mimic and viral infection. *Developmental & Comparative Immunology*, *44*(1), 86–93. https://doi.org/10.1016/j.dci.2013.11.019

Shahbandeh, M., (2023). Global salmonids supply by type 2021. *Statista*. Retrieved July 5, 2023, from https://www.statista.com/statistics/1026343/global-salmonids-supply/#statisticContainer

Shapouri-Moghaddam, A., Mohammadian, S., Vazini, H., Taghadosi, M., Esmaeili, S. A., Mardani, F., ... & Sahebkar, A. (2018). Macrophage plasticity, polarization, and function in health and disease. *Journal of cellular physiology*, *233*(9), 6425-6440.

Sharpe, C. S. (2007). Physiological stress responses to automated and hand vaccine injection procedures in yearling coho salmon. North American journal of aquaculture, 69(2), 180-184.

Silver, N., Best, S., Jiang, J., & Thein, S. L. (2006). Selection of housekeeping genes for gene expression studies in human reticulocytes using real-time PCR. *BMC Molecular Biology*, *7*(1), 33. https://doi.org/10.1186/1471-2199-7-33

Skjesol, A., Hansen, T., Shi, C.-Y., Thim, H. L., & Jørgensen, J. B. (2010). Structural and functional studies of STAT1 from Atlantic salmon (Salmo salar). *BMC Immunology*, *11*(1), 17. https://doi.org/10.1186/1471-2172-11-17

Skugor, S., Glover, K., Nilsen, F., & Krasnov, A. (2008). Local and systemic gene expression responses of Atlantic salmon (Salmo salar L.) to infection with the salmon louse (Lepeophtheirus salmonis). *BMC Genomics*, *9*(1), 498. https://doi.org/10.1186/1471-2164-9-498

Solem, S. T., Jørgensen, J. B., & Robertsen, B. (1995). Stimulation of respiratory burst and phagocytic activity in Atlantic salmon (Salmo salar L.) macrophages by lipopolysaccharide. *Fish & Shellfish Immunology*, *5*(7), 475–491. https://doi.org/10.1016/S1050-4648(95)80049-2

Sommerset, I., Bang Jensen, B., Bornø, B., Haukaas, A. and Brun, E. (2021). The Health Situation in Norwegian Aquaculture 2020. *Norwegian Veterinary Institute: Oslo, Norway.*

Stearley, R. F., & Smith, G. R. (1993). Phylogeny of the Pacific Trouts and Salmons (Oncorhynchus) and Genera of the Family Salmonidae. *Transactions of the American Fisheries Society*, *122*(1), 1–33. https://doi.org/10.1577/1548-8659(1993)122<0001:POTPTA>2.3.CO;2

Stentiford, G. D., Neil, D. M., Peeler, E. J., Shields, J. D., Small, H. J., Flegel, T. W., Vlak, J. M., Jones, B., Morado, F., Moss, S., Lotz, J., Bartholomay, L., Behringer, D. C., Hauton, C., & Lightner, D. V. (2012). Disease will limit future food supply from the global crustacean fishery and aquaculture sectors. *Journal of Invertebrate Pathology*, *110*(2), 141–157. https://doi.org/10.1016/j.jip.2012.03.013

Summathed, T., Zou, J., Wadsworth, S., & Secombes, C. (2013). Identification and expression analysis of IFN-gamma related (IFN-γrel) genes in Atlantic salmon Salmo

salar. *Fish & Shellfish Immunology*, *34*(6), 1740. https://doi.org/10.1016/j.fsi.2013.03.320

Sumpter, J. P. (1997). The endocrinology of stress. *Fish stress and health in aquaculture*, 819, 95-118.

Sun, B., Skjæveland, I., Svingerud, T., Zou, J., Jørgensen, J., & Robertsen, B. (2011). Antiviral Activity of Salmonid Gamma Interferon against Infectious Pancreatic Necrosis Virus and Salmonid Alphavirus and Its Dependency on Type I Interferon. *Journal of Virology*, *85*(17), 9188–9198. https://doi.org/10.1128/jvi.00319-11

Tadiso, T. M., Krasnov, A., Skugor, S., Afanasyev, S., Hordvik, I., & Nilsen, F. (2011). Gene expression analyses of immune responses in Atlantic salmon during early stages of infection by salmon louse (Lepeophtheirus salmonis) revealed bi-phasic responses coinciding with the copepod-chalimus transition. *BMC genomics*, *12*(1), 1-17.

Tartor, H., Luis Monjane, A., & Grove, S. (2020). Quantification of Defensive Proteins in Skin Mucus of Atlantic salmon Using Minimally Invasive Sampling and High-Sensitivity ELISA. *Animals*, *10*(8), 1374. https://doi.org/10.3390/ani10081374

Taylor, E. W., & Leite, C. A. C. (2022). How fish vary heart rate to match the respiratory cycle. In *Reference Module in Life Sciences* (p. B9780323908016000173). Elsevier. https://doi.org/10.1016/B978-0-323-90801-6.00017-3

Taylor, S., Wakem, M., Dijkman, G., Alsarraj, M., & Nguyen, M. (2010). A practical approach to RT-qPCR—Publishing data that conform to the MIQE guidelines. *Methods*, *50*(4), S1–S5. https://doi.org/10.1016/j.ymeth.2010.01.005

Teffer, A. K., Carr, J., Tabata, A., Schulze, A., Bradbury, I., Deschamps, D., Gillis, C.-A., Brunsdon, E. B., Mordecai, G., & Miller, K. M. (2020). A molecular assessment of infectious agents carried by Atlantic salmon at sea and in three eastern Canadian rivers, including aquaculture escapees and North American and European origin wild stocks. *FACETS*, *5*(1), 234–263. https://doi.org/10.1139/facets-2019-0048

Tiainen, T., Larsen, J. L., & Pelkonen, S. (1994). Characterization of Vibrio anguillarum strains isolated from diseased fish in Finland. *Acta Veterinaria Scandinavica*, *35*(4), 355–362. https://doi.org/10.1186/BF03548308

Torrissen, O., Jones, S., Asche, F., Guttormsen, A., Skilbrei, O. T., Nilsen, F., Horsberg, T. E., & Jackson, D. (2013). Salmon lice—Impact on wild salmonids and salmon aquaculture. *Journal of Fish Diseases*, *36*(3), 171–194. https://doi.org/10.1111/jfd.12061

Tsujita, T., Tsukada, H., Nakao, M., Oshiumi, H., Matsumoto, M., & Seya, T. (2004). Sensing bacterial flagellin by membrane and soluble orthologs of Toll-like receptor 5 in rainbow trout (Onchorhynchus mikiss). *The Journal of Biological Chemistry*, *279*(47), 48588–48597. https://doi.org/10.1074/jbc.M407634200

Tsukada, H., Fukui, A., Tsujita, T., Matsumoto, M., Iida, T., & Seya, T. (2005). Fish soluble Toll-like receptor 5 (TLR5S) is an acute-phase protein with integral flagellin-recognition activity. *International Journal of Molecular Medicine*, *15*(3), 519–525.

Tuomi, J. M., Voorbraak, F., Jones, D. L., & Ruijter, J. M. (2010). Bias in the Cq value observed with hydrolysis probe based quantitative PCR can be corrected with the

estimated PCR efficiency value. *Methods*, *50*(4), 313–322. https://doi.org/10.1016/j.ymeth.2010.02.003

Valdenegro-Vega, V. A., Crosbie, P., Bridle, A., Leef, M., Wilson, R., & Nowak, B. F. (2014). Differentially expressed proteins in gill and skin mucus of Atlantic salmon (Salmo salar) affected by amoebic gill disease. *Fish & Shellfish Immunology*, *40*(1), 69–77. https://doi.org/10.1016/j.fsi.2014.06.025

Valenzuela-Aviles, P., Torrealba, D., Figueroa, C., Mercado, L., Dixon, B., Conejeros, P., & Gallardo-Matus, J. (2022). Why vaccines fail against Piscirickettsiosis in farmed salmon and trout and how to avoid it: A review. *Frontiers in Immunology*, *13*, 1019404. https://doi.org/10.3389/fimmu.2022.1019404

Valero, Y., Martínez-Morcillo, F., Esteban, M., Chaves-Pozo, E., & Cuesta, A. (2015). Fish Peroxiredoxins and Their Role in Immunity. *Biology*, *4*(4), 860–880. https://doi.org/10.3390/biology4040860

van der Meer-Janssen, Y. P. M., van Galen, J., Batenburg, J. J., & Helms, J. B. (2010). Lipids in host–pathogen interactions: Pathogens exploit the complexity of the host cell lipidome. *Progress in Lipid Research*, *49*(1), 1–26. https://doi.org/10.1016/j.plipres.2009.07.003

Vandesompele, J., De Preter, K., Pattyn, F., Poppe, B., Van Roy, N., De Paepe, A., & Speleman, F. (2002). Accurate normalization of real-time quantitative RT-PCR data by geometric averaging of multiple internal control genes. *Genome Biology*, *3*(7), research0034.1. https://doi.org/10.1186/gb-2002-3-7-research0034

Waly, D., Muthupandian, A., Fan, C.-W., Anzinger, H., & Magor, B. G. (2022). Immunoglobulin VDJ repertoires reveal hallmarks of germinal centers in unique cell clusters isolated from zebrafish (Danio rerio) lymphoid tissues. *Frontiers in Immunology, 13*. https://doi.org/10.3389/fimmu.2022.1058877

Wang, J., Li, Y., Jaramillo-Torres, A., Einen, O., Jakobsen, J. V., Krogdahl, Å., & Kortner, T. M. (2023). Exploring gut microbiota in adult Atlantic salmon (Salmo salar L.): Associations with gut health and dietary prebiotics. *Animal Microbiome*, *5*(1), 47.

Weber, A., Wasiliew, P., & Kracht, M. (2010). Interleukin-1 (IL-1) Pathway. *Science Signaling*, *3*(105), cm1–cm1. https://doi.org/10.1126/scisignal.3105cm1

Weichselbaum, E., Coe, S., Buttriss, J., & Stanner, S. (2013). Fish in the diet: A review. *Nutrition Bulletin*, *38*(2), 128–177. https://doi.org/10.1111/nbu.12021

Wendelaar Bonga, S. E. (1997). The stress response in fish. *Physiological reviews*, *77*(3), 591-625.

Wiegertjes, G. F., Wentzel, A. S., Spaink, H. P., Elks, P. M., & Fink, I. R. (2016). Polarization of immune responses in fish: The 'macrophages first' point of view. *Molecular Immunology*, *69*, 146–156. https://doi.org/10.1016/j.molimm.2015.09.026

WOAH. (2023). WOAH - World Organisation for Animal Health. https://www.woah.org/en/what-we-do/animal-health-and-welfare/animal-diseases/

Xie, F., Wang, J., & Zhang, B. (2023). RefFinder: A web-based tool for comprehensively analyzing and identifying reference genes. *Functional & Integrative Genomics*, *23*(2), 125. https://doi.org/10.1007/s10142-023-01055-7

Xie, F., Xiao, P., Chen, D., Xu, L., & Zhang, B. (2012). miRDeepFinder: A miRNA analysis tool for deep sequencing of plant small RNAs. *Plant Molecular Biology*, *80*(1), 75–84. https://doi.org/10.1007/s11103-012-9885-2

Yang, X. O., Pappu, B. P., Nurieva, R., Akimzhanov, A., Kang, H. S., Chung, Y., Ma, L., Shah, B., Panopoulos, A. D., Schluns, K. S., Watowich, S. S., Tian, Q., Jetten, A. M., & Dong, C. (2008). T Helper 17 Lineage Differentiation Is Programmed by Orphan Nuclear Receptors RORα and RORγ. *Immunity*, *28*(1), 29–39. https://doi.org/10.1016/j.immuni.2007.11.016

Ye, J., Kaattari, I. M., & Kaattari, S. L. (2011). The differential dynamics of antibody subpopulation expression during affinity maturation in a teleost. *Fish & Shellfish Immunology*, *30*(1), 372–377. https://doi.org/10.1016/j.fsi.2010.11.013

Yu, Y., Ding, L., Huang, Z., Xu, H., & Xu, Z. (2021). Commensal bacteria-immunity crosstalk shapes mucosal homeostasis in teleost fish. *Reviews in Aquaculture*, *13*(4), 2322–2343. https://doi.org/10.1111/raq.12570

Zeng, J., Yang, Z., Zhong, Y., Zheng, Y., Hao, J., Luo, G., & Yan, Q. (2022). Metabolomics insights into the interaction between Pseudomonas plecoglossicida and Epinephelus coioides. *Scientific Reports*, *12*(1), 13309. https://doi.org/10.1038/s41598-022-17387-6

Zhang, Y.-A., Salinas, I., & Oriol Sunyer, J. (2011). Recent findings on the structure and function of teleost IgT. *Fish & Shellfish Immunology*, *31*(5), 627–634. https://doi.org/10.1016/j.fsi.2011.03.021

Zhu, W., & Su, J. (2022). Immune functions of phagocytic blood cells in teleost. *Reviews in Aquaculture*, *14*(2), 630-646.

Zou, J., Carrington, A., Collet, B., Dijkstra, J. M., Yoshiura, Y., Bols, N., & Secombes, C. (2005). Identification and Bioactivities of IFN-γ in Rainbow Trout Oncorhynchus mykiss: The First Th1-Type Cytokine Characterized Functionally in Fish1. *The Journal of Immunology*, *175*(4), 2484–2494. https://doi.org/10.4049/jimmunol.175.4.2484

Zou, J., & Secombes, C. J. (2011). Teleost fish interferons and their role in immunity. *Developmental & Comparative Immunology*, *35*(12), 1376–1387. https://doi.org/10.1016/j.dci.2011.07.001

Zuo, S., Karami, A. M., Ødegård, J., Mathiessen, H., Marana, M. H., Jaafar, R. M., ... & Buchmann, K. (2020). Immune gene expression and genome-wide association analysis in rainbow trout with different resistance to Yersinia ruckeri infection. Fish & Shellfish Immunology, 106, 441-450.

Appendix. Full list of gene expression results by OpenArray™ TaqMan® RT-qPCR in addition to section 2.3.2.

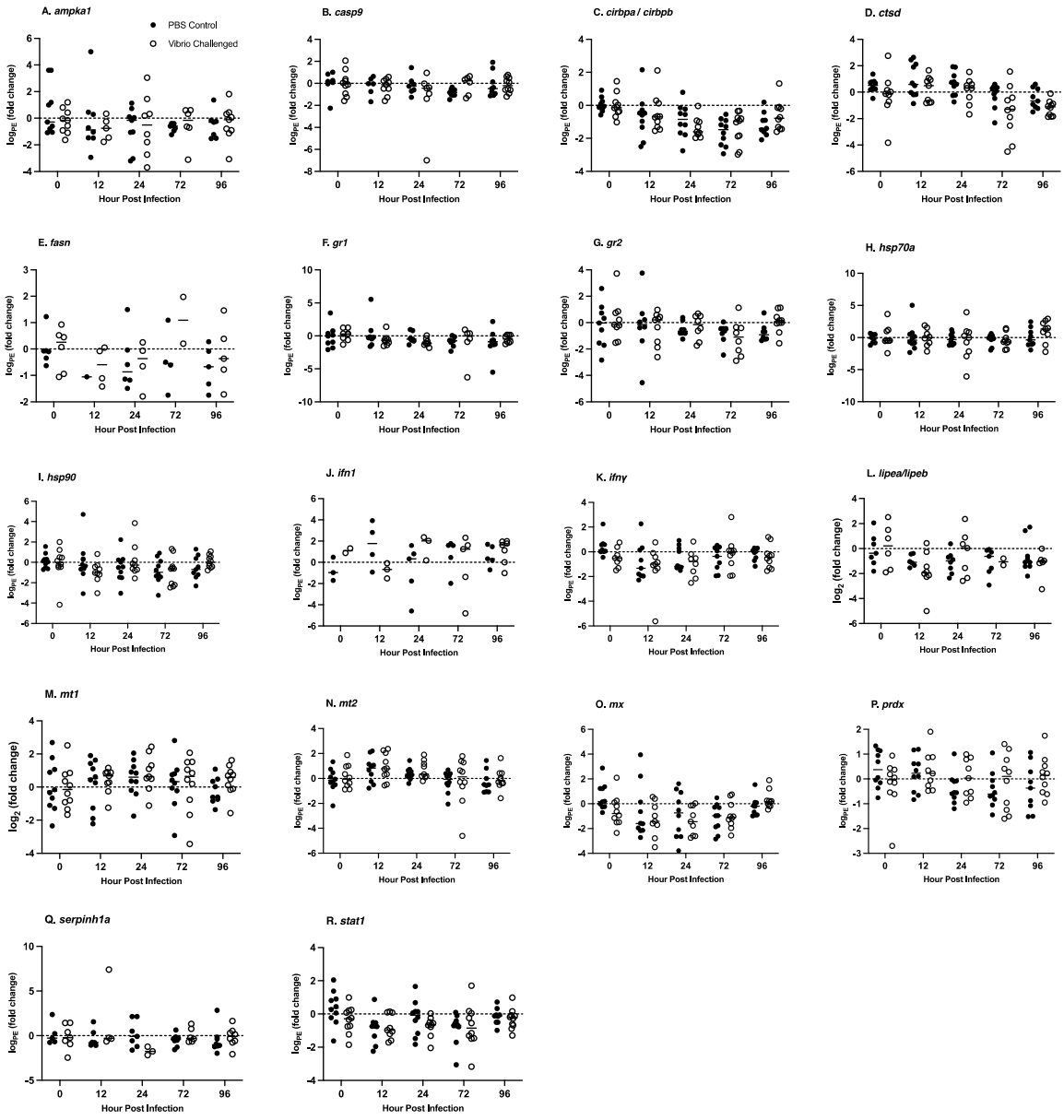

Figure 1. Spleen immune transcript expression throughout live *V. anguillarum* challenge, OpenArray™ TaqMan® RT-qPCR method. Transcript expression levels were assessed via OpenArray™ TaqMan® RT-qPCR on 12 h, 24 h, 72 h, and 96 h following i.p. injection with live *V. anguillarum*. Each treatment group had 10 individuals. All data was

normalized to the reference gene *rpl13a* and expressed as a $\log_{PE}$ (fold change) over the 0 h control group. A p-value of less than 0.05 was considered to be statistically significant.

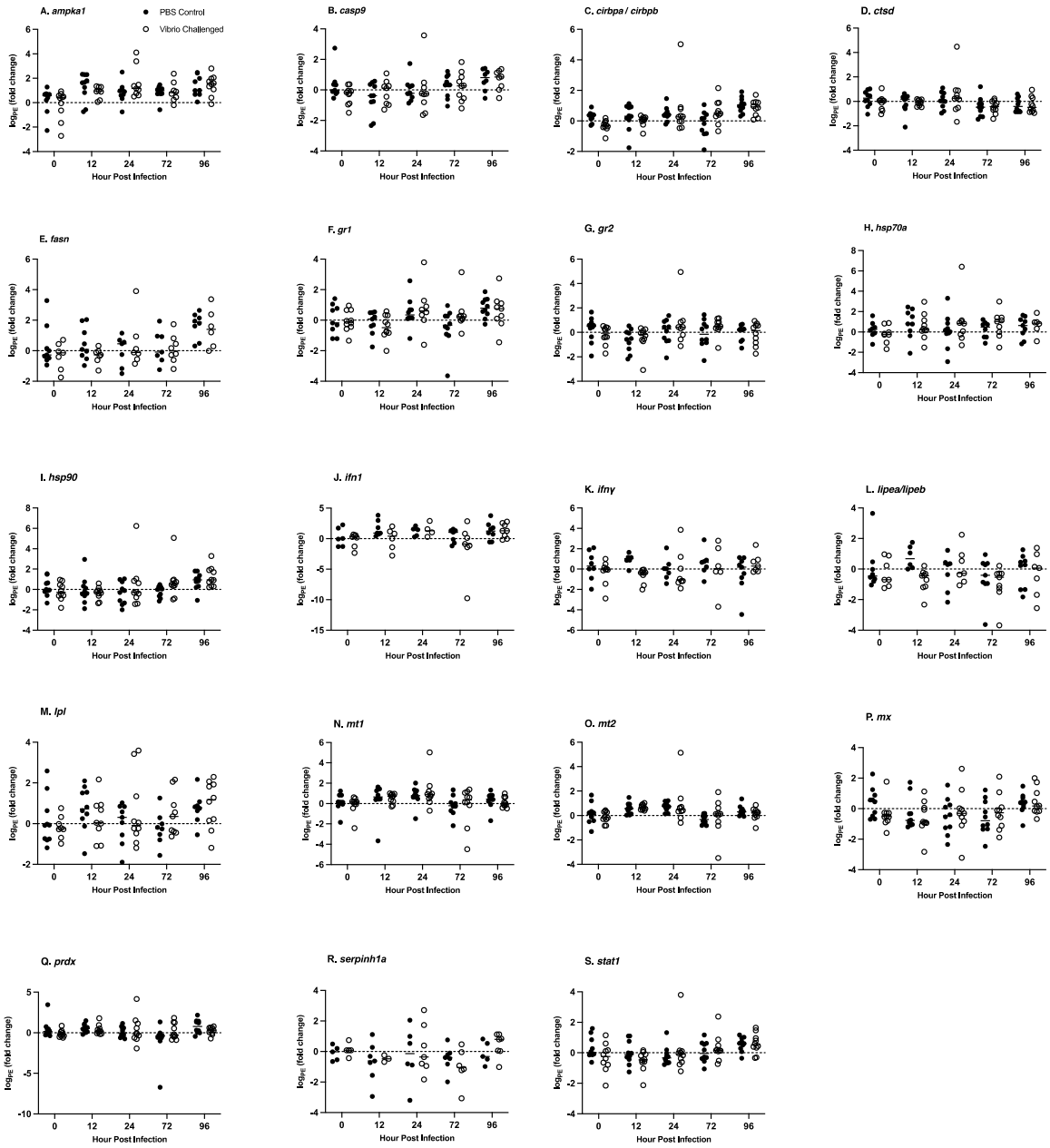

Figure 2. Head kidney immune transcript expression throughout live *V. anguillarum* challenge, OpenArray™ TaqMan® RT-qPCR method. Transcript expression levels were assessed via OpenArray™ TaqMan® RT-qPCR on 12 h, 24 h, 72 h, and 96 h following i.p. injection with live *V. anguillarum*. Each treatment group had 10 individuals. All data was

normalized to the reference gene *rpl13a* and expressed as a $\log_{PE}$ (fold change) over the 0 h control group. A p-value of less than 0.05 was considered to be statistically significant.

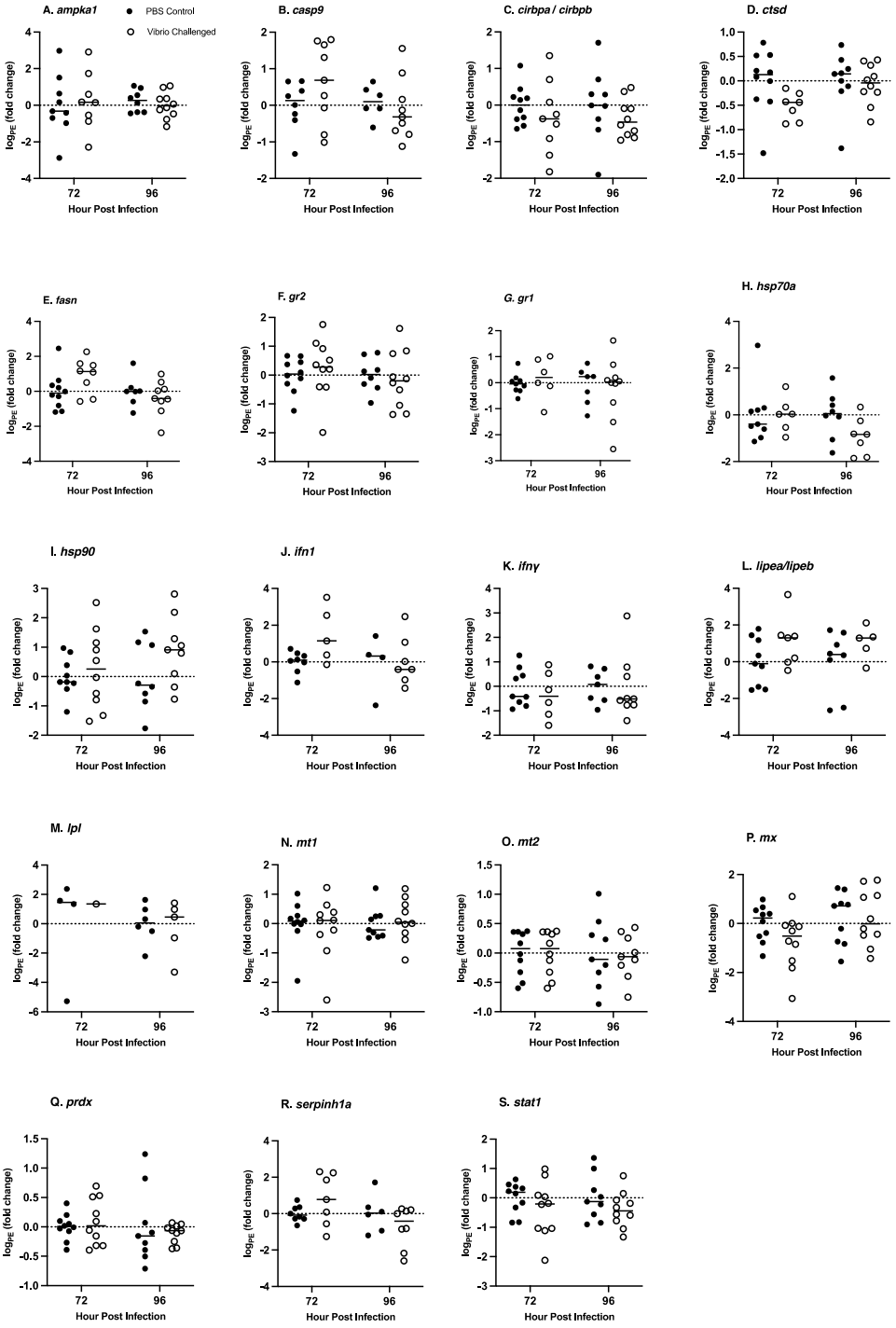

Figure 3. Gill immune transcript expression throughout live *V. anguillarum* challenge, OpenArray™ TaqMan® RT-qPCR method. Transcript expression levels were assessed via OpenArray™ TaqMan® RT-qPCR on 72 h and 96 h following i.p. injection with live *V.*

anguillarum. Each treatment group had 10 individuals. All data was normalized to the reference gene *rpl13a* and expressed as a $\log_{PE}$ (fold change) over the combined 72 h and 96 h control group. A p-value of less than 0.05 was considered to be statistically significant.

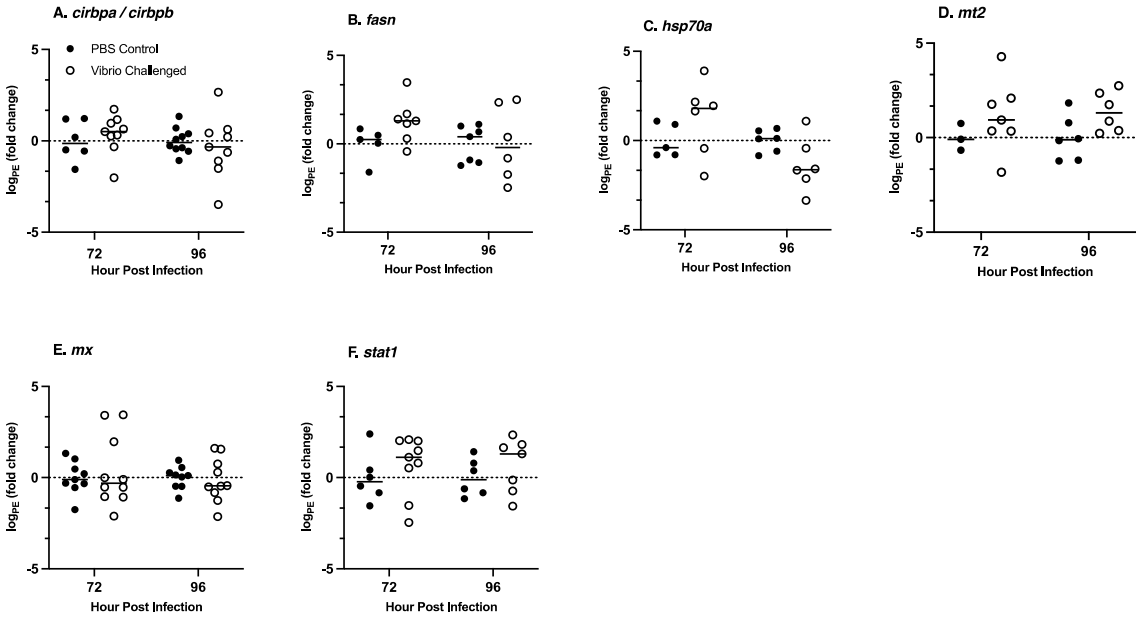

Figure 4. Mucus immune transcript expression throughout live *V. anguillarum* challenge, OpenArray™ TaqMan® RT-qPCR method. Transcript expression levels were assessed via OpenArray™ TaqMan® RT-qPCR on 72 h and 96 h following i.p. injection with live *V. anguillarum*. Each treatment group had 10 individuals. All data was normalized to the reference gene *rpl13a* and expressed as a $\log_{PE}$ (fold change) over the combined 72 h and 96 h control group. A p-value of less than 0.05 was considered to be statistically significant.